Nuclear Science
NEA/NSC/DOC(2003)3

ISBN 92-64-02123-X

Burn-up Credit Criticality Benchmark

Phase IV-A: Reactivity Prediction Calculations for Infinite Arrays of PWR MOX Fuel Pin Cells

Gregory J. O'Connor
Radioactive Materials Transport Division (RMTD)
Department for Transport, Local Government and the Regions (DTLR)
United Kingdom

Russell L. Bowden, Peter R. Thorne
Safety & Environmental Risk Management
Research & Technology
BNFL

NUCLEAR ENERGY AGENCY
ORGANISATION FOR ECONOMIC CO-OPERATION AND DEVELOPMENT

ORGANISATION FOR ECONOMIC CO-OPERATION AND DEVELOPMENT

Pursuant to Article 1 of the Convention signed in Paris on 14th December 1960, and which came into force on 30th September 1961, the Organisation for Economic Co-operation and Development (OECD) shall promote policies designed:

- to achieve the highest sustainable economic growth and employment and a rising standard of living in Member countries, while maintaining financial stability, and thus to contribute to the development of the world economy;
- to contribute to sound economic expansion in Member as well as non-member countries in the process of economic development; and
- to contribute to the expansion of world trade on a multilateral, non-discriminatory basis in accordance with international obligations.

The original Member countries of the OECD are Austria, Belgium, Canada, Denmark, France, Germany, Greece, Iceland, Ireland, Italy, Luxembourg, the Netherlands, Norway, Portugal, Spain, Sweden, Switzerland, Turkey, the United Kingdom and the United States. The following countries became Members subsequently through accession at the dates indicated hereafter: Japan (28th April 1964), Finland (28th January 1969), Australia (7th June 1971), New Zealand (29th May 1973), Mexico (18th May 1994), the Czech Republic (21st December 1995), Hungary (7th May 1996), Poland (22nd November 1996), Korea (12th December 1996) and the Slovak Republic (14 December 2000). The Commission of the European Communities takes part in the work of the OECD (Article 13 of the OECD Convention).

NUCLEAR ENERGY AGENCY

The OECD Nuclear Energy Agency (NEA) was established on 1st February 1958 under the name of the OEEC European Nuclear Energy Agency. It received its present designation on 20th April 1972, when Japan became its first non-European full Member. NEA membership today consists of 28 OECD Member countries: Australia, Austria, Belgium, Canada, Czech Republic, Denmark, Finland, France, Germany, Greece, Hungary, Iceland, Ireland, Italy, Japan, Luxembourg, Mexico, the Netherlands, Norway, Portugal, Republic of Korea, Slovak Republic, Spain, Sweden, Switzerland, Turkey, the United Kingdom and the United States. The Commission of the European Communities also takes part in the work of the Agency.

The mission of the NEA is:

- to assist its Member countries in maintaining and further developing, through international co-operation, the scientific, technological and legal bases required for a safe, environmentally friendly and economical use of nuclear energy for peaceful purposes, as well as
- to provide authoritative assessments and to forge common understandings on key issues, as input to government decisions on nuclear energy policy and to broader OECD policy analyses in areas such as energy and sustainable development.

Specific areas of competence of the NEA include safety and regulation of nuclear activities, radioactive waste management, radiological protection, nuclear science, economic and technical analyses of the nuclear fuel cycle, nuclear law and liability, and public information. The NEA Data Bank provides nuclear data and computer program services for participating countries.

In these and related tasks, the NEA works in close collaboration with the International Atomic Energy Agency in Vienna, with which it has a Co-operation Agreement, as well as with other international organisations in the nuclear field.

FOREWORD

The reactivity of nuclear fuel decreases with irradiation (or burn-up) due to the transformation of heavy nuclides and the formation of fission products. Burn-up credit studies aim at accounting for fuel irradiation in criticality studies of the nuclear fuel cycle (transport, storage…).

The OECD/NEA Expert Group on Burn-up Credit was established in 1991 to address scientific and technical issues connected with the use of burn-up credit in nuclear fuel cycle operations. Several benchmark exercises were conducted in order to compare computation tools used in this context. Phases I and II of these benchmarks addressed burn-up credit issues when the uranium oxide fuel involved was irradiated in pressurised water reactors (PWRs). Phase III concentrated on uranium fuels irradiated in boiling water reactors (BWRs). The present report, the first in a series of two reports, concerns mixed uranium and plutonium oxide (MOX) fuels irradiated in pressurised water reactors.

Electronic versions of all of the benchmark reports are available on the NEA website at www.nea.fr/html/science/wpncs/buc. Attention should be drawn to the fact that the printed version of this publication is in black and white; several of the figures were, however, originally produced in colour and can best be viewed either on CD-ROM or at the Internet address mentioned above.

Acknowledgements

The NEA Secretariat wishes to thank all those who have contributed to this study, in particular, Russ Bowden and Peter Thorne for the preparation of the benchmark specifications; the participants for their calculation of the benchmark and the submission of solutions to the exercises; Greg O'Connor for his analysis of the results and the preparation of the present report; and Bénédicte Roque, Hiroshi Okuno and Dennis Mennerdahl for their peer reviews.

Abstract

The report describes the final results of the Phase IV-A Burn-up Credit Benchmark conducted by the Expert Group on Burn-up Credit Criticality Safety under the auspices of the Nuclear Energy Agency (NEA) of the Organisation for Economic Co-operation and Development (OECD).

The intention of the benchmark was to undertake an initial investigation into the reactivity effects observed with MOX fuel for combinations of the computer codes and data libraries currently being used around the world. The exercise was based upon the calculation of infinite PWR fuel pin cell reactivity for fresh and irradiated MOX fuels, using isotopic number densities provided by the benchmark co-ordinators.

In total, 37 contributions were submitted to the Phase IV-A benchmark exercise, from 17 different companies/organisations in 10 countries around the world. The participants were asked to perform 63 separate reactivity calculations covering three different initial MOX compositions, with a range of burn-ups, cooling times and fuel representations.

Analysis of the contributions for this benchmark has shown that there is a spread in the k_{eff} results of between 2.0-2.5% about the mean, depending on the MOX composition. This spread does not appear to be dependent on the burn-up of the fuel (neglecting the results that include curium). Consequently, the spread in the results for the fresh MOX fuel is just as large as that for the irradiated fuel.

The analysis has also shown that the calculations which include curium gives rise to a larger spread in the results than those calculations with the curium removed. It is considered that discrepancies in the nuclear data for the ^{244}Cm and ^{245}Cm nuclides could be the cause for the larger spread in the participants' k_{eff} results when curium is included in the fuel composition.

The addition of the curium isotopes into the fuel inventory also leads to an increase in the reactivity of the system of the order of 1 000 ppm. This is seen to occur for MOX fuel only and not UOX fuel. It is therefore recommended that the curium isotopes be included in the spent fuel compositions of MOX fuel.

Although the Wigner-Seitz approximation has previously been shown to be acceptable for UO_2 pin cell calculations, it can be seen from the reports presented in Appendices III and IV that this approximation for MOX fuels introduces a reactivity error of the order of 500 pcm. It is therefore recommended that the Wigner-Seitz approximation not be used for MOX fuel.

Keywords

Burn-up credit, PWR, MOX, infinite, pin cell, reactivity, benchmark, OECD/NEA, burn-up, criticality.

TABLE OF CONTENTS

1. Introduction

The investigation of burn-up credit for mixed oxide (MOX) fuels is an ongoing objective of the OECD/NEA Burn-up Credit Working Group, following the study of burn-up credit methods for PWR and BWR UO_2 fuels [1-6].

The first phase of this benchmarking programme for MOX systems, referred to as Phase IV-A, was to undertake an initial investigation of the reactivity effects observed with MOX fuel. This exercise was based upon the calculation of infinite PWR fuel pin cell reactivity for fresh and irradiated MOX fuels, using isotopic number densities provided by the benchmark co-ordinators.

The requested calculations considered the effect of burn-up, cooling time and initial MOX composition, i.e. initial plutonium vector and MOX plutonium content upon the pin cell reactivity. Consideration was given to the impact of the initial MOX composition using three different initial MOX fuels, which were chosen to represent the range of current interest in MOX fuel:

- A reference MOX fuel case, Case A, appropriate to a typical plutonium vector for material derived from the reprocessing of thermal reactor UO_2 fuels, often referred to as "first generation" MOX.
- A MOX fuel case appropriate to the disposition of weapons plutonium in MOX, Case B.
- A MOX fuel case appropriate to future MOX fuels that might be produced using the plutonium recovered from the reprocessing of irradiated MOX, i.e. the "later generation" of MOX fuel from a plutonium recycling strategy, Case C.

In order to keep the initial exercise as simple as possible, it was agreed that there be no requirement to consider MOX fuels that were truly equivalent in terms of their lifetime performance in the reactor. For the purposes of the Phase IV-A benchmark, it was judged sufficient to analyse the reactivity effect of the initial plutonium vectors for three MOX fuels with broadly the same initial fissile plutonium content.

The 63 requested calculations are presented in Table 1.1 and were chosen to cover combinations of the following parameters for the three MOX fuel types:

- Burn-up:
  - Fresh fuel.
  - 20 GWd/teHM.
  - 40 GWd/teHM.
  - 60 GWd/teHM.
- Cooling:
  - One year.
  - Five years.
- Fuel representation:
  - Major and minor actinides.
  - Actinides and fission products.

Table 1.1. Specified calculations

MOX case	Cooling time (years)	Fission products modelled?	Actinides modelled?	Burn-up (GWd/teHM)			
				Fresh	20	40	60
A	1	Yes	Major	Case 1	Case 2	Case 3	Case 4
		No	Major		Case 5	Case 6	Case 7
			All		Case 8	Case 9	Case 10
	5	Yes	Major		Case 11	Case 12	Case 13
		No	Major		Case 14	Case 15	Case 16
			All		Case 17	Case 18	Case 19
B	1	Yes	Major	Case 20	Case 21	Case 22	Case 23
		No	Major		Case 24	Case 25	Case 26
			All		Case 27	Case 28	Case 29
	5	Yes	Major		Case 30	Case 31	Case 32
		No	Major		Case 33	Case 34	Case 35
			All		Case 36	Case 37	Case 38
C	1	Yes	Major	Case 39	Case 40	Case 41	Case 42
			All		Case 43	Case 44	Case 45
		No	Major		Case 46	Case 47	Case 48
			All		Case 49	Case 50	Case 51
	5	Yes	Major		Case 52	Case 53	Case 54
			All		Case 55	Case 56	Case 57
		No	Major		Case 58	Case 59	Case 60
			All		Case 61	Case 62	Case 63

The complete specification of this benchmark is presented in Appendix I. The specification of major actinides and fission products is consistent with previous burn-up credit benchmark exercises. In the context of this benchmark, the term “all actinides” was used to include the presence of the curium isotopes.

The pin cell geometry for the Phase IV-A exercise is presented in Figure 1.1. The fuel pin consists of a 0.412 cm radius fuel pellet surrounded by 0.063 cm thick zircalloy-4 cladding, with no intervening air gap between the fuel and the cladding. The fuel pin is within a square cell of 1.33 cm side dimension, and is surrounded by full density water. Reflective boundary conditions are modelled on all sides of the pin cell geometry.

2. Benchmark contributions

A total of 37 contributions were made to the Phase IV-A benchmark exercise, from 17 different companies/organisations covering 10 countries around the world. Details of the codes and nuclear data libraries used by the benchmark participants are presented in Table 2.1. A detailed description of the participants’ methods, data and assumptions can be obtained from Appendix II.

Figure 1.1. Geometry of MOX fuel pin cell for PWR

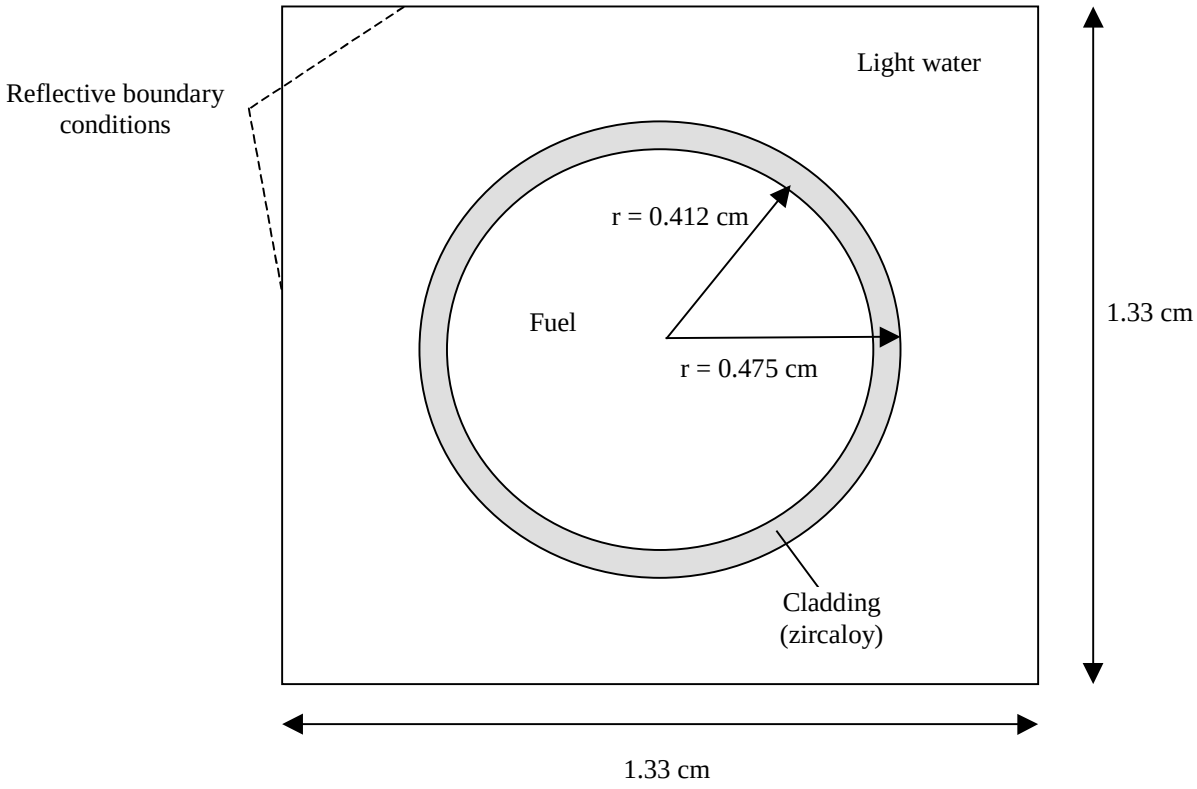

Table 2.1. Participant, code and nuclear data source

#	Institute	Country	Criticality code	Groups	Nuclear data source	Processing method	Comments
1	EDF/DER	France	TRIPOLI-4	Point	JEF2		
2	PNC	Japan	KENO-Va	44	ENDF/B-V	AMPX/SCALE-4.3	CSAS25
3	BNFL	UK	MONK7B	Point	UKNDL	GALAXY/GENEX/DICE	
4	BNFL	UK	WIMS7B	172	JEF2.2	NJOY/HEAD	
5	BNFL	UK	KENO-Va	27	ENDF/B-IV	AMPX/SCALE-4.3	CSAS25
6	BNFL	UK	KENO-Va	44	ENDF/B-V	AMPX/SCALE-4.3	CSAS25
7	JAERI	Japan	MVP94.1	Point	JENDL-3.2	LICEM	
8	JAERI	Japan	SRAC95	107	JENDL-3.2		
9	CEA	France	APOLLO2	172	JEF2.2	NJOY/THEMIS	
10	Siemens	Germany	KENO-Va	44	ENDF/B-V	AMPX/SCALE-4.3	CSAS25
11	Siemens	Germany	MCNP4B2	Point	ENDF/B-VI	NJOY	
12	AEAT	UK	WIMS7B	172	JEF2.2	NJOY/HEAD	
13	AEAT	UK	MONK7B	Point	JEF2.2	NJOY/DICE	
14	AEAT	UK	KENO-Va	238	ENDF/B-V	AMPX/SCALE-4.3	CSAS25
15	IPPE	RF	WIMS/ABBN	69	FOND-2	NJOY	

Table 2.1. Participant, code and nuclear data source (*cont.*)

#	Institute	Country	Criticality code	Groups	Nuclear data source	Processing method	Comments
16	EMS	Sweden	XSDRNPM	44	ENDF/B-V	AMPX/SCALE-4.3	CSAS1X
17	EMS	Sweden	XSDRNPM	27	ENDF/B-IV	AMPX/SCALE-4.3	CSAS1X
18	EMS	Sweden	XSDRNPM	238	ENDF/B-V	AMPX/SCALE-4.3	CSAS1X
19	IPSN	France	APOLLO2	172	JEF2.2	NJOY/THEMIS	
20	DETR	UK	MONK	Point	UKNDL	GALAXY/GENEX/DICE	
21	NUPEC	Japan	ANISN	137	ENDF/B-IV/ JENDL-3.2	MGCL-JINS	
22	NUPEC	Japan	XSDRNPM	44	ENDF/B-V	AMPX/SCALE-4.3	CSAS1X
23	NUPEC	Japan	XSDRNPM	27	ENDF/B-IV	AMPX/SCALE-4.3	CSAS1X
24	NUPEC	Japan	MVP	Point	JENDL-3.2		
25	NUPEC	Japan	MCNP4A	Point	JENDL-3.2		
26	ORNL	USA	XSDRNPM	44	ENDF/B-V	AMPX/SCALE-4.3	CSAS1X
27	ORNL	USA	NEWT	44	ENDF/B-V	AMPX/SCALE-4.3	CSASN
28	ORNL	USA	KENO-Va	44	ENDF/B-V	AMPX/SCALE-4.3	CSAS25
29	ORNL	USA	XSDRNPM	238	ENDF/B-V	AMPX/SCALE-4.3	CSAS1X
30	ORNL	USA	NEWT	238	ENDF/B-V	AMPX/SCALE-4.3	CSASN
31	ORNL	USA	KENO-Va	238	ENDF/B-V	AMPX/SCALE-4.3	CSAS25
32	PSI	Switzerland	BOXER	70	JEF1	ETOBOX	
33	ANL	USA	VIM	Point	ENDF/B-VI	UNIDOP/AURIX	
34	KEPCO	Korea	HELIOS	89	ENDF/B-VI		
35	KFKI	Hungary	MCNP4C	Point	ENDF/B-VI	NJOY	
36	KFKI	Hungary	MCNP4C	Point	JEF2.2	NJOY	
37	EMS	Sweden	MCNP4C2	Point	ENDF/B-VI	NJOY	

3. Results

The results from the participants to the Phase IV-A exercise are presented in Tables 3.1, 3.2 and 3.3 for the three different MOX fuel cases, respectively. In addition, these tables also present the mean calculated neutron multiplication and the standard deviation on this value from the 37 individual contributions. This result is a simple arithmetic mean of the various results, but it is acknowledged that many of the contributions from the benchmark participants have a common method of solution, particularly the results provided using the SCALE-4.3 suite of codes.

The results from each contributor are graphically presented in Figure 3.1. The absolute neutron multiplication factors are plotted for each of the 63 benchmark cases. It appears from the data presented in Figure 3.1, that the participants have all predicted similar neutron multiplication factors (k_{eff}s) for each of the benchmark cases. However, this is due to the scale of the graph and further analysis is required to examine the results in more detail.

Table 3.1. Multiplication factors from participants (MOX composition A)

Case #	Burn-up (GWd/te)	Cooling (years)	FPs	Actinides	Participant												
					1	2	3	4	5	6	7	8	9	10	11	12	13
1	0	0	N/A	Major	1.3036	1.2966	1.3012	1.2961	1.3040	1.2996	1.3029	1.3038	1.3045	1.2986	1.2999	1.2998	1.3021
2	20	1	Yes	Major	1.1812	1.1790	1.1819	1.1758	1.1859	1.1809	1.1835	1.1854	1.1838	1.1799	1.1850	1.1793	1.1841
3	40	1	Yes	Major	1.1112	1.1100	1.1106	1.1041	1.1129	1.1119	1.1120	1.1147	1.1119	1.1099	1.1141	1.1074	1.1132
4	60	1	Yes	Major	1.0510	1.0535	1.0559	1.0464	1.0561	1.0558	1.0544	1.0577	1.0540	1.0543	1.0599	1.0495	1.0533
5	20	1	No	Major	1.2461	1.2397	1.2460	1.2386	1.2455	1.2440	1.2438	1.2463	1.2468	1.2413	1.2417	1.2423	1.2460
6	40	1	No	Major	1.2089	1.2041	1.2102	1.2003	1.2071	1.2051	1.2066	1.2077	1.2085	1.2035	1.2050	1.2038	1.2092
7	60	1	No	Major	1.1760	1.1742	1.1812	1.1708	1.1775	1.1781	1.1767	1.1779	1.1788	1.1758	1.1736	1.1741	1.1771
8	20	1	No	All	1.2450	1.2405	1.2447	1.2384		1.2440	1.2440	1.2460	1.2466	1.2422	1.2395	1.2421	1.2468
9	40	1	No	All	1.2091	1.2041	1.2126	1.2015		1.2063	1.2059	1.2083	1.2097	1.2055	1.2058	1.2050	1.2107
10	60	1	No	All	1.1844	1.1814	1.1885	1.1760		1.1829	1.1796	1.1814	1.1837	1.1830	1.1773	1.1790	1.1855
11	20	5	Yes	Major	1.1345	1.1329	1.1330	1.1276	1.1366	1.1351	1.1376	1.1397	1.1357	1.1340	1.1363	1.1310	1.1346
12	40	5	Yes	Major	1.0545	1.0537	1.0528	1.0460	1.0542	1.0558	1.0548	1.0588	1.0537	1.0554	1.0573	1.0492	1.0554
13	60	5	Yes	Major	0.9870	0.9906	0.9884	0.9808	0.9906	0.9913	0.9912	0.9938	0.9881	0.9910	0.9936	0.9837	0.9898
14	20	5	No	Major	1.2024	1.1978	1.2011	1.1933	1.2012	1.2002	1.2031	1.2038	1.2016	1.1980	1.1964	1.1969	1.1998
15	40	5	No	Major	1.1560	1.1535	1.1569	1.1482	1.1545	1.1554	1.1564	1.1584	1.1564	1.1537	1.1538	1.1516	1.1556
16	60	5	No	Major	1.1208	1.1200	1.1261	1.1155	1.1208	1.1246	1.1235	1.1253	1.1235	1.1215	1.1181	1.1187	1.1241
17	20	5	No	All	1.2003	1.1973	1.2021	1.1932		1.2007	1.2010	1.2037	1.2016	1.1990	1.1978	1.1969	1.2012
18	40	5	No	All	1.1554	1.1560	1.1575	1.1500		1.1568	1.1571	1.1595	1.1582	1.1559	1.1543	1.1534	1.1583
19	60	5	No	All	1.1272	1.1292	1.1345	1.1220		1.1311	1.1283	1.1303	1.1301	1.1299	1.1256	1.1253	1.1292

Table 3.1. Multiplication factors from participants (MOX composition A) (*cont.*)

Case #	Burn-up (GWd/te)	Cooling (years)	FPs	Actinides	Participant												
					14	15	16	17	18	19	20	21	22	23	24	25	26
1	0	0	N/A	Major	1.2984	1.2893	1.2974	1.3000	1.2916	1.3021	1.3029	1.3070	1.2943	1.2996	1.3014	1.3079	1.2947
2	20	1	Yes	Major	1.1792	1.1720	1.1779	1.1827	1.1741	1.1816	1.1817	1.1879	1.1776	1.1825	1.1832	1.1876	1.1779
3	40	1	Yes	Major	1.1074	1.1013	1.1081	1.1110	1.1041	1.1099	1.1112	1.1164	1.1079	1.1110	1.1110	1.1162	1.1081
4	60	1	Yes	Major	1.0539	1.0437	1.0524	1.0531	1.0480	1.0521	1.0549	1.0582	1.0522	1.0533	1.0548	1.0603	1.0523
5	20	1	No	Major	1.2391	1.2327	1.2386	1.2428	1.2342	1.2444	1.2463	1.2499	1.2382	1.2425	1.2449	1.2498	1.2386
6	40	1	No	Major	1.2025	1.1951	1.2013	1.2043	1.1961	1.2063	1.2087	1.2117	1.2010	1.2041	1.2059	1.2115	1.2013
7	60	1	No	Major	1.1712	1.1657	1.1729	1.1742	1.1670	1.1768	1.1800	1.1818	1.1726	1.1741	1.1764	1.1801	1.1728
8	20	1	No	All	1.2403	1.2325	1.2386		1.2340	1.2442	1.2448		1.2383		1.2450	1.2483	1.2386
9	40	1	No	All	1.2029	1.1962	1.2033		1.1975	1.2075	1.2115		1.2031		1.2072	1.2134	1.2033
10	60	1	No	All	1.1788	1.1701	1.1795		1.1724	1.1817	1.1891		1.1793		1.1789	1.1844	1.1795
11	20	5	Yes	Major	1.1354	1.1253	1.1317	1.1338	1.1279	1.1333	1.1324	1.1390	1.1315	1.1336	1.1359	1.1434	1.1317
12	40	5	Yes	Major	1.0546	1.0446	1.0519	1.0525	1.0480	1.0518	1.0542	1.0574	1.0518	1.0525	1.0545	1.0613	1.0519
13	60	5	Yes	Major	0.9877	0.9794	0.9883	0.9875	0.9843	0.9864	0.9880	0.9916	0.9883	0.9878	0.9906	0.9961	0.9882
14	20	5	No	Major	1.1956	1.1891	1.1955	1.1966	1.1908	1.1992	1.2011	1.2039	1.1952	1.1963	1.2007	1.2062	1.1955
15	40	5	No	Major	1.1500	1.1446	1.1514	1.1512	1.1461	1.1542	1.1561	1.1591	1.1512	1.1510	1.1560	1.1622	1.1514
16	60	5	No	Major	1.1196	1.1120	1.1197	1.1181	1.1138	1.1215	1.1249	1.1262	1.1195	1.1181	1.1242	1.1296	1.1196
17	20	5	No	All	1.1962	1.1890	1.1957		1.1908	1.1992	1.2000		1.1954		1.2006	1.2059	1.1957
18	40	5	No	All	1.1542	1.1463	1.1539		1.1480	1.1559	1.1614		1.1536		1.1579	1.1605	1.1539
19	60	5	No	All	1.1253	1.1182	1.1274		1.1206	1.1280	1.1352		1.1272		1.1280	1.1353	1.1274

Table 3.1. Multiplication factors from participants (MOX composition A) (*cont.*)

Case #	Burn-up (GWd/te)	Cooling (years)	FPs	Actinides	Participant											Mean	St dev	St dev/mean
					27	28	29	30	31	32	33	34	35	36	37			
1	0	0	N/A	Major	1.2980	1.2979	1.2929	1.2989	1.2978	1.3061	1.3108	1.3037	1.2987	1.3042	1.2981	**1.3002**	0.0045	3.4900E-03
2	20	1	Yes	Major	1.1807	1.1802	1.1753	1.1807	1.1795	1.1868	1.1862	1.1864	1.1806	1.1835	1.1809	**1.1814**	0.0038	3.1802E-03
3	40	1	Yes	Major	1.1107	1.1108	1.1053	1.1103	1.1093	1.1155	1.1161	1.1161	1.1094	1.1120	1.1108	**1.1106**	0.0035	3.1591E-03
4	60	1	Yes	Major	1.0546	1.0543	1.0491	1.0538	1.0527	1.0583	1.0600	1.0591	1.0534	1.0550	1.0525	**1.0539**	0.0036	3.4330E-03
5	20	1	No	Major	1.2415	1.2413	1.2355	1.2412	1.2406	1.2491	1.2491	1.2465	1.2418	1.2462	1.2396	**1.2428**	0.0042	3.4085E-03
6	40	1	No	Major	1.2039	1.2041	1.1973	1.2028	1.2017	1.2110	1.2107	1.2084	1.2037	1.2078	1.2043	**1.2050**	0.0041	3.4192E-03
7	60	1	No	Major	1.1751	1.1755	1.1681	1.1732	1.1724	1.1816	1.1810	1.1787	1.1744	1.1783	1.1744	**1.1754**	0.0039	3.3127E-03
8	20	1	No	All	1.2416	1.2416	1.2353	1.2411	1.2407	1.2489	1.2486	1.2464	1.2412	1.2456	1.2408	**1.2423**	0.0041	3.2793E-03
9	40	1	No	All	1.2060	1.2053	1.1987	1.2042	1.2027	1.2125	1.2112	1.2096	1.2051	1.2096	1.2049	**1.2061**	0.0042	3.5103E-03
10	60	1	No	All	1.1819	1.1812	1.1736	1.1788	1.1778	1.1875	1.1868	1.1833	1.1796	1.1839	1.1794	**1.1809**	0.0043	3.6676E-03
11	20	5	Yes	Major	1.1345	1.1345	1.1291	1.1343	1.1333	1.1392	1.1394	1.1386	1.1337	1.1359	1.1323	**1.1343**	0.0036	3.1973E-03
12	40	5	Yes	Major	1.0544	1.0542	1.0491	1.0539	1.0539	1.0578	1.0591	1.0581	1.0528	1.0541	1.0523	**1.0537**	0.0034	3.2642E-03
13	60	5	Yes	Major	0.9903	0.9908	0.9854	0.9897	0.9891	0.9927	0.9948	0.9932	0.9888	0.9891	0.9891	**0.9891**	0.0035	3.5194E-03
14	20	5	No	Major	1.1987	1.1985	1.1921	1.1978	1.1957	1.2046	1.2037	1.2018	1.1972	1.2008	1.1966	**1.1986**	0.0039	3.2809E-03
15	40	5	No	Major	1.1541	1.1537	1.1473	1.1527	1.1516	1.1595	1.1593	1.1567	1.1520	1.1561	1.1522	**1.1538**	0.0038	3.2995E-03
16	60	5	No	Major	1.1220	1.1217	1.1150	1.1199	1.1196	1.1268	1.1272	1.1238	1.1194	1.1230	1.1193	**1.1213**	0.0039	3.4398E-03
17	20	5	No	All	1.1989	1.1983	1.1921	1.1979	1.1968	1.2046	1.2050	1.2018	1.1976	1.2008	1.1963	**1.1986**	0.0039	3.2700E-03
18	40	5	No	All	1.1566	1.1563	1.1492	1.1547	1.1539	1.1616	1.1598	1.1585	1.1544	1.1578	1.1541	**1.1556**	0.0036	3.0977E-03
19	60	5	No	All	1.1299	1.1301	1.1218	1.1269	1.1259	1.1343	1.1326	1.1299	1.1268	1.1308	1.1269	**1.1282**	0.0040	3.5331E-03

Table 3.2. Multiplication factors from participants (MOX composition B)

Case #	Burn-up (GWd/te)	Cooling (years)	FPs	Actinides	Participant												
					1	2	3	4	5	6	7	8	9	10	11	12	13
20	0	0	N/A	Major	1.4148	1.4163	1.4100	1.4077	1.4087	1.4221	1.4186	1.4190	1.4163	1.4180	1.4099	1.4108	1.4136
21	20	1	Yes	Major	1.2247	1.2232	1.2221	1.2176	1.2237	1.2258	1.2272	1.2282	1.2257	1.2249	1.2260	1.2207	1.2249
22	40	1	Yes	Major	1.1144	1.1116	1.1119	1.1067	1.1150	1.1125	1.1149	1.1167	1.1141	1.1131	1.1160	1.1097	1.1132
23	60	1	Yes	Major	1.0321	1.0337	1.0373	1.0267	1.0340	1.0354	1.0351	1.0369	1.0338	1.0328	1.0390	1.0294	1.0329
24	20	1	No	Major	1.2969	1.2937	1.2941	1.2898	1.2934	1.2958	1.2968	1.2982	1.2981	1.2939	1.2924	1.2931	1.2970
25	40	1	No	Major	1.2220	1.2166	1.2221	1.2158	1.2193	1.2193	1.2210	1.2222	1.2235	1.2183	1.2170	1.2189	1.2236
26	60	1	No	Major	1.1697	1.1682	1.1737	1.1653	1.1690	1.1692	1.1702	1.1712	1.1730	1.1684	1.1672	1.1682	1.1720
27	20	1	No	All	1.2968	1.2935	1.2918	1.2898		1.2971	1.2975	1.2981	1.2981	1.2954	1.2931	1.2931	1.2974
28	40	1	No	All	1.2239	1.2177	1.2236	1.2160		1.2193	1.2212	1.2223	1.2237	1.2178	1.2178	1.2191	1.2225
29	60	1	No	All	1.1735	1.1708	1.1739	1.1673		1.1739	1.1718	1.1726	1.1750	1.1710	1.1705	1.1702	1.1742
30	20	5	Yes	Major	1.1971	1.1975	1.1916	1.1901	1.1951	1.1997	1.2017	1.2020	1.1981	1.1991	1.2001	1.1932	1.1975
31	40	5	Yes	Major	1.0616	1.0644	1.0611	1.0569	1.0631	1.0656	1.0661	1.0685	1.0642	1.0647	1.0651	1.0597	1.0636
32	60	5	Yes	Major	0.9713	0.9715	0.9709	0.9637	0.9717	0.9731	0.9736	0.9752	0.9706	0.9721	0.9749	0.9661	0.9713
33	20	5	No	Major	1.2748	1.2710	1.2708	1.2667	1.2713	1.2744	1.2755	1.2765	1.2748	1.2723	1.2702	1.2699	1.2744
34	40	5	No	Major	1.1810	1.1780	1.1787	1.1745	1.1769	1.1801	1.1823	1.1832	1.1823	1.1781	1.1771	1.1775	1.1830
35	60	5	No	Major	1.1196	1.1205	1.1240	1.1158	1.1203	1.1229	1.1230	1.1240	1.1235	1.1206	1.1177	1.1186	1.1222
36	20	5	No	All	1.2735	1.2705	1.2717	1.2667		1.2748	1.2754	1.2765	1.2748	1.2721	1.2709	1.2699	1.2742
37	40	5	No	All	1.1829	1.1777	1.1810	1.1748		1.1811	1.1832	1.1833	1.1826	1.1799	1.1786	1.1778	1.1826
38	60	5	No	All	1.1242	1.1240	1.1293	1.1184		1.1250	1.1246	1.1258	1.1261	1.1239	1.1230	1.1212	1.1252

Table 3.2. Multiplication factors from participants (MOX composition B) (*cont.*)

Case #	Burn-up (GWd/te)	Cooling (years)	FPs	Actinides	Participant												
					14	15	16	17	18	19	20	21	22	23	24	25	26
20	0	0	N/A	Major	1.4137	1.4012	1.4161	1.4069	1.4103	1.4153	1.4080	1.4162	1.4156	1.4060	1.4194	1.4262	1.4162
21	20	1	Yes	Major	1.2236	1.2133	1.2221	1.2214	1.2190	1.2243	1.2186	1.2261	1.2218	1.2211	1.2275	1.2297	1.2221
22	40	1	Yes	Major	1.1137	1.1037	1.1107	1.1113	1.1079	1.1128	1.1101	1.1152	1.1105	1.1113	1.1143	1.1208	1.1106
23	60	1	Yes	Major	1.0332	1.0243	1.0323	1.0315	1.0290	1.0326	1.0331	1.0350	1.0322	1.0318	1.0351	1.0404	1.0322
24	20	1	No	Major	1.2940	1.2831	1.2918	1.2906	1.2884	1.2965	1.2920	1.2973	1.2914	1.2901	1.2978	1.3036	1.2918
25	40	1	No	Major	1.2175	1.2100	1.2160	1.2172	1.2127	1.2222	1.2214	1.2231	1.2158	1.2170	1.2211	1.2284	1.2160
26	60	1	No	Major	1.1649	1.1604	1.1665	1.1669	1.1623	1.1716	1.1709	1.1725	1.1663	1.1669	1.1705	1.1767	1.1668
27	20	1	No	All	1.2923	1.2831	1.2918		1.2884	1.2965	1.2935		1.2914		1.2967	1.3031	1.2918
28	40	1	No	All	1.2179	1.2102	1.2164		1.2130	1.2224	1.2220		1.2161		1.2222	1.2280	1.2164
29	60	1	No	All	1.1695	1.1624	1.1691		1.1645	1.1737	1.1757		1.1689		1.1722	1.1777	1.1694
30	20	5	Yes	Major	1.1977	1.1866	1.1958	1.1940	1.1924	1.1968	1.1924	1.1983	1.1955	1.1938	1.2009	1.2069	1.1958
31	40	5	Yes	Major	1.0644	1.0550	1.0624	1.0618	1.0596	1.0629	1.0622	1.0649	1.0623	1.0620	1.0668	1.0722	1.0623
32	60	5	Yes	Major	0.9713	0.9624	0.9707	0.9692	0.9676	0.9696	0.9680	0.9714	0.9707	0.9697	0.9738	0.9783	0.9706
33	20	5	No	Major	1.2709	1.2608	1.2699	1.2672	1.2662	1.2733	1.2697	1.2739	1.2695	1.2667	1.2753	1.2832	1.2699
34	40	5	No	Major	1.1789	1.1701	1.1766	1.1756	1.1731	1.1808	1.1813	1.1817	1.1764	1.1755	1.1823	1.1874	1.1766
35	60	5	No	Major	1.1215	1.1124	1.1189	1.1173	1.1147	1.1222	1.1258	1.1232	1.1187	1.1173	1.1238	1.1290	1.1192
36	20	5	No	All	1.2708	1.2608	1.2699		1.2662	1.2733	1.2728		1.2696		1.2758	1.2811	1.2699
37	40	5	No	All	1.1781	1.1704	1.1771		1.1734	1.1812	1.1799		1.1769		1.1831	1.1892	1.1771
38	60	5	No	All	1.1230	1.1149	1.1219		1.1173	1.1248	1.1271		1.1218		1.1248	1.1302	1.1222

Table 3.2. Multiplication factors from participants (MOX composition B) (*cont.*)

Case #	Burn-up (GWd/te)	Cooling (years)	FPs	Actinides	Participant													
					27	28	29	30	31	32	33	34	35	36	37	Mean	St dev	St dev/mean
20	0	0	N/A	Major	1.4180	1.4182	1.4112	1.4154	1.4146	1.4178	1.4146	1.4184	1.4111	1.4148	1.4110	**1.4141**	0.0049	3.4759E-03
21	20	1	Yes	Major	1.2239	1.2242	1.2200	1.2243	1.2239	1.2281	1.2279	1.2279	1.2223	1.2251	1.2213	**1.2236**	0.0034	2.7639E-03
22	40	1	Yes	Major	1.1123	1.1122	1.1089	1.1129	1.1129	1.1174	1.1172	1.1180	1.1121	1.1144	1.1122	**1.1128**	0.0033	2.9274E-03
23	60	1	Yes	Major	1.0337	1.0341	1.0300	1.0337	1.0322	1.0378	1.0378	1.0389	1.0328	1.0350	1.0328	**1.0335**	0.0033	3.1528E-03
24	20	1	No	Major	1.2937	1.2934	1.2895	1.2942	1.2934	1.2996	1.2978	1.2973	1.2923	1.2972	1.2931	**1.2941**	0.0037	2.8716E-03
25	40	1	No	Major	1.2176	1.2180	1.2140	1.2182	1.2172	1.2254	1.2244	1.2231	1.2184	1.2225	1.2170	**1.2193**	0.0038	3.0869E-03
26	60	1	No	Major	1.1678	1.1676	1.1633	1.1674	1.1675	1.1751	1.1747	1.1730	1.1674	1.1723	1.1668	**1.1690**	0.0036	3.0686E-03
27	20	1	No	All	1.2937	1.2937	1.2895	1.2941	1.2933	1.2996	1.2982	1.2973	1.2917	1.2966	1.2929	**1.2943**	0.0038	2.9275E-03
28	40	1	No	All	1.2180	1.2170	1.2142	1.2184	1.2176	1.2256	1.2247	1.2233	1.2177	1.2226	1.2182	**1.2196**	0.0039	3.1918E-03
29	60	1	No	All	1.1705	1.1700	1.1655	1.1696	1.1688	1.1775	1.1762	1.1750	1.1699	1.1742	1.1705	**1.1714**	0.0035	3.0240E-03
30	20	5	Yes	Major	1.1975	1.1971	1.1934	1.1976	1.1972	1.2009	1.1998	1.2007	1.1952	1.1976	1.1956	**1.1968**	0.0038	3.1454E-03
31	40	5	Yes	Major	1.0639	1.0641	1.0605	1.0643	1.0639	1.0678	1.0686	1.0683	1.0627	1.0639	1.0621	**1.0636**	0.0032	3.0417E-03
32	60	5	Yes	Major	0.9719	0.9722	0.9685	0.9719	0.9715	0.9747	0.9754	0.9756	0.9707	0.9714	0.9699	**0.9712**	0.0031	3.2128E-03
33	20	5	No	Major	1.2719	1.2725	1.2673	1.2719	1.2720	1.2769	1.2745	1.2745	1.2691	1.2740	1.2701	**1.2717**	0.0039	3.0548E-03
34	40	5	No	Major	1.1784	1.1780	1.1743	1.1785	1.1777	1.1846	1.1847	1.1823	1.1776	1.1817	1.1772	**1.1790**	0.0036	3.0229E-03
35	60	5	No	Major	1.1203	1.1195	1.1157	1.1197	1.1188	1.1260	1.1257	1.1239	1.1186	1.1225	1.1175	**1.1207**	0.0035	3.1366E-03
36	20	5	No	All	1.2720	1.2718	1.2673	1.2719	1.2703	1.2769	1.2759	1.2745	1.2693	1.2739	1.2697	**1.2720**	0.0038	2.9558E-03
37	40	5	No	All	1.1789	1.1785	1.1747	1.1788	1.1781	1.1849	1.1833	1.1826	1.1779	1.1821	1.1774	**1.1797**	0.0037	3.1284E-03
38	60	5	No	All	1.1234	1.1235	1.1183	1.1223	1.1217	1.1289	1.1278	1.1264	1.1213	1.1252	1.1218	**1.1236**	0.0034	2.9985E-03

Table 3.3. Multiplication factors from participants (MOX composition C)

Case #	Burn-up (GWd/te)	Cooling (years)	FPs	Actinides	Participant												
					1	2	3	4	5	6	7	8	9	10	11	12	13
39	0	0	N/A	Major	1.2007	1.1922	1.2038	1.1913	1.2035	1.1947	1.1967	1.1983	1.2004	1.1919	1.1956	1.1952	1.1980
40	20	1	Yes	Major	1.1118	1.1092	1.1170	1.1028	1.1168	1.1102	1.1102	1.1126	1.1116	1.1091	1.1123	1.1065	1.1114
41	40	1	Yes	Major	1.0616	1.0666	1.0687	1.0570	1.0704	1.0659	1.0653	1.0684	1.0656	1.0669	1.0683	1.0605	1.0668
42	60	1	Yes	Major	1.0263	1.0293	1.0319	1.0186	1.0302	1.0309	1.0285	1.0313	1.0270	1.0308	1.0335	1.0220	1.0298
43	20	1	Yes	All	1.1083	1.1079	1.1167	1.1026		1.1099	1.1096	1.1122	1.1114	1.1093	1.1119	1.1064	1.1121
44	40	1	Yes	All	1.0679	1.0723	1.0748	1.0605		1.0719	1.0685	1.0707	1.0692	1.0717	1.0724	1.0641	1.0694
45	60	1	Yes	All	1.0400	1.0428	1.0492	1.0299		1.0449	1.0358	1.0401	1.0385	1.0446	1.0463	1.0335	1.0393
46	20	1	No	Major	1.1649	1.1623	1.1705	1.1571	1.1683	1.1647	1.1638	1.1654	1.1662	1.1612	1.1620	1.1610	1.1658
47	40	1	No	Major	1.1483	1.1479	1.1557	1.1405	1.1510	1.1488	1.1473	1.1493	1.1497	1.1490	1.1472	1.1443	1.1502
48	60	1	No	Major	1.1381	1.1358	1.1437	1.1276	1.1368	1.1371	1.1341	1.1368	1.1367	1.1366	1.1344	1.1312	1.1389
49	20	1	No	All	1.1672	1.1613	1.1690	1.1567		1.1658	1.1631	1.1648	1.1658	1.1619	1.1612	1.1606	1.1651
50	40	1	No	All	1.1538	1.1528	1.1613	1.1432		1.1539	1.1499	1.1511	1.1524	1.1531	1.1495	1.1470	1.1541
51	60	1	No	All	1.1479	1.1499	1.1575	1.1375		1.1517	1.1424	1.1448	1.1468	1.1505	1.1452	1.1413	1.1496
52	20	5	Yes	Major	1.0562	1.0565	1.0590	1.0476	1.0604	1.0579	1.0566	1.0601	1.0564	1.0562	1.0570	1.0512	1.0547
53	40	5	Yes	Major	1.0033	1.0053	1.0084	0.9955	1.0068	1.0077	1.0069	1.0093	1.0041	1.0061	1.0081	0.9989	1.0048
54	60	5	Yes	Major	0.9597	0.9643	0.9648	0.9524	0.9637	0.9662	0.9640	0.9669	0.9605	0.9650	0.9676	0.9555	0.9626
55	20	5	Yes	All	1.0547	1.0570	1.0585	1.0478		1.0565	1.0578	1.0600	1.0566	1.0573	1.0578	1.0514	1.0566
56	40	5	Yes	All	1.0064	1.0132	1.0131	1.0001		1.0137	1.0086	1.0126	1.0088	1.0121	1.0146	1.0036	1.0111
57	60	5	Yes	All	0.9752	0.9787	0.9844	0.9656		0.9797	0.9739	0.9774	0.9740	0.9806	0.9797	0.9689	0.9757
58	20	5	No	Major	1.1136	1.1111	1.1158	1.1039	1.1138	1.1135	1.1123	1.1153	1.1131	1.1113	1.1106	1.1077	1.1150
59	40	5	No	Major	1.0933	1.0916	1.0989	1.0833	1.0922	1.0943	1.0926	1.0951	1.0925	1.0924	1.0884	1.0870	1.0908
60	60	5	No	Major	1.0755	1.0798	1.0835	1.0689	1.0762	1.0806	1.0786	1.0808	1.0779	1.0797	1.0764	1.0724	1.0778
61	20	5	No	All	1.1127	1.1116	1.1184	1.1039		1.1132	1.1123	1.1150	1.1131	1.1124	1.1107	1.1077	1.1129
62	40	5	No	All	1.0944	1.0985	1.1025	1.0873		1.1017	1.0962	1.0980	1.0965	1.0981	1.0931	1.0910	1.0957
63	60	5	No	All	1.0908	1.0957	1.1024	1.0812		1.0970	1.0886	1.0908	1.0905	1.0953	1.0907	1.0849	1.0933

Table 3.3. Multiplication factors from participants (MOX composition C) (*cont.*)

Case #	Burn-up (GWd/te)	Cooling (years)	FPs	Actinides	Participant												
					14	15	16	17	18	19	20	21	22	23	24	25	26
39	0	0	N/A	Major	1.1934	1.1827	1.1887	1.1986	1.1866	1.1973	1.2031	1.2032	1.1884	1.1985	1.1965	1.2014	1.1887
40	20	1	Yes	Major	1.1070	1.0973	1.1063	1.1123	1.1013	1.1089	1.1135	1.1193	1.1076	1.1137	1.1118	1.1154	1.1063
41	40	1	Yes	Major	1.0644	1.0521	1.0634	1.0659	1.0574	1.0630	1.0682	1.0727	1.0632	1.0659	1.0671	1.0689	1.0633
42	60	1	Yes	Major	1.0257	1.0140	1.0272	1.0270	1.0208	1.0247	1.0322	1.0341	1.0270	1.0271	1.0274	1.0332	1.0271
43	20	1	Yes	All	1.1081	1.0971	1.1068		1.1013	1.1087	1.1147		1.1080		1.1101	1.1144	1.1067
44	40	1	Yes	All	1.0681	1.0550	1.0684		1.0613	1.0665	1.0760		1.0681		1.0670	1.0722	1.0683
45	60	1	Yes	All	1.0413	1.0237	1.0408		1.0329	1.0361	1.0461		1.0406		1.0362	1.0413	1.0407
46	20	1	No	Major	1.1600	1.1497	1.1591	1.1645	1.1532	1.1633	1.1676	1.1715	1.1588	1.1643	1.1629	1.1683	1.1590
47	40	1	No	Major	1.1445	1.1333	1.1449	1.1470	1.1372	1.1469	1.1534	1.1559	1.1446	1.1468	1.1479	1.1523	1.1448
48	60	1	No	Major	1.1302	1.1206	1.1336	1.1330	1.1249	1.1343	1.1412	1.1430	1.1334	1.1329	1.1355	1.1386	1.1335
49	20	1	No	All	1.1611	1.1492	1.1594		1.1530	1.1629	1.1696		1.1591		1.1629	1.1677	1.1594
50	40	1	No	All	1.1488	1.1355	1.1497		1.1407	1.1495	1.1615		1.1494		1.1506	1.1543	1.1497
51	60	1	No	All	1.1419	1.1290	1.1471		1.1364	1.1443	1.1564		1.1468		1.1427	1.1486	1.1470
52	20	5	Yes	Major	1.0550	1.0436	1.0530	1.0559	1.0482	1.0537	1.0599	1.0616	1.0528	1.0528	1.0579	1.0606	1.0530
53	40	5	Yes	Major	1.0037	0.9921	1.0035	1.0034	0.9980	1.0015	1.0070	1.0101	1.0034	1.0034	1.0054	1.0105	1.0035
54	60	5	Yes	Major	0.9622	0.9491	0.9622	0.9601	0.9565	0.9585	0.9621	0.9666	0.9621	0.9603	0.9639	0.9671	0.9622
55	20	5	Yes	All	1.0545	1.0437	1.0537		1.0485	1.0539	1.0612		1.0534		1.0558	1.0607	1.0536
56	40	5	Yes	All	1.0074	0.9962	1.0093		1.0029	1.0062	1.0138		1.0092		1.0092	1.0140	1.0093
57	60	5	Yes	All	0.9761	0.9610	0.9773		0.9702	0.9718	0.9837		0.9771		0.9745	0.9780	0.9772
58	20	5	No	Major	1.1063	1.0982	1.1080	1.1099	1.1022	1.1102	1.1189	1.1174	1.1078	1.1078	1.1129	1.1174	1.1080
59	40	5	No	Major	1.0895	1.0778	1.0896	1.0883	1.0822	1.0896	1.0983	1.0977	1.0894	1.0894	1.0927	1.0986	1.0896
60	60	5	No	Major	1.0751	1.0636	1.0766	1.0730	1.0684	1.0756	1.0852	1.0833	1.0764	1.0729	1.0793	1.0837	1.0766
61	20	5	No	All	1.1094	1.0982	1.1086		1.1023	1.1102	1.1176		1.1084		1.1130	1.1193	1.1086
62	40	5	No	All	1.0940	1.0814	1.0953		1.0868	1.0937	1.1046		1.0951		1.0954	1.0997	1.0953
63	60	5	No	All	1.0880	1.0747	1.0918		1.0818	1.0880	1.1015		1.0916		1.0884	1.0934	1.0918

Table 3.3. Multiplication factors from participants (MOX composition C) (*cont.*)

Case #	Burn-up (GWd/te)	Cooling (years)	FPs	Actinides	Participant													
					27	28	29	30	31	32	33	34	35	36	37	Mean	St dev	St dev/mean
39	0	0	N/A	Major	1.1927	1.1911	1.1880	1.1948	1.1931	1.2011	1.2024	1.1986	1.1956	1.2008	1.1945	**1.1957**	0.0053	4.4363E-03
40	20	1	Yes	Major	1.1101	1.1091	1.1027	1.1090	1.1070	1.1149	1.1170	1.1133	1.1093	1.1120	1.1085	**1.1101**	0.0046	4.1534E-03
41	40	1	Yes	Major	1.0669	1.0665	1.0587	1.0646	1.0628	1.0699	1.0731	1.0687	1.0651	1.0661	1.0634	**1.0652**	0.0043	4.0091E-03
42	60	1	Yes	Major	1.0304	1.0299	1.0221	1.0277	1.0261	1.0322	1.0309	1.0310	1.0275	1.0288	1.0274	**1.0279**	0.0042	4.1204E-03
43	20	1	Yes	All	1.1105	1.1096	1.1027	1.1090	1.1080	1.1148	1.1162	1.1132	1.1095	1.1118	1.1097	**1.1094**	0.0042	3.8085E-03
44	40	1	Yes	All	1.0720	1.0713	1.0626	1.0687	1.0675	1.0740	1.0759	1.0718	1.0686	1.0697	1.0692	**1.0690**	0.0045	4.1820E-03
45	60	1	Yes	All	1.0443	1.0440	1.0342	1.0401	1.0383	1.0450	1.0436	1.0410	1.0400	1.0406	1.0395	**1.0399**	0.0051	4.9261E-03
46	20	1	No	Major	1.1630	1.1627	1.1546	1.1613	1.1591	1.1691	1.1702	1.1652	1.1621	1.1667	1.1614	**1.1630**	0.0048	4.0912E-03
47	40	1	No	Major	1.1485	1.1477	1.1386	1.1450	1.1437	1.1532	1.1543	1.1486	1.1459	1.1498	1.1449	**1.1473**	0.0048	4.1599E-03
48	60	1	No	Major	1.1368	1.1364	1.1263	1.1324	1.1306	1.1407	1.1383	1.1354	1.1339	1.1367	1.1326	**1.1347**	0.0047	4.1787E-03
49	20	1	No	All	1.1634	1.1625	1.1544	1.1611	1.1593	1.1688	1.1690	1.1649	1.1618	1.1664	1.1607	**1.1624**	0.0047	4.0236E-03
50	40	1	No	All	1.1535	1.1526	1.1421	1.1487	1.1471	1.1570	1.1595	1.1512	1.1498	1.1532	1.1494	**1.1508**	0.0054	4.6725E-03
51	60	1	No	All	1.1506	1.1497	1.1378	1.1442	1.1423	1.1533	1.1501	1.1445	1.1450	1.1488	1.1443	**1.1459**	0.0058	5.0199E-03
52	20	5	Yes	Major	1.0567	1.0569	1.0495	1.0556	1.0539	1.0604	1.0631	1.0630	1.0550	1.0566	1.0557	**1.0558**	0.0042	4.0036E-03
53	40	5	Yes	Major	1.0069	1.0067	0.9993	1.0050	1.0039	1.0088	1.0115	1.0073	1.0041	1.0051	1.0040	**1.0047**	0.0040	4.0285E-03
54	60	5	Yes	Major	0.9653	0.9656	0.9578	0.9630	0.9617	0.9659	0.9679	0.9646	0.9621	0.9622	0.9613	**0.9623**	0.0041	4.2706E-03
55	20	5	Yes	All	1.0574	1.0575	1.0498	1.0560	1.0546	1.0606	1.0639	1.0632	1.0557	1.0568	1.0555	**1.0558**	0.0043	4.0417E-03
56	40	5	Yes	All	1.0129	1.0118	1.0042	1.0100	1.0085	1.0138	1.0164	1.0116	1.0092	1.0100	1.0086	**1.0095**	0.0044	4.3487E-03
57	60	5	Yes	All	0.9806	0.9799	0.9715	0.9770	0.9759	0.9805	0.9816	0.9766	0.9758	0.9755	0.9752	**0.9761**	0.0048	4.9631E-03
58	20	5	No	Major	1.1120	1.1114	1.1036	1.1102	1.1087	1.1167	1.1180	1.1125	1.1103	1.1136	1.1101	**1.1111**	0.0046	4.1109E-03
59	40	5	No	Major	1.0934	1.0930	1.0836	1.0900	1.0890	1.0965	1.0972	1.0918	1.0897	1.0925	1.0896	**1.0911**	0.0046	4.2128E-03
60	60	5	No	Major	1.0800	1.0794	1.0697	1.0757	1.0739	1.0824	1.0812	1.0770	1.0754	1.0781	1.0742	**1.0769**	0.0046	4.2857E-03
61	20	5	No	All	1.1127	1.1125	1.1038	1.1104	1.1090	1.1169	1.1183	1.1126	1.1103	1.1135	1.1090	**1.1112**	0.0046	4.1816E-03
62	40	5	No	All	1.0993	1.0991	1.0882	1.0947	1.0935	1.1015	1.1022	1.0957	1.0946	1.0977	1.0938	**1.0956**	0.0049	4.4460E-03
63	60	5	No	All	1.0955	1.0950	1.0832	1.0895	1.0875	1.0971	1.0968	1.0885	1.0891	1.0924	1.0891	**1.0908**	0.0057	5.2289E-03

Figure 3.1. Neutron multiplication factor against case number

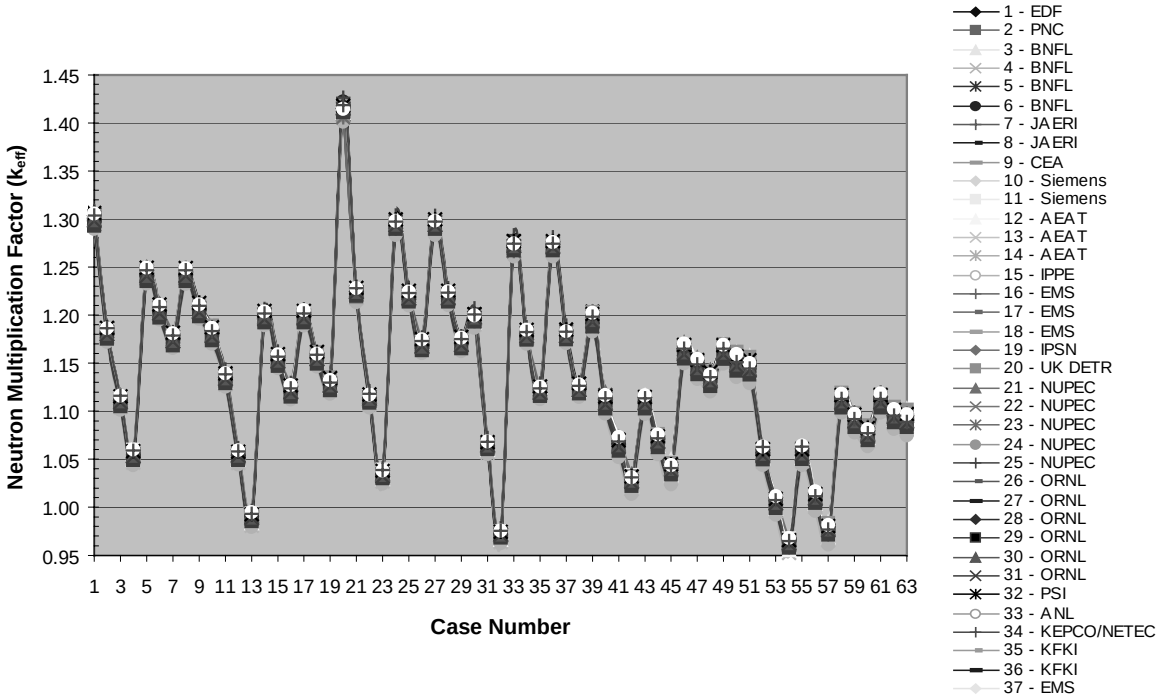

4. Analysis of results

In order to examine the contributions from the participants more rigorously, the standard deviation for each benchmark case was calculated and divided by the average k_{eff} for that case. These results are graphically presented in Figure 4.1.

Figure 4.1. Standard deviation/average k_{eff} against case number

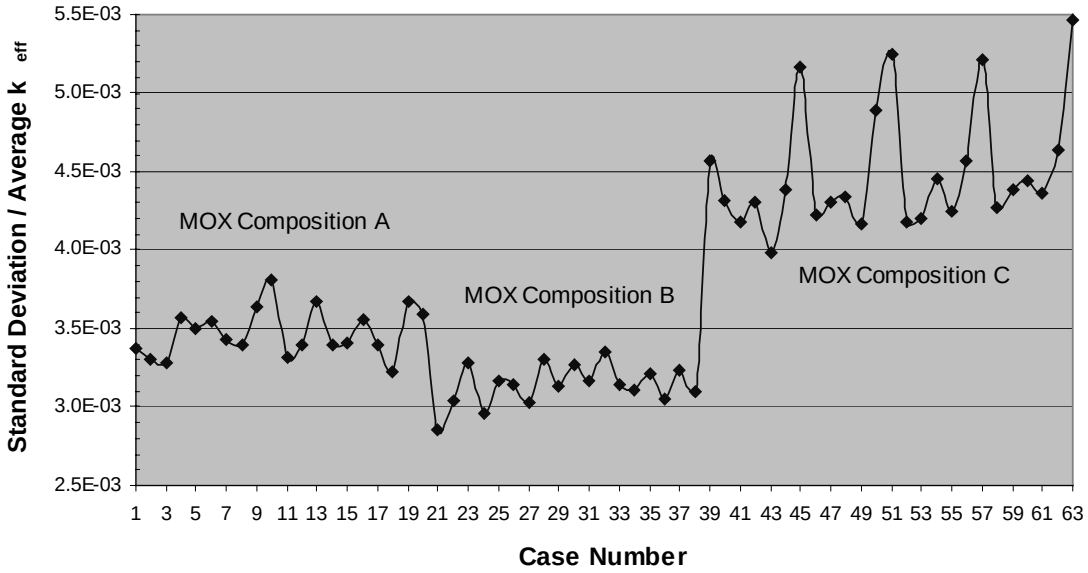

It can be seen from the results presented in Figure 4.1 that three distinct groups have emerged. These groups correspond to the different MOX compositions used in the benchmark, MOX compositions A, B and C.

- MOX composition A – 1st generation MOX.
- MOX composition B – MOX produced from the disposition of weapons.
- MOX composition C – Later-generation MOX.

Across Cases 1-19 and 20-38 (MOX compositions A and B, respectively), it can be seen that the spread of results is approximately constant. This implies that the spread in the results is independent of burn-up for these two MOX compositions.

It can also be seen that the baseline spread in the MOX composition C results, Cases 39-63, is higher than for either MOX compositions A or B. This shall be analysed further in Section 4.1.

From the MOX composition C results, it can be seen that there are peaks in the spread of the participants' results. These peaks correspond to Cases 45, 51, 57 and 63. From examination of the fuel inventory for these cases, it is seen that these peaks correspond to the cases where high concentrations of curium were modelled in the spent fuel inventory composition. It is therefore considered likely that discrepancies in the curium nuclear data between the various participants have caused the peaks in the spread of the results for MOX composition C. This shall be analysed further in Section 4.2.

The graph presented in Figure 4.2 shows the percentage difference relative to the mean for the MOX composition C results.

Figure 4.2. Spread of results for MOX composition C (multiple MOX recycle)

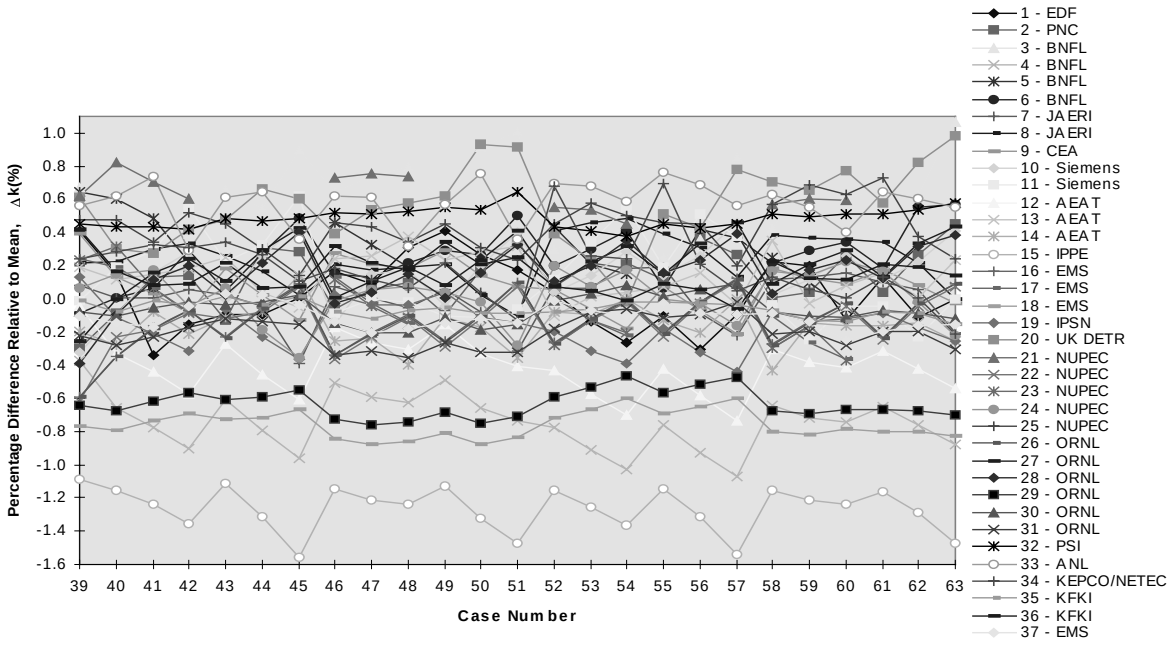

The main point of note from Figure 4.2 is that there is a 2.5% spread in the results around the mean value, even for fresh MOX fuel. This spread in the results is maintained across the range of burn-ups, cooling times and spent fuel representations considered in the Phase IV-A benchmark exercise. Similar trends were seen for MOX compositions A and B (first generation MOX and MOX derived from the disposition of weapons), although the spread in the results is reduced to 2.0%.

The participants of this benchmark have used a variety of criticality codes, nuclear data sources, energy group structures and modelling techniques to perform the calculations. One of these modelling techniques (Wigner-Sietz) is considered to be inadequate for the reactivity prediction of MOX fuel, as discussed in Section 4.5. If the contributions that have used this method and also those contributions that have used a group structure with less than 80 energy groups, the spread in the results for MOX composition C, multiple recycle MOX reduces to about 1%. A reasonable number of results are still being used for this analysis and it is shown that even when different methods and data are used for the benchmark, consistent results are produced.

It is difficult to discern a trend in the results presented in Figure 4.2. Consequently, it was decided to produce two further graphs that separated the results into two sets. As 14 contributions used the criticality code SCALE, it was considered appropriate to split the results into SCALE and non-SCALE contributions. These separated contributions are presented in Figures 4.3 and 4.4 respectively.

It can be seen from the SCALE results presented in Figure 4.3 that there is still a large spread in the results. The SCALE nuclear data libraries used have a 27, 44 or 238 energy group structure. However, the spread in the results may also be due to the method of processing the data (the energy spectra used to collapse the cross-section data into groups). For example, the 44 energy group library was collapsed using a PWR 17×17 UOX fuel spectrum, whereas the 238 energy group library was collapsed from point data using a more general energy spectrum. Also, the SCALE results that used the 238 energy group library and the Monte Carlo (CSAS25) route are much more consistent with the average results of the participants.

It can be seen from close examination of the data presented in Table 3.3 (graphically presented in Figure 4.4) that contribution 3, BNFL, consistently overpredicts the mean of the other non-SCALE participants' results. This participant used the MONK7B code with the UKNDL nuclear data library. Contribution 13, AEAT, was also performed with MONK7B but with the JEF-2.2 nuclear data library. It can also be seen from this table that this contribution predicts k_{eff} values close to the mean of the other results.

Figure 4.3. Spread of SCALE results for MOX composition C (multiple MOX recycle)

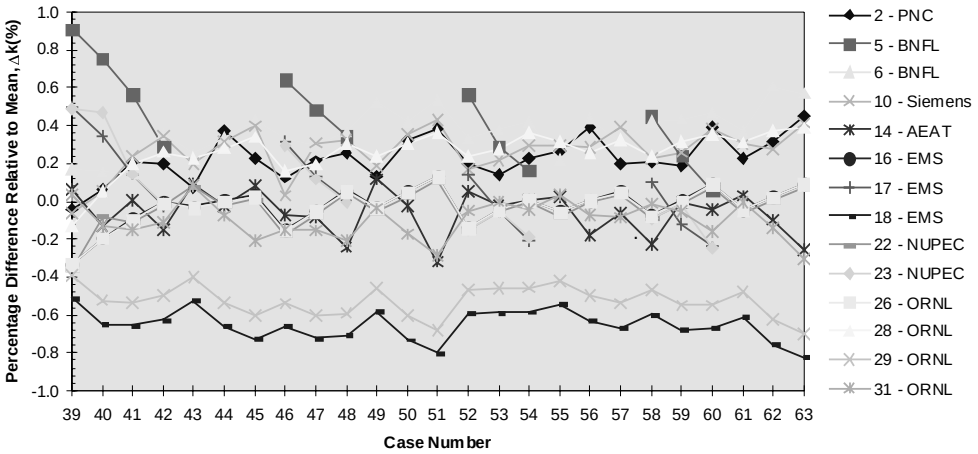

Figure 4.4. Spread of non-SCALE results for MOX composition C (multiple MOX recycle)

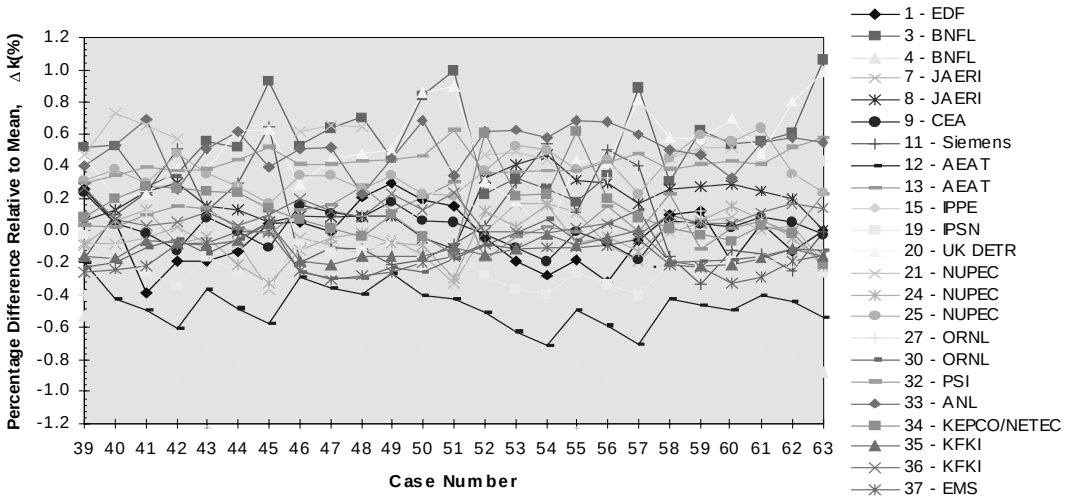

According to Ref. [7], the United Kingdom Nuclear Data Library (UKNDL) was first collated in 1964 for 8 220 energy groups. Further revisions and new evaluations led to the 1973 edition. In the early 1980s, work began on processing the 1980 edition of the UKNDL into a form suitable for Monte Carlo calculations. This involved the use of a code called MOULD to produce the Monte Carlo data from the UKNDL tabulations. During the course of this work further improvements were made to the UKNDL resulting in the 1981 edition.

Some data in the UKNDL continuous energy database have been taken from the JEF-2 library; for example data used for the thermalisation treatment, as well as fission product and higher actinide nuclide data not present in UKNDL. Contribution 3, BNFL, used this hybrid UKNDL/JEF-2.2 nuclear data library.

More recently a predominantly JEF-2 based library (Joint Evaluated File) for MONK in 13 193 energy groups has been produced. This data is of a better quality than the UKNDL and comparable with ENDF/B-VI. The JEF-2 based library is now being recommended in preference to the UKNDL based library for criticality applications in the UK. Contribution 13, AEAT, used the JEF-2.2 nuclear data library.

As the same criticality code, MONK, was used for both contributions 3 and 13, the discrepancy in the k_{eff} results was due solely to the differences in the nuclear data libraries used. It was therefore considered appropriate to perform further calculations using these two nuclear data libraries so as to try to identify the particular nuclides that cause the discrepancy in the k_{eff} results between contributions 3 and 13.

Discrepancies in the nuclear data between contributions 3 and 13 may indicate which nuclides are responsible for the discrepancies in the k_{eff} results for all the contributions.

4.1 Baseline spread analysis

The data presented in Figure 4.1 indicates that the spread in the results for the three MOX compositions does not appear to be dependent on the burn-up of the fuel (neglecting the results that include curium). It is therefore considered that any further analysis on the baseline spread of the results can be performed using the fresh fuel case for MOX composition C, Case 39.

The fresh fuel inventory for MOX composition C consists only of the uranium and plutonium nuclides. As stated earlier in Section 4, it can be seen from Figure 4.1 that the baseline spread for the MOX composition C results, Cases 39-63, is higher than for either MOX composition A or B. The spread in the results must therefore be due to at least one of the uranium or plutonium nuclides.

In order to try to identify which of the uranium or plutonium nuclides may be causing the spread in the fresh fuel cases, Case 39, the fresh fuel case for MOX composition C, was repeated with the MONK code using both the UKNDL and JEF-2.2 data libraries. As the MONK7B criticality code has been superseded by MONK8A, a cross-check calculation was initially carried out which confirmed that the latest version of the code produces a statistically similar k_{eff} result to the previous version.

It is considered that removing a particular uranium or plutonium nuclide from the base case model, Case 39, should produce a similar reactivity worth when using either the UKNDL or JEF-2.2 nuclear data library. If it does not and a significantly different reactivity worth is calculated, this may indicate that differences in the nuclear data for this particular nuclide could be contributing to the discrepancies in k_{eff} between these two contributions.

Each of the uranium and plutonium isotopes was removed in turn from the base case model and the new neutron multiplication factor for the system was calculated. The calculations were run three times each down to a standard deviation (σ) of 0.0005. This equates to a reactivity change (Δk) of approximately 50 pcm when k_{eff} is close to unity.

The reactivity worth of removing each of the uranium and plutonium isotopes was calculated using the formula:

$$\text{Reactivity Worth (pcm)} = 10^5.\ln(k_{ref}/k_i)$$

Where k_{ref} is the k_{eff} for the base case model, k_i is the k_{eff} of the system without the nuclide and pcm is per cent milli. The results produced are presented in Table 4.1.1.

Table 4.1.1. Reactivity worth of nuclides from fresh fuel case MOX composition C (Case 39) using the nuclear data libraries UKNDL and JEF-2.2

Nuclide	Reactivity worth using UKNDL	Reactivity worth using JEF-2.2	Difference in reactivity worth
^{234}U	-8 pcm	17 pcm	25 pcm
^{235}U	606 pcm	577 pcm	29 pcm
^{238}U	-14 254 pcm	-15 245 pcm	992 pcm
^{238}Pu	-1 017 pcm	-1 431 pcm	414 pcm
^{239}Pu	26 920 pcm	28 173 pcm	1 252 pcm
^{240}Pu	-21 558 pcm	-21 855 pcm	297 pcm
^{241}Pu	10 347 pcm	10 508 pcm	161 pcm
^{242}Pu	-3 020 pcm	-3 155 pcm	135 pcm

Case 39 using the UKNDL nuclear data library and the MONK8A code gave a k_{eff} = 1.2035. Case 39 using the JEF-2.2 nuclear data library and the MONK8A code gave a k_{eff} = 1.2000.

A positive value for the reactivity worth indicates that the k_{eff} of the system would increase if this nuclide were added to the fuel inventory. Conversely, a negative value for the reactivity worth indicates that the k_{eff} of the system would decrease if this nuclide were added to the fuel inventory.

The reactivity worth for each of the nuclides was calculated by completely removing them in turn from the fuel inventory. As ^{238}U accounts for approximately 91.8 w/o of the heavy metal mass in the fuel, changes in the reactivity of the model could be due to nuclear data errors in the nuclides that are left, and not data errors in the ^{238}U nuclide that was removed. It is therefore considered that this method cannot be used for accurately calculating the reactivity worth of the ^{238}U nuclide.

It can be seen that the difference in the reactivity worth calculated for the ^{239}Pu nuclide between the UKNDL and JEF-2.2 nuclear data libraries is larger than any of the other uranium or plutonium nuclides. Examination of the fresh fuel MOX composition C number densities (Case 39) shows that MOX composition C has a lower ^{239}Pu concentration than either of MOX compositions A or B. It is therefore considered unlikely that these two nuclides contribute to the large spread in the baseline results for MOX composition C.

It can be seen from the above table that the two nuclear data libraries, UKNDL and JEF-2.2, produce a very low value for the reactivity worth for the ^{234}U nuclide. As the standard deviation in these calculations is approximately 50 pcm, it is considered that this nuclide is not the cause for the discrepancies in k_{eff} between contributions 3 and 13.

The difference in the reactivity worth calculated using the two nuclear data libraries for the ^{235}U nuclides is also quite low. It is therefore considered that this nuclide is not the cause for the discrepancy in k_{eff} between contributions 3 and 13.

From the results presented in Table 4.1.1, it can be seen that the difference in the reactivity worth calculated for the ^{238}Pu nuclide is quite large using the UKNDL and JEF-2.2 nuclear data libraries. This discrepancy is equivalent to a Δk of 0.4% when the k_{eff} of the model is close to unity and it could be a contributing factor in the k_{eff} discrepancy between contributions 3 and 13. However, it is likely that this discrepancy is due to an improvement in the ^{238}Pu capture cross-section over time as it dates back to the 1960s for the UKNDL and from the 1980s for the JEF-2.2 nuclear data library.

The differences in the reactivity worth for the ^{240}Pu, ^{241}Pu and ^{242}Pu nuclides between the two nuclear data libraries are above the 50 pcm standard deviation threshold. It is therefore possible that these three nuclides could contribute to the discrepancy in k_{eff} between contributions 3 and 13.

4.2 Curium analysis

As stated earlier in Section 4, it is considered that the peaks in the spread of the MOX composition C results, presented in Figure 4.1, are due to the addition of the curium isotopes (^{242}Cm, ^{243}Cm, ^{244}Cm or ^{245}Cm) into the spent fuel inventory of the model.

From further examination of the data, it can be seen that the peaks in the spread of the MOX composition C results occurs for cooling times of both one and five years. This implies that the large spread in the results between the various participants can only be due to long-lived curium nuclides. Hence, the ^{242}Cm nuclide, which has a relatively short half-life (163 days), would decay significantly over a five-year cooling period and would not be the cause of the large spread in the results seen in Figure 4.1. Further analysis will therefore concentrate only on the nuclides ^{243}Cm, ^{244}Cm and ^{245}Cm.

The base case calculation chosen was Case 63, as it can be seen from Figure 4.1 that this case produced the largest spread in the participants' results. Case 63 included all the major actinides, including curium, but excluded the fission products. The fuel was burnt up to 60 GWd/teHM and cooled for five years.

As above, the calculations were performed using the two nuclear data libraries, UKNDL and JEF-2.2, with the MONK8A code. The results produced are presented in Table 4.2.1.

Table 4.2.1. Reactivity worth of nuclides from the high curium inventory case (Case 63) using the nuclear data libraries UKNDL and JEF-2.2

Nuclide	Reactivity worth using UKNDL	Reactivity worth using JEF-2.2	Difference in reactivity worth
^{243}Cm	67 pcm	31 pcm	36 pcm
^{244}Cm	-314 pcm	-505 pcm	191 pcm
^{245}Cm	2 069 pcm	1 820 pcm	249 pcm

Case 63 using the UKNDL nuclear data library and the MONK8A code gave a k_{eff} = 1.1020. Case 63 using the JEF-2.2 nuclear data library and the MONK8A code gave a k_{eff} = 1.0921.

As in Table 4.1.1, a positive value for the reactivity worth indicates that the k_{eff} of the system would increase if this nuclide were added to the fuel inventory. Conversely, a negative value for the reactivity worth indicates that the k_{eff} of the system would decrease if this nuclide were added to the fuel inventory.

It can be seen from the results presented in Table 4.2.1 that the reactivity worths calculated for the ^{243}Cm nuclide using the nuclear data libraries UKNDL and JEF-2.2 are statistically indistinguishable. However, relatively large discrepancies are seen for the reactivity worths calculated for both the ^{244}Cm and ^{245}Cm nuclides. It is therefore considered likely that either of these two nuclides could be the cause of the k_{eff} discrepancy between contributions 3 and 13 for Case 63 and potentially the cause of the peaks in the spread of the MOX composition C results seen in Figure 4.1.

Figure 4.2.1 indicates the effect of including the curium isotopes in the reactivity calculation for the three MOX fuel cases. The impact of curium is clearly dependent upon the quality of the initial plutonium vector. For the multiple recycle MOX fuel, Case C, the positive reactivity effect of the curium isotopes is of the order of 1 000 pcm at a burn-up of 60 GWd/teHM. The majority of this reactivity effect is associated with the build-up of the isotope ^{245}Cm, which is not compensated for by the absorber ^{244}Cm. This suggests a need to confirm the adequacy of spent fuel representations for spent MOX fuel.

Figure 4.2.1. Effect of curium inclusion on mean result for all MOX cases, no fission products, one year cooling

Cases 1, 5-10, 20, 24-29, 39, 46-51

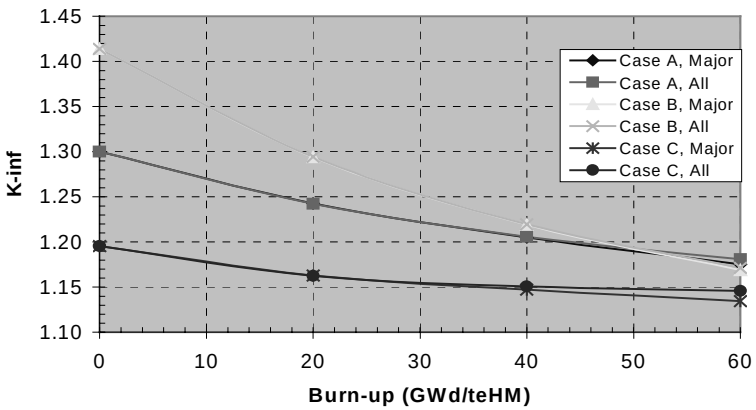

4.3 Statistical analysis of participants' results

A statistical analysis of the participants' results was carried out. For each benchmark case, the results were grouped by the percentage that they deviated from the mean. A representative sample of the bar chart graphs plotted (Cases 1, 39 and 63) are presented in Figures 4.3.1, 4.3.2 and 4.3.3, respectively.

Figure 4.3.1. Phase IV-A burn-up credit benchmark Case 1

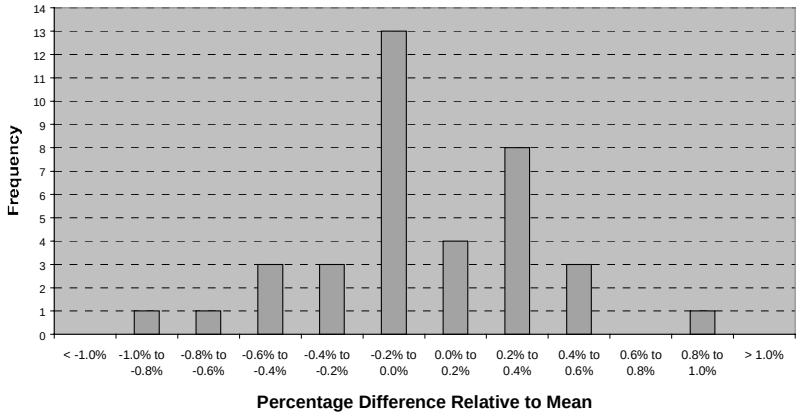

Figure 4.3.2. Phase IV-A burn-up credit benchmark Case 39

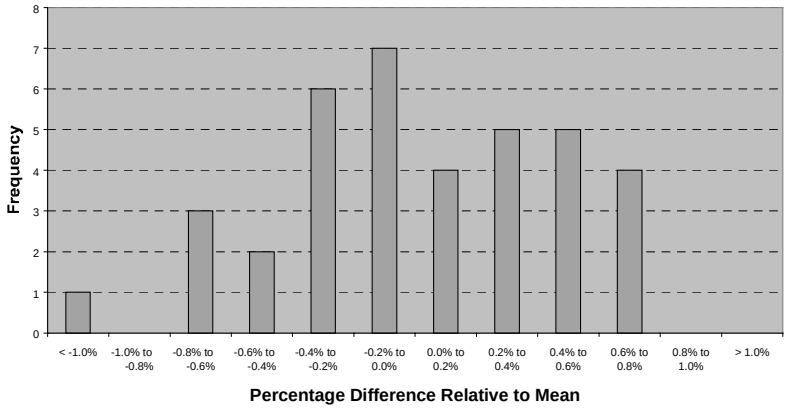

Figure 4.3.3. Phase IV-A burn-up credit benchmark Case 63

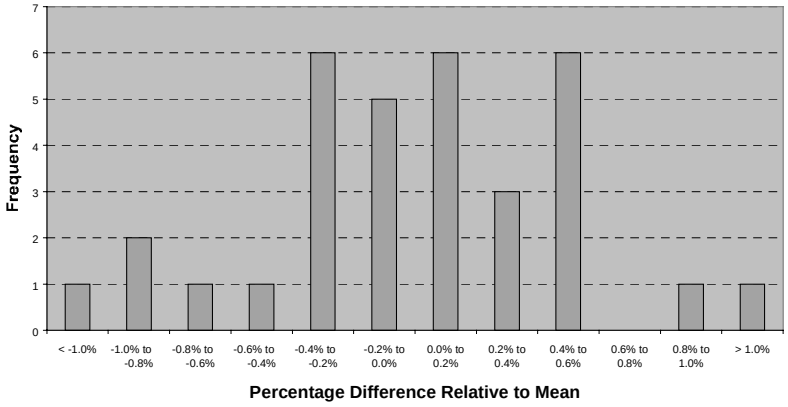

For MOX compositions A and B (Cases 1 to 38), the statistical analysis produced graphs similar to the graph plotted for Case 1, presented in Figure 4.3.1, i.e. a normal distribution. A normal distribution is expected for a random scattering of values around the mean.

However, it was seen for the MOX composition C cases (Cases 39 to 63) that the statistical analysis did not produce a normal distribution. This indicates that the participants' results for MOX composition C, presented in Figures 4.3.2 and 4.3.3, are not scattered randomly around the mean.

4.4 Analysis of extra contributions from the benchmark participants

It was highlighted in Sections 4.1 and 4.2 that discrepancies in the nuclear data libraries for the nuclides ^{238}Pu, ^{244}Cm and ^{245}Cm may be the cause for the differences in the k_{eff} results between contributions 3 and 13. It is also possible that these nuclides could be the cause for the large spread in results for all the participants' contributions.

In order to test whether this hypothesis is correct, a request was sent out to the burn-up credit group for the participants of the Phase IV-A Benchmark to repeat Cases 39 and 63, but with the following nuclides removed: ^{238}Pu, ^{244}Cm and ^{245}Cm. The participants were also requested to remove the ^{242}Pu nuclide from their calculations as it was initially thought that this nuclide was responsible for the large spread in the baseline results in Figure 4.1. The reactivity worth results calculated by the participants who took part in this exercise are presented in Table 4.4.1.

Table 4.4.1. Reactivity worth for the nuclides of interest calculated by a selection of the participants

Contribution	Reactivity worth (Case 39)		Reactivity worth (Case 63)	
	^{238}Pu	^{242}Pu	^{244}Cm	^{245}Cm
3 – MONK8A, point group, UKNDL (DTLR)	-1 017 pcm	-3 020 pcm	-314 pcm	2 069 pcm
9 – APOLLO2, 172 group, JEF-2.2 (CEA)	-1 417 pcm	-3 157 pcm	-625 pcm	1 764 pcm
13 – MONK8A, point group, JEF-2.2 (DTLR)	-1 431 pcm	-3 155 pcm	-505 pcm	1 820 pcm
16 – XSDRNPM, 44 group, ENDF/B-V (EMS)	-1 417 pcm	-3 148 pcm	-300 pcm	1 669 pcm
18 – XSDRNPM, 238 group, ENDF/B-V (EMS)	-1 421 pcm	-3 276 pcm	-442 pcm	1 662 pcm
26 – XSDRNPM, 44 group, ENDF/B-V (ORNL)	-1 418 pcm	-3 148 pcm	-300 pcm	1 670 pcm
32 – BOXER, 70 group, JEF-1 (PSI)	-1 410 pcm	-3 178 pcm	-515 pcm	1 841 pcm
37 – MCNP4C2, point group, ENDF/B-VI (EMS)	-1 446 pcm	-3 250 pcm	-441 pcm	1 543 pcm

Analysis of these reactivity worth results indicates that there is a large discrepancy with the nuclear data associated with the ^{244}Cm nuclide and to a lesser extent, the ^{245}Cm nuclide. However, there does not appear to be a significant discrepancy with the predicted reactivity worth of the ^{238}Pu nuclide. In order to determine whether the ^{238}Pu nuclide is responsible for the large baseline spread in the MOX composition C results, it is likely that further data is required from the remaining participants of the Phase IV-A Burn-up Credit Benchmark.

^{242}Pu self-shielding can become important for MOX fuel with highly degraded plutonium. However, it can be seen from the above table that the discrepancies between the reactivity worths calculated by the participants for the ^{242}Pu nuclide are not significant. This would suggest that each of the participants have used a nuclear data library with a sufficient number of energy groups to adequately model the ^{242}Pu thermal resonances. However, in order to determine whether all the participants that took part in the Phase IV-A benchmark have adequately modelled ^{242}Pu self-shielding, further data is required from the remaining participants.

4.5 Studies based on the Phase IV-A Burn-up Credit Benchmark

Two of the contributors to the benchmark have assessed the impact of the Wigner-Seitz approximation in modelling the MOX pin cell geometry, the reports of which are included in Appendices III and IV.

The Wigner-Seitz approximation uses a cylindrical outer boundary with white boundary conditions to replace the square boundary associated with a pin in a square lattice. Whilst this approximation has previously been shown to be acceptable for UO_2 pin cell calculations, it can be seen from the reports presented in Appendices III and IV that this approximation for MOX fuels introduces a reactivity error of the order of 500 pcm. These reports also highlight the fact that using nuclear data libraries with an insufficient number of groups may not adequately model the low energy resonances of plutonium.

The report presented in Appendix IV includes results using MCNP4C2 with ENDF/B-VI.5 and other nuclear cross-section data sets. Although submitted after the deadline for inclusion in the main report, this information may be useful for the reader.

5. Conclusion

The OECD/NEA Expert Group on Burn-up Credit Criticality Safety has produced this benchmark with the intention of undertaking an initial investigation into the reactivity effects observed with MOX fuel for combinations of the computer codes and data libraries currently being used around the world. The exercise was based upon the calculation of infinite PWR fuel pin cell reactivity for fresh and irradiated MOX fuels, using isotopic number densities provided by the benchmark co-ordinators.

In total, 37 contributions were submitted to the Phase IV-A benchmark exercise, from 17 different companies/organisations in 10 countries around the world. The participants were asked to perform 63 separate reactivity calculations covering three different initial MOX compositions, with a range of burn-ups, cooling times and fuel representations.

Analysis of the contributions for this benchmark has shown that there is a spread in the k_{eff} results of between 2.0-2.5% about the mean, depending on the MOX composition. This spread does not appear to be dependent on the burn-up of the fuel (neglecting the results that include curium). Consequently, the spread in the results for the fresh MOX fuel is just as large as that for the irradiated fuel.

The analysis has also shown that the calculations that include the curium isotopes give rise to a larger spread in the results than those calculations with the curium removed. It is considered that discrepancies in the nuclear data for the ^{244}Cm and ^{245}Cm nuclides could be the cause for the larger spread in the participants' k_{eff} results when curium is included in the fuel composition.

The addition of the curium isotopes into the fuel inventory also leads to an increase in the reactivity of the system of the order of 1 000 ppm. This is seen to occur for MOX fuel only and not UOX fuel. It is therefore recommended that the curium isotopes be included in the spent fuel composition of MOX fuel.

Although the Wigner-Seitz approximation has previously been shown to be acceptable for UO_2 pin cell calculations, it can be seen from the reports presented in Appendices III and IV that this approximation for MOX fuels introduces a reactivity error of the order of 500 pcm. It is therefore recommended that the Wigner-Seitz approximation not be used for MOX fuel.

Acknowledgements

The authors would like to thank the participants of this international benchmark study for their contributions and also the peer reviewers, H. Okuno, D. Mennerdahl, B. Roque and C.J. Dean for their invaluable comments.

REFERENCES

[1] Makoto Takano, "Burn-up Credit Criticality Benchmark Final Results of Phase 1A, Infinite Array of PWR Pin Cells", JAERI-M-94-003, NEA/NSC/DOC(1993)22, January 1994.

[2] M.D. DeHart, M.C. Brady, C.V. Parks, "OECD/NEA Burn-up Credit Calculational Criticality Benchmark Phase-IB, Isotopic Prediction: Final Report", ORNL-6901, NEA/NSC/DOC(1996)6, June 1996.

[3] M. Takano, H. Okuno "OECD/NEA Burn-up Credit Criticality Benchmark: Results of Phase IIA, PWR Spent Fuel Rods Effect of Axial Burn-up Profile", JAERI-Research 96-003, NEA/NSC/DOC(1996)1, February 1996.

[4] A. Nouri, "Burn-up Credit Criticality Benchmark Analysis of Phase II-B Results: Conceptual PWR Spent Fuel Transportation Cask", IPSN/98-05, NEA/NSC/DOC(1998)1, May 1998.

[5] H. Okuno, Y. Naito, Y. Ando, "OECD/NEA Burn-up Credit Criticality Benchmark Phase III-A, Criticality Calculations of BWR Spent Fuel Assemblies in Storage and Transport", JAERI-Research 2000-041, NEA/NSC/DOC(2000)12, September 2000.

[6] H. Okuno, Y. Naito, K. Suyama, "OECD/NEA Burn-up Credit Criticality Benchmark Phase III-B: Burn-up Calculations of BWR Spent Fuel Assemblies in Storage and Transport", JAERI-Research 2002-001, NEA/NSC/DOC(2002)2, February 2002.

[7] "MONK, A Monte Carlo Program for Nuclear Criticality Safety and Reactor Physics Analyses", ANSWERS/MONK(98)6, Issue 3, User Guide for Version 8, The ANSWERS Software Service, June 2001.

Appendix I

PROBLEM SPECIFICATION FOR THE OECD/NEA NSC BURN-UP CREDIT BENCHMARK PHASE IV-A: MIXED OXIDE (MOX) FUELS

Russell L. Bowden, Peter R. Thorne
Safety & Environmental Risk Management
Research & Technology
British Nuclear Fuels

1. Introduction

Since 1991, the criticality working group of the NEA NSC (formerly the NEA CRP) has been investigating the methods and data associated with the calculation of burn-up credit in criticality safety assessments. During this period, consideration has been given to uranium oxide fuels in both pressurised water and boiling water reactors (PWRs and BWRs). These benchmark exercises, denoted as Phases I to III, have covered the calculation of fuel inventory and the calculation of reactivity in storage array and transport flask configurations. The international consensus approach to the benchmarks adopted by the working group generates a great deal of confidence in the assessment methods. Participation in these exercises has produced useful data and a deeper understanding of the issues associated with the calculation of burn-up credit.

The next challenge for the burn-up credit method lies in its application to mixed oxide (MOX) fuels, i.e. fuel containing a mixture of uranium and plutonium oxides. A comprehensive MOX benchmark study would contain all of the elements of the previous phases, but with the added difficulties associated with the non-unique specification of MOX fuels and the manner in which they would be utilised within existing thermal reactor designs. The definition of a universally attractive benchmark exercise is further complicated by the different incentives for adopting a MOX fuel strategy amongst the member countries of the group participants.

Experience from the earlier benchmark exercises has shown that the first step in any benchmark programme must not be overly ambitious if it is to succeed in establishing some common ground between the participants. In recognition of this, it is proposed that the initial MOX burn-up credit benchmark, denoted as Phase IV-A, should be centred upon a simplified MOX fuel configuration.

The Phase IV-A benchmark exercise concerns the calculation of infinite PWR fuel pin cell reactivity for fresh and irradiated MOX fuels. The fuel compositions have been derived by the benchmark co-ordinators, BNFL, using the WIMS7 reactor lattice code. The nuclear data was provided by the 172-group WIMS “1996” nuclear data set, which is based upon JEF-2.2 evaluations. These calculations used a simplified MOX only representation of the core, and irradiated the fuel in a single cycle at a power of 35 MW/teHM, with a constant boron loading of 500 ppm in the core coolant. A comprehensive description of the calculation method adopted can be found in Ref. [1].

2. Parameters and case numbers

The neutron multiplication factor is required for a total of 63 cases, covering various combinations of initial MOX fuel composition, burn-up, cooling and spent fuel representation (i.e. "actinide only" or "fission product" burn-up credit). The selected parameters and case numbers are shown in Table 1.

In the context of this benchmark exercise, the term "major actinides" is taken to represent the following nuclides:

^{234}U, ^{235}U, ^{236}U, ^{238}U, ^{238}Pu, ^{239}Pu, ^{240}Pu, ^{241}Pu, ^{242}Pu, ^{237}Np, ^{241}Am and ^{243}Am

consistent with previous benchmark problems.

The fission products considered in this exercise are the 15 major fission product absorbers addressed in previous benchmarks, namely:

^{95}Mo, ^{99}Tc, ^{101}Ru, ^{103}Rh, ^{109}Ag, ^{133}Cs, ^{143}Nd, ^{145}Nd, ^{147}Sm, ^{149}Sm, ^{150}Sm, ^{151}Sm, ^{152}Sm, ^{153}Eu, ^{155}Gd

The simple pin cell model means that the completion of the exercise is estimated to require approximately one day of effort for the criticality assessor.

3. Geometry data

The geometry for the Phase IV-A exercise is an infinite PWR fuel cell lattice, analogous to that used in the Phase I-A exercise for PWR UO_2 fuel, as shown in Figure 1.

Fuel pin pitch:	1.33 cm square pin array
Fuel pellet radius:	0.412 cm
Cladding thickness:	0.063 cm (no air gap between fuel and clad)

4. Material data

The pin cell materials shown in Figure 1 are as follows:

Cladding:	Zircaloy
Pin cell moderator:	Water
Fuel:	Mixed oxide fuel (as defined in Section 5)

For the purposes of the benchmark exercise, the non-fissile material compositions should be modelled as specified in Table 1.

5. MOX fuel compositions

The original proposal for the MOX benchmarking exercise (Ref. [1]) suggested that three different MOX fuels should be considered, chosen to represent the range of potential interest within the group for MOX fuels. The proposed MOX fuels were representative of:

- A reference MOX fuel case, appropriate to a typical plutonium vector for material derived from the reprocessing of thermal reactor UO_2 fuels, often designated “first generation” MOX, referred to as MOX Case A.

- A MOX fuel case appropriate to the disposition of weapons plutonium in MOX, referred to as MOX Case B.

- A MOX fuel case appropriate to future MOX fuels that might be produced using the plutonium recovered from the reprocessing of irradiated MOX, i.e. the “later generation” of MOX fuel from a plutonium recycling strategy, referred to as MOX Case C.

The plutonium isotopic compositions for these MOX fuels are presented in Table 2. In all cases, the uranium oxide component of the MOX is assumed to be depleted, with a ^{235}U content of 0.25 w/o $^{235}U/U$, which is typical of current MOX fuel fabrication. The uranium isotopic composition is shown in Table 3. The initial MOX fuel enrichments for the three MOX cases are shown in Table 4.

The fuel compositions for the requested calculations are shown in Tables 5, 6 and 7 for the MOX fuel cases A, B and C respectively. These compositions will also be provided to the participants on floppy disk or CD format, in order to ease the handling of the various fuel compositions in the calculations.

6. Specified format for submission of results

The results should be submitted via e-mail to the benchmark organisers, using the e-mail address shown on the front page of this specification. In order to facilitate the data manipulation, the participants are requested to submit their results in the following format:

1 Date.

2 Institute.

3 Contact person.

4 E-mail address or telefax number of the contact person.

5 Computer code.

6-68 Multiplication factors for the requested cases.

69 Please describe your analysis environment here. It will be included in the Phase IV-A report. The description should include:

- Institute and country.
- Participants.
- Neutron data library.
- Neutron data processing code or method.
- Neutron energy groups.
- Description of your code system.
- Geometry modelling.
- Omitted or substituted nuclides (if any).
- Employed convergence limit or statistical errors for the eigenvalue calculations.
- Other information (if any).

REFERENCE

[1] R.L. Bowden and G.J O'Connor, "Derivation of Isotopic Number Densities for the Specification of the OECD/NEANSC Burn-up Credit Benchmark, Phase IV-A (MOX Fuels)", BNFL Report CR5172, Rev. 1, July 1997.

Table 1. Non-fissile material compositions

Zircaloy	
Nuclide	**Atoms/barn.cm**
Zr	4.2982E-2
Fe	1.4838E-4
Cr	7.5891E-5
Water	
H	6.6724E-2
O	3.3362E-2

Table 2. Plutonium isotopic compositions in fresh MOX fuel

Nuclide	**Isotopic composition, w/o in Pu_{total}**		
	MOX Case A	**MOX Case B**	**MOX Case C**
^{238}Pu	1.8	0.05	4.0
^{239}Pu	59.0	93.6	36.0
^{240}Pu	23.0	6.0	28.0
^{241}Pu	12.2	0.3	12.0
^{242}Pu	4.0	0.05	20.0

Table 3. Uranium isotopic compositions in fresh MOX fuel

Nuclide	**w/o in U_{total}**
^{234}U	0.00119
^{235}U	0.25000
^{238}U	99.74881

Table 4. Initial MOX fuel enrichments

MOX fuel type	MOX fuel plutonium content, w/o Pu_{total}/[U+Pu]	MOX fuel enrichment, w/o $Pu_{fissile}$/[U+Pu]
Case A	5.6	3.987
Case B	4.0	3.756
Case C	8.0	3.840

Table 5. Specified calculations

MOX case	Cooling time (years)	Fission products modelled?	Actinides modelled	Burn-up (GWd/teHM)			
				Fresh	20	40	60
A	1	Yes	Major	Case 1	Case 2	Case 3	Case 4
		No	Major		Case 5	Case 6	Case 7
			All		Case 8	Case 9	Case 10
	5	Yes	Major		Case 11	Case 12	Case 13
		No	Major		Case 14	Case 15	Case 16
			All		Case 17	Case 18	Case 19
B	1	Yes	Major	Case 20	Case 21	Case 22	Case 23
		No	Major		Case 24	Case 25	Case 26
			All		Case 27	Case 28	Case 29
	5	Yes	Major		Case 30	Case 31	Case 32
		No	Major		Case 33	Case 34	Case 35
			All		Case 36	Case 37	Case 38
C	1	Yes	Major	Case 39	Case 40	Case 41	Case 42
			All		Case 43	Case 44	Case 45
		No	Major		Case 46	Case 47	Case 48
			All		Case 49	Case 50	Case 51
	5	Yes	Major		Case 52	Case 53	Case 54
			All		Case 55	Case 56	Case 57
		No	Major		Case 58	Case 59	Case 60
			All		Case 61	Case 62	Case 63

Table 6. Material compositions for MOX Case A

Nuclide	Atoms/barn.cm for given fuel burn-up and cooling time						
	Fresh	20 GWd/teHM		40 GWd/teHM		60 GWd/teHM	
		One year cooling	Five years cooling	One year cooling	Five years cooling	One year cooling	Five years cooling
^{234}U	2.7999E-7	6.3600E-7	1.3530E-6	7.7718E-7	1.5879E-6	9.1664E-7	1.8564E-6
^{235}U	5.8570E-5	4.2219E-5	4.2287E-5	2.9018E-5	2.9070E-5	1.9181E-5	1.9223E-5
^{236}U	–	3.7252E-6	3.8580E-6	6.1753E-6	6.2984E-6	7.5360E-6	7.6448E-6
^{238}U	2.3074E-2	2.2732E-2	2.2732E-2	2.2365E-2	2.2365E-2	2.1986E-2	2.1986E-2
^{238}Pu	2.4700E-5	2.2785E-5	2.2389E-5	2.5504E-5	2.5364E-5	2.9509E-5	2.9410E-5
^{239}Pu	8.0623E-4	5.9182E-4	5.9176E-4	4.5028E-4	4.5024E-4	3.6327E-4	3.6325E-4
^{240}Pu	3.1298E-4	3.1445E-4	3.1491E-4	2.9067E-4	2.9250E-4	2.5605E-4	2.5961E-4
^{241}Pu	1.6533E-4	1.8251E-4	1.5056E-4	1.8125E-4	1.4953E-4	1.6525E-4	1.3633E-4
^{242}Pu	5.3981E-5	7.0592E-5	7.0592E-5	9.1733E-5	9.1733E-5	1.1211E-4	1.1211E-4
^{237}Np	–	1.6134E-6	1.6134E-6	3.0746E-6	3.0746E-6	4.1997E-6	4.1997E-6
^{241}Am	–	1.8432E-5	5.0375E-5	2.2303E-5	5.4028E-5	2.1568E-5	5.0491E-5
^{243}Am	–	1.3528E-5	1.3528E-5	2.4023E-5	2.4023E-5	3.2566E-5	3.2566E-5
^{16}O	4.8992E-2	4.8992E-2	4.8992E-2	4.8992E-2	4.8992E-2	4.8992E-2	4.8992E-2
^{242}Cm	–	3.2217E-7	6.4678E-10	6.7186E-7	1.3488E-9	8.4273E-7	1.6918E-9
^{243}Cm	–	2.8535E-8	2.6018E-8	1.1090E-7	1.0111E-7	1.8772E-7	1.7116E-7
^{244}Cm	–	4.1736E-6	3.5812E-6	1.3749E-5	1.1798E-5	2.8565E-5	2.2194E-5
^{245}Cm	–	3.0261E-7	3.0261E-7	1.6967E-6	1.6967E-6	3.9227E-6	3.9227E-6
^{95}Mo	–	2.3101E-5	2.3261E-5	4.4441E-5	4.4599E-5	6.3363E-5	6.3520E-5
^{99}Tc	–	2.8609E-5	2.8610E-5	5.3736E-5	5.3736E-5	7.5064E-5	7.5064E-5
^{101}Ru	–	2.9847E-5	2.9847E-5	5.7774E-5	5.7774E-5	8.3092E-5	8.3092E-5
^{103}Rh	–	2.9106E-5	2.9111E-5	4.9708E-5	4.9714E-5	6.3144E-5	6.3149E-5
^{109}Ag	–	6.5892E-6	6.5892E-6	1.1408E-5	1.1408E-5	1.5024E-5	1.5024E-5
^{133}Cs	–	3.1181E-5	3.1181E-5	5.7100E-5	5.7100E-5	7.7818E-5	7.7818E-5
^{143}Nd	–	2.1008E-5	2.1008E-5	3.8610E-5	3.8610E-5	5.2176E-5	5.2176E-5
^{145}Nd	–	1.4896E-5	1.4896E-5	2.8038E-5	2.8038E-5	3.9157E-5	3.9157E-5
^{147}Sm	–	2.7653E-6	5.9794E-6	5.2265E-6	9.3872E-6	6.8435E-6	1.1221E-5
^{149}Sm	–	3.5704E-7	3.5704E-7	3.3504E-7	3.3504E-7	3.0728E-7	3.0728E-7
^{150}Sm	–	6.6564E-6	6.6564E-6	1.3820E-5	1.3820E-5	2.0276E-5	2.0276E-5
^{151}Sm	–	1.3380E-6	1.2968E-6	1.5043E-6	1.4580E-6	1.5866E-6	1.5379E-6
^{152}Sm	–	3.8440E-6	3.8439E-6	6.2143E-6	6.2143E-6	7.5692E-6	7.5692E-6
^{153}Eu	–	3.2743E-6	3.2743E-6	7.5074E-6	7.5074E-6	1.0848E-5	1.0848E-5
^{155}Gd	–	7.5755E-8	2.5948E-7	1.4403E-7	5.0261E-7	2.2005E-7	7.7899E-7

Table 7. Material compositions for MOX Case B

Nuclide	Atoms/barn.cm for given fuel burn-up and cooling time						
	Fresh	20 GWd/teHM		40 GWd/teHM		60 GWd/teHM	
		One year cooling	Five years cooling	One year cooling	Five years cooling	One year cooling	Five years cooling
^{234}U	2.8452E-7	2.2995E-7	2.6895E-7	2.1773E-7	3.6734E-7	2.6275E-7	5.7503E-7
^{235}U	5.9518E-5	4.0882E-5	4.0948E-5	2.5627E-5	2.5670E-5	1.4759E-5	1.4791E-5
^{236}U	–	3.9723E-6	4.0436E-6	6.5755E-6	6.6585E-6	7.8389E-6	7.9160E-6
^{238}U	2.3447E-2	2.3103E-2	2.3103E-2	2.2715E-2	2.2715E-2	2.2300E-2	2.2300E-2
^{238}Pu	4.8972E-7	1.1910E-6	1.2270E-6	4.5563E-6	4.7086E-6	9.6242E-6	9.8070E-6
^{239}Pu	9.1194E-4	5.7376E-4	5.7369E-4	3.7279E-4	3.7275E-4	2.7573E-4	2.7570E-4
^{240}Pu	5.8276E-5	1.6882E-4	1.6879E-4	1.9642E-4	1.9672E-4	1.8198E-4	1.8321E-4
^{241}Pu	3.8689E-6	7.4303E-5	6.1297E-5	1.1078E-4	9.1391E-5	1.1209E-4	9.2467E-5
^{242}Pu	4.8161E-7	8.9143E-6	8.9143E-6	3.0626E-5	3.0626E-5	5.6427E-5	5.6427E-5
^{237}Np	–	1.5675E-6	1.5675E-6	3.0228E-6	3.0228E-6	4.1080E-6	4.1080E-6
^{241}Am	–	5.9894E-6	1.8995E-5	1.0955E-5	3.0345E-5	1.2034E-5	3.1652E-5
^{243}Am	–	1.2867E-6	1.2867E-6	6.8336E-6	6.8336E-6	1.5293E-5	1.5293E-5
^{16}O	4.8965E-2	4.8965E-2	4.8965E-2	4.8965E-2	4.8965E-2	4.8965E-2	4.8965E-2
^{242}Cm	–	7.5157E-8	1.5088E-10	3.0247E-7	6.0723E-10	4.9610E-7	9.9596E-10
^{243}Cm	–	5.1466E-9	4.6925E-9	4.0239E-8	3.6690E-8	9.5010E-8	8.6628E-8
^{244}Cm	–	2.6410E-7	2.2662E-7	2.6910E-6	2.3090E-6	9.2627E-6	7.9480E-6
^{245}Cm	–	1.3681E-8	1.3681E-8	2.3729E-7	2.3729E-7	1.0624E-6	1.0624E-6
^{95}Mo	–	2.3871E-5	2.4036E-5	4.5718E-5	4.5879E-5	6.4917E-5	6.5075E-5
^{99}Tc	–	2.8946E-5	2.8946E-5	5.4176E-5	5.4176E-5	7.5371E-5	7.5371E-5
^{101}Ru	–	2.9955E-5	2.9955E-5	5.8079E-5	5.8079E-5	8.3707E-5	8.3707E-5
^{103}Rh	–	2.8121E-5	2.8126E-5	4.6580E-5	4.6585E-5	5.7355E-5	5.7360E-5
^{109}Ag	–	5.7370E-6	5.7370E-6	1.0105E-5	1.0105E-5	1.3457E-5	1.3457E-5
^{133}Cs	–	3.1383E-5	3.1383E-5	5.7177E-5	5.7177E-5	7.7393E-5	7.7393E-5
^{143}Nd	–	2.0862E-5	2.0862E-5	3.7501E-5	3.7501E-5	4.9110E-5	4.9110E-5
^{145}Nd	–	1.4826E-5	1.4826E-5	2.7866E-5	2.7866E-5	3.8801E-5	3.8801E-5
^{147}Sm	–	2.6881E-6	5.8102E-6	4.9973E-6	8.9723E-6	6.3962E-6	1.0505E-5
^{149}Sm	–	2.7823E-7	2.7823E-7	2.5523E-7	2.5523E-7	2.3274E-7	2.3274E-7
^{150}Sm	–	6.6563E-6	6.6563E-6	1.3926E-5	1.3926E-5	2.0464E-5	2.0464E-5
^{151}Sm	–	1.0732E-6	1.0402E-6	1.1467E-6	1.1114E-6	1.1985E-6	1.1616E-6
^{152}Sm	–	3.8212E-6	3.8212E-6	5.9493E-6	5.9493E-6	7.0762E-6	7.0762E-6
^{153}Eu	–	3.2199E-6	3.2199E-6	7.4656E-6	7.4656E-6	1.0705E-5	1.0705E-5
^{155}Gd	–	5.8022E-8	2.0452E-7	1.1923E-7	4.2851E-7	1.8106E-7	6.5902E-7

Table 8. Material compositions for MOX Case C

Nuclide	Atoms/barn.cm for given fuel burn-up and cooling time						
	Fresh	20 GWd/teHM		40 GWd/teHM		60 GWd/teHM	
		One year cooling	Five years cooling	One year cooling	Five years cooling	One year cooling	Five years cooling
^{234}U	2.7318E-7	1.5063E-6	3.6143E-6	1.9068E-6	3.9071E-6	2.1766E-6	4.1510E-6
^{235}U	5.7145E-5	4.1669E-5	4.1734E-5	2.9739E-5	2.9794E-5	2.0961E-5	2.1009E-5
^{236}U	–	3.6788E-6	3.8787E-6	6.0137E-6	6.1853E-6	7.3406E-6	7.4879E-6
^{238}U	2.2513E-2	2.2161E-2	2.2161E-2	2.1796E-2	2.1796E-2	2.1428E-2	2.1428E-2
^{238}Pu	7.8503E-5	6.7431E-5	6.5740E-5	6.3615E-5	6.2454E-5	6.2619E-5	6.1686E-5
^{239}Pu	7.0356E-4	5.6858E-4	5.6852E-4	4.8007E-4	4.8003E-4	4.2049E-4	4.2046E-4
^{240}Pu	5.4493E-4	4.7278E-4	4.7425E-4	4.0401E-4	4.0879E-4	3.4474E-4	3.5312E-4
^{241}Pu	2.3257E-4	2.4534E-4	2.0240E-4	2.3568E-4	1.9443E-4	2.1323E-4	1.7590E-4
^{242}Pu	3.8610E-4	3.7523E-4	3.7523E-4	3.6946E-4	3.6946E-4	3.6386E-4	3.6386E-4
^{237}Np	–	1.6899E-6	1.6899E-6	3.1985E-6	3.1985E-6	4.3720E-6	4.3720E-6
^{241}Am	–	2.5361E-5	6.8303E-5	3.0694E-5	7.1945E-5	3.0366E-5	6.7687E-5
^{243}Am	–	4.0530E-5	4.0530E-5	6.4516E-5	6.4516E-5	7.8878E-5	7.8878E-5
^{16}O	4.9031E-2	4.9031E-2	4.9031E-2	4.9031E-2	4.9031E-2	4.9031E-2	4.9031E-2
^{242}Cm	–	4.1769E-7	8.3855E-10	8.4517E-7	1.6895E-9	1.0431E-6	2.0941E-9
^{243}Cm	–	3.8856E-8	3.5428E-8	1.4606E-7	1.3318E-7	2.4454E-7	2.2297E-7
^{244}Cm	–	1.1769E-5	1.0098E-5	3.4867E-5	2.9918E-5	6.0098E-5	5.1568E-5
^{245}Cm	–	9.0845E-7	9.0845E-7	4.5435E-6	4.5435E-6	9.6412E-6	9.6412E-6
^{95}Mo	–	2.2735E-5	2.2892E-5	4.3787E-5	4.3944E-5	6.2588E-5	6.2743E-5
^{99}Tc	–	2.8403E-5	2.8403E-5	5.3414E-5	5.3414E-5	7.4849E-5	7.4849E-5
^{101}Ru	–	2.9798E-5	2.9798E-5	5.7667E-5	5.7667E-5	8.3006E-5	8.3006E-5
^{103}Rh	–	2.9664E-5	2.9669E-5	5.1912E-5	5.1917E-5	6.7750E-5	6.7756E-5
^{109}Ag	–	6.9595E-6	6.9595E-6	1.2094E-5	1.2094E-5	1.6067E-5	1.6067E-5
^{133}Cs	–	3.1031E-5	3.1031E-5	5.6923E-5	5.6923E-5	7.7931E-5	7.7931E-5
^{143}Nd	–	2.1064E-5	2.1064E-5	3.9138E-5	3.9138E-5	5.3831E-5	5.3831E-5
^{145}Nd	–	1.4931E-5	1.4931E-5	2.8137E-5	2.8137E-5	3.9433E-5	3.9433E-5
^{147}Sm	–	2.7739E-6	6.0029E-6	5.2757E-6	9.4928E-6	7.0109E-6	1.1512E-5
^{149}Sm	–	4.0641E-7	4.0641E-7	4.0019E-7	4.0019E-7	3.8076E-7	3.8076E-7
^{150}Sm	–	6.6678E-6	6.6678E-6	1.3785E-5	1.3785E-5	2.0207E-5	2.0207E-5
^{151}Sm	–	1.4686E-6	1.4235E-6	1.7611E-6	1.7070E-6	1.9357E-6	1.8762E-6
^{152}Sm	–	3.8100E-6	3.8100E-6	6.3411E-6	6.3411E-6	8.0271E-6	8.0271E-6
^{153}Eu	–	3.3404E-6	3.3404E-6	7.5293E-6	7.5293E-6	1.0865E-5	1.0865E-5
^{155}Gd	–	8.5534E-8	2.8847E-7	1.6237E-7	5.5419E-7	2.5211E-7	8.6971E-7

Figure 1. Geometry of MOX fuel pin cell for PWR

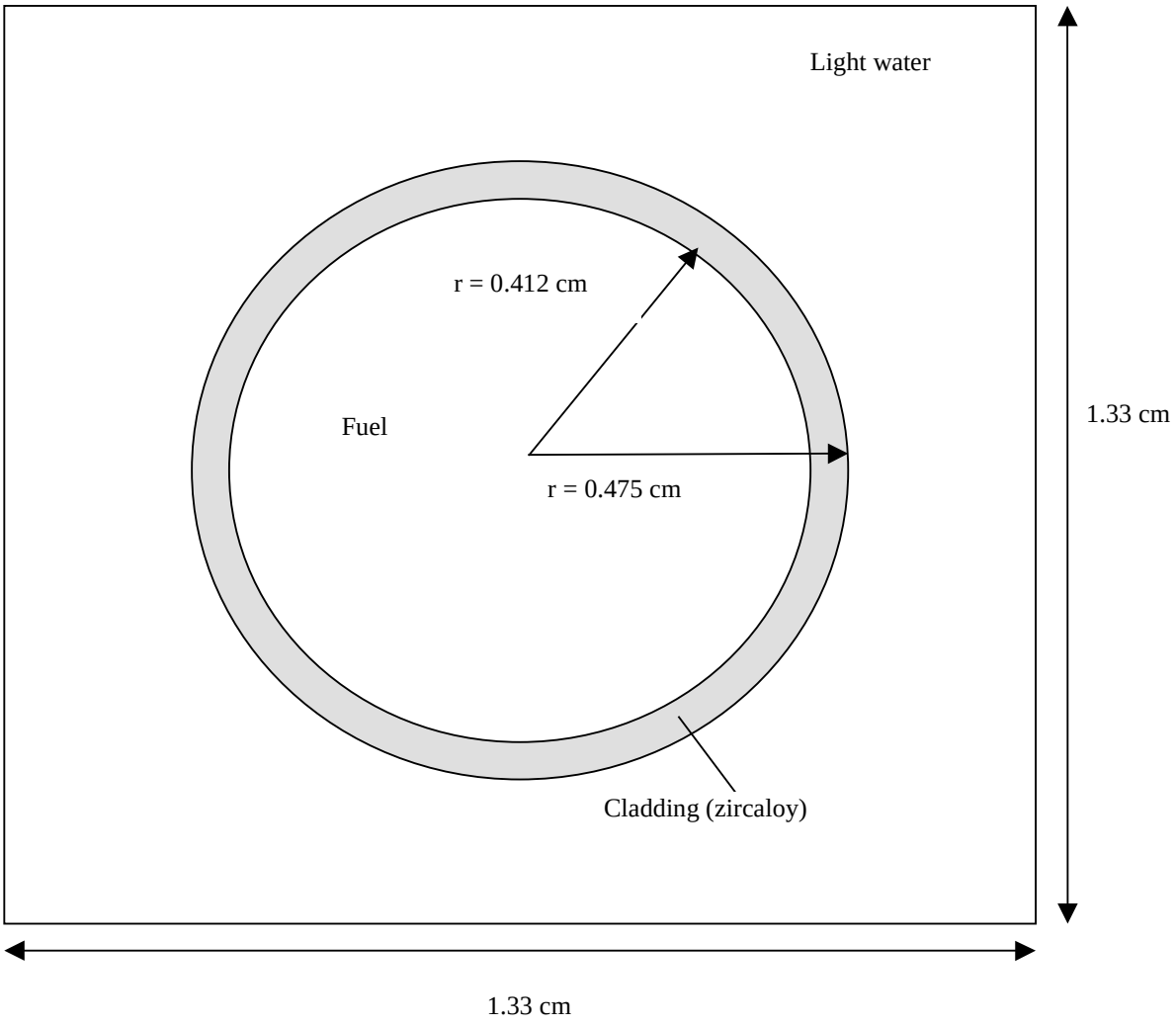

Appendix II

PARTICIPANTS AND ANALYSIS METHODS

1. EDF/DER, France

Institute: Électricité de France (EDF)
Participants: Patrice Risch, Claude Garzenne
Computer code: TRIPOLI-4
Data library: JEF-2
Comments: TRIPOLI-4 three-dimensional neutron and gamma Monte Carlo code, developed by CEA Saclay. Three-dimensional geometry modelled with 366 cm axial length. No substituted or omitted nuclides. Sigma between 1.4E-4 and 2.7E-4. 100*5 000 neutrons simulated.

2. PNC, Japan

Institute: PNC Tokai Works
Participants: Ichiro Nojiri
Computer code: SCALE-4.3
Data library: 44-group ENDF/B-V (44GROUPNDF5)
Comments: Neutron data processed via BONAMI and NITAWL-II. No nuclides substituted or omitted. Employed convergence of $\sigma = \pm 0.0007$. All materials taken at 300 K.

3. BNFL, United Kingdom

Institute: British Nuclear Fuels
Participants: Russell Bowden, Peter Thorne, Gregory O'Connor
Computer code: MONK7B
Data library: MONK 8220-point UKNDL nuclear data library
Comments: Some data in the UKNDL continuous energy database have been taken from the JEF-2 library; for example data used for the thermalisation treatment, as well as fission product and higher actinide nuclide data not present in UKNDL. Calculations performed on a Sun Sparc Server 1000E, using the Solaris 2.5 operating system. No nuclides substituted or omitted from the calculations. Convergence of eigenvalue to less than 0.0010.

4. BNFL, United Kingdom

Institute: British Nuclear Fuels
Participants: Russell Bowden, Peter Thorne, Gregory O'Connor
Computer code: WIMS7B
Data library: 172-group WIMS "1996" JEF-2.2 nuclear data library
Comments: Calculations performed on a Sun Sparc Server 1000E, using the Solaris 2.5 operating system. No nuclides substituted or omitted from the calculations. Calculations performed in full 172-group structure of data library, with resonance treatment via the subgroup method in WIMS.

5. BNFL, United Kingdom

Institute: British Nuclear Fuels
Participants: Russell Bowden, Peter Thorne, Gregory O'Connor
Computer code: SCALE-4.3
Data library: 27-group ENDF/B-IV (27BURNUPLIB)
Comments: Calculations performed on a Compaq Pentium-166 PC, using the MS-DOS 6.22 operating system. Calculations used the CSAS25 sequence in SCALE-4.3, i.e. data processed via BONAMI and NITAWL-II, prior to calculation with KENO Va. Calculations with curium were not completed, as these isotopes are not available on the data library.

6. BNFL, United Kingdom

Institute: British Nuclear Fuels
Participants: Russell Bowden, Peter Thorne, Gregory O'Connor
Computer code: SCALE-4.3
Data library: 44-group ENDF/B-V (44GROUPNDF5)
Comments: Calculations performed on a Compaq Pentium-166 PC, using the MS-DOS 6.22 operating system. No nuclides substituted or omitted from the calculations. Calculations used the CSAS25 sequence in SCALE-4.3, i.e. data processed via BONAMI and NITAWL-II, prior to calculation with KENO Va.

7. JAERI, Japan

Institute: Japan Atomic Energy Research Institute
Participants: Kenya Suyama
Computer code: MVP94.1
Data library: JENDL-3.2
Comments: Continuous energy JENDL-3.2 data library, with the data processed via the LICEM code. MVP94.1 is a continuous-energy Monte Carlo code developed by JAERI, tuned for vector and parallel processor systems for faster calculation. No nuclides were substituted or omitted. Calculations were performed with 5 000 particles/generation, with a total of 300 generations, the first 50 generations being skipped from the eigenvalue calculation.

8. JAERI, Japan

Institute: Japan Atomic Energy Research Institute
Participants: Kenya Suyama
Computer code: SRAC95
Data library: JENDL-3.2
Comments: One hundred seven (107) group JENDL-3.2 data library used for eigenvalue problem. SRAC is the JAERI thermal reactor standard code system, with SRAC95 being the latest version released in 1996. SRAC has been used for many reactor analyses. SRAC uses collision probability method to calculate group constants. A generalised Dancoff correction factor was introduced for infinite arrays of multi-region cells including several absorber lumps with different nuclide concentrations using the collision probability method. A fixed boundary source problem is available in the cell calculation by the collision probability method. It can provide a proper spectrum to an isolated cell that can not have its own

spectrum. One feature of SRAC is the ultra-fine resonance calculation. It uses collision probability method with an almost continuous energy library to treat neutron resonance absorption.

Square and cylinder divided by concentric circles (1-D calculation). No nuclides substituted or omitted. Employed convergence limit on eigenvalue of 1.0E-5. The 107-group effective group constants were calculated by collision probability method in fixed source mode by SRAC95. Then we calculate eigenvalue problem by collision probability method using these constants of 107-groups. Ultra-fine (150 000 groups) resonance calculation was selected for 961 eV to 3.9279 eV. This sequence is the most general method to calculate eigenvalues using the SRAC system.

9. CEA, France

Institute: Commissariat à l'Énergie Atomique (CEA)
Participants: Benedicte Roque, Alain Santamarina
Computer code: APOLLO2
Data library: CEA93
Comments: The neutron data library used is the CEA93 library in a 172-group structure. These multi-group cross-sections and effective cross-sections were processed by NJOY from the JEF-2 European file. The calculations were performed using the French code APOLLO2 extensively, used in light water reactor studies and in the CRISTAL criticality safety package. APOLLO2 is a modular code which solves both the Boltzmann integral equation and the integro-differential equation (S_n method). APOLLO2 allows the use of several collision probability methods to solve the integral equation: exact 2-D P_{ij}, multi-cell P_{ij} based on the interface current method. The one used for the benchmark is the exact 2-D P_{ij} method. In our calculations, the MOX fuel pin is divided into six concentric zones. Self-shielded cross-sections are calculated for ^{238}U in each concentric zone; an accurate "background matrix" formalism is used for resonant reaction rate calculation, allowing space-dependent resonance self-shielding and rim effect modelling. For the other actinides, ^{240}Pu, ^{239}Pu, ^{241}Pu, ^{242}Pu, ^{238}Pu, ^{241}Am, ^{235}U and Zr we used an "average" self-shielding formalism. The whole set of nuclides required for the benchmark is available in the CEA93 library.

10. Siemens, Germany

Institute: Siemens AG, Power Generation Group (KWU), Dept. NDM3
Participants: Jens Christian Neuber
Computer code: SCALE-4.3
Data library: 44-group ENDF/B-V (44GROUPNDF5)
Comments: Calculations performed using sequence CSAS25 in the SCALE-4.3 system, with neutron data processed via BONAMI and NITAWL-II. No nuclides substituted or omitted from calculations. Typical standard deviations of 0.0006 for requested calculations.

11. Siemens, Germany

Institute: Siemens AG, Power Generation Group (KWU), Dept. NDM3
Participants: Jens Christian Neuber
Computer code: MCNP4B2
Data library: ENDF/B-VI for actinides, plus fission product and clad material data from various sources, e.g. KIDMAN1
Comments: 10×10 square pitch array modelled in calculations with a periodic boundary condition (x/y faces), and mirror image reflection (z faces). No nuclides substituted or omitted from calculations. Typical standard deviations of 0.0010 for requested calculations.

12. AEAT, United Kingdom

Institute: AEA Technology
Participants: David Hanlon, Jim Gulliford
Computer code: WIMS7B
Data library: 172-group WIMS "1997" JEF-2.2 data library
Comments: One hundred seventy-two (172) group calculation using the PRES-PIJ-RES subgroup resonance treatment. Two-dimensional calculation with no nuclides substituted or omitted. Final PIP k_∞ calculation converged to 10^{-5}.

13. AEAT, United Kingdom

Institute: AEA Technology
Participants: David Hanlon, Jim Gulliford
Computer code: MONK7B
Data library: MONK "1996" DICE nuclear data library
Comments: Monte Carlo calculation using 1 000 neutrons per stage and 10 superhistories, ~340 000 sampled neutrons per calculation. Three-dimensional model, with ^{242}Cm omitted from the calculations. Standard deviation on k_∞ calculations is 0.0010 in all cases.

14. AEAT, United Kingdom

Institute: AEA Technology
Participants: David Hanlon, Jim Gulliford
Computer code: SCALE-4.3
Data library: 238-group ENDF/B-V (238GROUPNDF5)
Comments: CSAS25 route used in SCALE-4.3 to give Monte Carlo calculation using 1 000 neutrons per generation and run for 303 generations, i.e. 303 000 sampled neutrons per calculation. Three-dimensional calculation with no nuclides omitted. Standard deviation on k_∞ calculation is 0.0010 in all cases.

15. IPPE, Russian Federation

Institute: State Scientific Centre of Russian Federation, Institute of Physics and Power Engineering (SSC IPPE)
Participants: Gennadi Jerdev, Svetlana Zabrodskaia, Anatoli Tsiboulia
Computer code: WIMS/ABBN
Data library: 69-group WIMS/ABBN data library (FOND-2 evaluations)
Comments: The calculations were performed at the State Scientific Centre of the Russian Federation, Institute of Physics and Power Engineering (SSC IPPE), in the ABBN Nuclear Cross-sections Laboratory. The WIMS/ABBN neutron data library

obtained on the basis of neutron data FOND-2 (IPPE, Obninsk) was used for the calculations. The WIMS/ABBN 69-group data library was used, retrieved from the FOND-2 evaluated data files with the code NJOY. The WIMS/ABBN code system is a modification of the standard WIMS-D4 code. The WIMS/ABBN data library differs from the standard WIMS-D4 library by the amount of nuclides, number of resonance tables and burn-up chains included. Different fission spectra are available in calculations. The special treatment of the resonance self-shielding for ^{242}Pu in the vicinity of 2.6 eV is used. The equivalent cylinder model was used for the calculations.

16. EMS, Sweden

Institute: E Mennerdahl Systems
Participants: Dennis Mennerdahl
Computer code: SCALE-4.3
Data library: 44-group ENDF/B-V (44GROUPNDF5)
Comments: CSAS1X sequence from SCALE-4.3 used together with 44-group ENDF/B-V library. Standard values for convergence used.

17. EMS, Sweden

Institute: E Mennerdahl Systems
Participants: Dennis Mennerdahl
Computer code: SCALE-4.3
Data library: 27-group ENDF/B-IV (27BURNUPLIB)
Comments: CSAS1X sequence from SCALE-4.3 used together with 27-group ENDF/B-IV library. Standard values for convergence used. Calculations with curium were not completed, as these isotopes are not available on the data library.

18. EMS, Sweden

Institute: E Mennerdahl Systems
Participants: Dennis Mennerdahl
Computer code: SCALE-4.3
Data library: 238-group ENDF/B-V (238GROUPNDF5)
Comments: CSAS1X sequence from SCALE-4.3 used together with 238-group ENDF/B-V library. Standard values for convergence used.

19. IPSN, France

Institute: Institut de Protection et de Sûreté Nucléaire
Participants: Xavier Boudin, Eric Letang
Computer code: APOLLO2
Data library: CEA93
Comments: Neutron data library used is the CEA93 library (172-groups library based on JEF-2 evaluation). Calculations were performed using the APOLLO2 code (the cylindrical pin cell model is used). The fuel pin is divided in six concentric zones where the self-shielding cross-sections are calculated using the "background matrix" formalism. All nuclides specified in the benchmark are available in the neutron data library used for the calculations.

20. DETR, United Kingdom

Institute: Department of Environment, Transport and the Regions
Participants: Jim Stewart
Computer code: MONK
Data library: UKNDL
Comments: None

21. NUPEC, Japan

Institute: Institute of Nuclear Safety, Nuclear Power Engineering Corporation (NUPEC-INS)
Participants: Susumu Mitake, Fumihiro Masukawa, Osamu Sato
Computer code: ANISN
Data library: MGCL-JINS
Comments: One-dimensional infinite cylinder modelled (Wigner cell model) using the discrete ordinates code ANISN. Effective cross-section calculation performed by the Bondarenko method using MAIL-JINS, with the 137-group MGCL-JINS cross-section library, drawn from ENDF/B-IV and JENDL-3.2 data. Calculations performed with S_8 angular quadrature, P_3 order of scattering and an eigenvalue convergence criteria of 0.001%. Cases with all actinides were omitted due to the lack of cross-section data for the curium isotopes (except ^{244}Cm) in the MGCL-JINS library.

22. NUPEC, Japan

Institute: Institute of Nuclear Safety, Nuclear Power Engineering Corporation (NUPEC-INS)
Participants: Susumu Mitake, Fumihiro Masukawa, Osamu Sato
Computer code: SCALE-4.3
Data library: 44-group ENDF/B-V (44GROUPNDF5)
Comments: One-dimensional infinite cylinder modelled (Wigner cell model) using the discrete ordinates code XSDRNPM within SCALE-4.3. CSAS1X calculational sequence used with the 44-group ENDF/B-V library. Calculations performed with S_8 angular quadrature, P_3 order of scattering and an eigenvalue convergence criteria of 0.01%.

23. NUPEC, Japan

Institute: Institute of Nuclear Safety, Nuclear Power Engineering Corporation (NUPEC-INS)
Participants: Susumu Mitake, Fumihiro Masukawa, Osamu Sato
Computer code: SCALE-4.3
Data library: 27-group ENDF/B-IV (27BURNUPLIB)
Comments: One-dimensional infinite cylinder modelled (Wigner cell model) using the discrete ordinates code XSDRNPM within SCALE-4.3. CSAS1X calculational sequence used with the 27-group ENDF/B-IV library. Calculations performed with S_8 angular quadrature, P_3 order of scattering and an eigenvalue convergence criteria of 0.01%. Cases with all actinides were omitted due to the lack of cross-section data for the curium isotopes (except ^{244}Cm) in the 27-group data library.

24. NUPEC, Japan

Institute: Institute of Nuclear Safety, Nuclear Power Engineering Corporation (NUPEC-INS)
Participants: Susumu Mitake, Fumihiro Masukawa, Osamu Sato
Computer code: MVP
Data library: JENDL-3.2
Comments: Infinite lattice of square pitch cell with mirror reflection boundaries modelled on all faces of a cubic cell. Calculations performed with the continuous energy three-dimensional Monte Carlo code MVP, which includes an improved method for treating self-shielding effects of unresolved resonances using a probability table method assuming infinite diluted cross-sections. Calculations completed with 1 000 neutrons per batch for 510 batches, with 10 initial batches skipped.

25. NUPEC, Japan

Institute: Institute of Nuclear Safety, Nuclear Power Engineering Corporation (NUPEC-INS)
Participants: Susumu Mitake, Fumihiro Masukawa, Osamu Sato
Computer code: MCNP4A
Data library: FSXLIB-J3R2 (JENDL-3.2)
Comments: Infinite lattice of square pitch cell with mirror reflection boundaries modelled on all faces of a cubic cell. Calculations performed with the continuous energy three-dimensional Monte Carlo code MCNP4A and the FSXLIB-J3R2 library made from JENDL-3.2 evaluations. Calculations completed with 1 000 neutrons per batch for 510 batches, with 10 initial batches skipped to obtain the multiplication factors with statistical errors below 0.1%.

26. ORNL, United States

Institute: Oak Ridge National Laboratory
Participants: Mark DeHart
Computer code: SCALE-4.3
Data library: 44-group ENDF/B-V (44GROUPNDF5)
Comments: All cross-sections were processed automatically by the CSAS1X sequence of SCALE-4.3. CSAS1X uses the BONAMI code to apply the Bondarenko resonance self-shielding method for nuclides with Bondarenko data (unresolved energy range; nuclides with resonance structure but no ENDF resonance data); it then invokes NITAWL-II to perform Nordheim resonance self-shielding corrections (resolved energy range). Calculations performed in 44 energy groups, with structure selected based on typical LWR spectra. The CSAS1X sequence then invokes XSDRNPM for the transport solution. All calculations were run on a DEC ALPHA Station 500. XSDRNPM is a one-dimensional discrete ordinates code. The model used was developed using cylindrical geometry in which the fuel and clad were represented explicitly and the square cell boundary was represented using a Wigner-Seitz approximation with white boundary conditions. S_8 quadrature was used together with a P_3 scattering approximation. No nuclides were substituted or omitted from the calculations. All calculations were performed with flux and eigenvalue convergence criteria of 1.0E-4.

27. ORNL, United States

Institute: Oak Ridge National Laboratory
Participants: Mark DeHart
Computer code: NEWT
Data library: 44-group ENDF/B-V (44GROUPNDF5)
Comments: All cross-sections were processed using the CSASN sequence of SCALE-4.3. CSASN uses the BONAMI code to apply the Bondarenko resonance self-shielding method for nuclides with Bondarenko data (unresolved energy range; nuclides with resonance structure but no ENDF resonance data); it then invokes NITAWL-II to perform Nordheim resonance self-shielding corrections (resolved energy range). Calculations performed in 44 energy groups, structure selected based on typical LWR spectra. Cross-section processing was performed using the CSASI module of SCALE-4.3. The transport solution was performed using NEWT running within SCALE-4.3. All calculations were run on a DEC ALPHA Station 500. NEWT is a two-dimensional discrete ordinates code that performs transport solutions on an arbitrary grid structure. A polygon-based grid structure was laid on top of a 5×5 square gird, representing cylindrical fuel and clad surfaces. A ¼ pin cell model was used, taking advantage of symmetry, and reflective boundary conditions were applied on all outer boundaries. S_6 quadrature was used together with a P_3 scattering approximation. No nuclides were substituted or omitted from the calculations. All calculations were performed with flux and eigenvalue convergence criteria of 1.0E-4.

28. ORNL, United States

Institute: Oak Ridge National Laboratory
Participants: Mark DeHart
Computer code: SCALE-4.3
Data library: 44-group ENDF/B-V (44GROUPNDF5)
Comments: All cross-sections were processed automatically by the CSAS25 sequence of SCALE-4.3. CSAS25 uses the BONAMI code to apply the Bondarenko resonance self-shielding method for nuclides with Bondarenko data (unresolved energy range; nuclides with resonance structure but no ENDF resonance data); it then invokes NITAWL-II to perform Nordheim resonance self-shielding corrections (resolved energy range). Calculations performed in 44 energy groups, with structure selected based on typical LWR spectra. The CSAS25 sequence then invokes KENO Va for the transport solution. All calculations were run on a DEC ALPHA Station 500. KENO Va is a multi-group-based 3-D Monte Carlo criticality code. Fuel and clad cylinders and the square boundary were modelled explicitly within KENO. The fuel was assumed to be 10 cm tall, but reflective boundary conditions were used on all boundaries to represent infinite fuel length in an infinite lattice. A P_3 scattering approximation was employed. No nuclides were substituted or omitted from the calculations. Typical statistical error on results of about 0.0004 for a 1-sigma confidence level. Calculations were based on a total of 2 100 generations of 1 000 neutrons each. The first 100 generations were skipped in the calculation of k_{eff} to allow for source convergence.

29. ORNL, United States

Institute: Oak Ridge National Laboratory
Participants: Mark DeHart
Computer code: SCALE-4.3
Data library: 238-group ENDF/B-V (238GROUPNDF5)
Comments: All cross-sections were processed automatically by the CSAS1X sequence of SCALE-4.3. CSAS1X uses the BONAMI code to apply the Bondarenko resonance self-shielding method for nuclides with Bondarenko data (unresolved energy range; nuclides with resonance structure but no ENDF resonance data); it then invokes NITAWL-II to perform Nordheim resonance self-shielding corrections (resolved energy range). Calculations performed in 238 energy groups, with structure selected based on typical LWR spectra. The CSAS1X sequence then invokes XSDRNPM for the transport solution. All calculations were run on a DEC ALPHAStation 500. XSDRNPM is a one-dimensional discrete ordinates code. The model used was developed using cylindrical geometry in which the fuel and clad were represented explicitly and the square cell boundary was represented using a Wigner-Seitz approximation with white boundary conditions. S_{16} quadrature was used together with a P_3 scattering approximation. No nuclides were substituted or omitted from the calculations. All calculations were performed with flux and eigenvalue convergence criteria of 1.0E-4.

30. ORNL, United States

Institute: Oak Ridge National Laboratory
Participants: Mark DeHart
Computer code: NEWT
Data library: 238-group ENDF/B-V (238GROUPNDF5)
Comments: All cross-sections were processed using the CSASN sequence of SCALE-4.3. CSASN uses the BONAMI code to apply the Bondarenko resonance self-shielding method for nuclides with Bondarenko data (unresolved energy range; nuclides with resonance structure but no ENDF resonance data); it then invokes NITAWL-II to perform Nordheim resonance self-shielding corrections (resolved energy range). Calculations performed in 238 energy groups, structure selected based on typical LWR spectra. Cross-section processing was performed using the CSASI module of SCALE-4.3. The transport solution was performed using NEWT running within SCALE-4.3. All calculations were run on a DEC ALPHAStation 500. NEWT is a two-dimensional discrete ordinates code that performs transport solutions on an arbitrary grid structure. A polygon-based grid structure was laid on top of a 5×5 square gird, representing cylindrical fuel and clad surfaces. A ¼ pin cell model was used, taking advantage of symmetry, and reflective boundary conditions were applied on all outer boundaries. S_8 quadrature was used together with a P_3 scattering approximation. No nuclides were substituted or omitted from the calculations. All calculations were performed with flux and eigenvalue convergence criteria of 1.0E-4.

31. ORNL, United States

Institute: Oak Ridge National Laboratory
Participants: Mark DeHart
Computer code: SCALE-4.3
Data library: 238-group ENDF/B-V (238GROUPNDF5)
Comments: All cross-sections were processed automatically by the CSAS25 sequence of SCALE-4.3. CSAS25 uses the BONAMI code to apply the Bondarenko resonance self-shielding method for nuclides with Bondarenko data (unresolved energy range; nuclides with resonance structure but no ENDF resonance data); it then invokes NITAWL-II to perform Nordheim resonance self-shielding corrections (resolved energy range). Calculations performed in 238 energy groups, with structure selected based on typical LWR spectra. The CSAS25 sequence then invokes KENO Va for the transport solution. All calculations were run on a DEC ALPHA Station 500. KENO Va is a multi-group-based 3-D Monte Carlo criticality code. Fuel and clad cylinders and the square boundary were modelled explicitly within KENO. The fuel was assumed to be 10 cm tall, but reflective boundary conditions were used on all boundaries to represent infinite fuel length in an infinite lattice. A P_3 scattering approximation was employed. No nuclides were substituted or omitted from the calculations. Typical statistical error on results of about 0.0004 for a 1-sigma confidence level. Calculations were based on a total of 2 100 generations of 1 000 neutrons each. The first 100 generations were skipped in the calculation of k_{eff} to allow for source convergence.

32. PSI, Switzerland

Institute: Paul Scherrer Institute
Participants: Peter Grimm
Computer code: BOXER
Data library: JEF-1
Comments: Cross-sections from JEF-1 (except ^{155}Gd from JENDL-2, zircaloy-2 from ENDF/B-IV), processed by the PSI code ETOBOX. Calculations performed in 70 groups (the 69-group WIMS structure + one group at 10-15 MeV, thermal cut-off 1.3 eV). Point data in the resonance range (1.3 eV-907 eV), typically 7 000-8 000 points. Tabulated resonance cross-sections collapsed to groups for E > 907 eV. Thermal scattering matrix for hydrogen in water from JEF-1 $S(\alpha,\beta)$ matrix. Calculations used the BOXER cell and two-dimensional transport and depletion code, which was developed at PSI. Resonance self-shielding calculated by a pointwise two-region collision probability calculation (1.3 eV < E < 907 eV), tabular interpolation versus temperature and equivalent dilution cross-section for E > 907 eV, Dancoff factor corrected for square cell outer boundary. The cell calculation was performed by one-dimensional integral transport calculation in cylindrical geometry with white boundary condition. Fundamental mode spectrum (k_{eff} = 1) in 70 groups by B1 method for homogenised cell. Cladding composition replaced by zircaloy-2, 4.3206E-2 atoms/barn.cm (sum of number densities for Zr, Fe and Cr in specification).

33. ANL, United States

Institute: Argonne National Laboratory
Participants: Roger Blomquist
Computer code: VIM
Data library: ENDF/B-VI
Comments: Calculations with ENDF/B-VI neutron data library using VIM cross-section processing codes entirely independent of NJOY (UNIDOP resolved resonance continuous energy code, using Reich-Moore, single and multi-level Breit-Wigner, and Adler-Adler resonance parameters, AURIX unresolved resonance probability tables code, truncated ENDF File 6 distributions to isotropic). Continuous energy data, with selected numbers of continuous energy points, e.g. 76 000 (^{235}U), 70 000 (^{238}U), 24 000 (^{239}Pu), 31 000 (^{50}Cr), etc. Calculations performed with VIM continuous-energy Monte Carlo neutron transport code (ENDF/B-V available at RSICC and OECD/NEA Data Bank), with power iteration on fission source distribution. No variance reduction used, except optimal combined eigenvalue estimator. Exact geometry modelled, using combinatorial geometry. No nuclides substituted or omitted. Eigenvalue uncertainties were ~0.0008, with five generations used to converge fission source.

34. KEPCO/NETEC and KAIST, Republic of Korea

Institute: Korea Electric Power Corporation (KEPCO/NETEC), Korea Advanced Institute of Science and Technology (KAIST)
Participants: Duck Joon Koh, Je Keun Chon, Byung Tae Kim (KEPCO/NETEC), Kyung Taek Lee, Chang Keun Jo, Nam Zin Cho (KAIST)
Computer code: HELIOS
Data library: HELIOS library generated from ENDF/B-VI
Comments: Calculations with 89-group HELIOS library (hy8918-961a.dat) based on ENDF/B-VI evaluations. Employed convergence limit of 2.0E-5 on eigenvalue.

35. KFKI, Hungary

Institute: KFKI Atomic Energy Research Institute
Participants: Gabor Hordosy
Computer code: MCNP4C
Data library: DLC-189
Comments: Continuous energy MCNP libraries from the DLC-189 data package were used with the .60c data set. For fission products other than ^{99}Tc, ^{109}Ag, ^{133}Cs, ^{153}Eu and ^{155}Gd, ENDF/B-V based libraries were used. For all other isotopes (actinides, structural material, H, O and the above-mentioned fission products ENDF/B-VI Rel. 1 and 2 based libraries were used. The statistical error (one standard deviation) of k_{eff} values varied between 2.4E-04 and 2.9E-04. The statistical error of each individual k_{eff} is given above together with the multiplication factor.

36. KFKI, Hungary

Institute: KFKI Atomic Energy Research Institute
Participants: Gabor Hordosy
Computer code: MCNP4C
Data library: JEF-2.2
Comments: Continuous energy MCNP libraries based on JEF-2.2 derived by ENEA, Bologna, contained in the CD NEA-1616/01 were used. The statistical error (one standard deviation) of k_{eff} values varied between 2.4E-04 and 3.0E-04. The statistical error of each individual k_{eff} is given above together with the multiplication factor.

37. EMS, Sweden

Institute: E Mennerdahl Systems
Participants: Dennis Mennerdahl
Computer code: MCNP4C2
Data library: ENDF/B-VI/V
Comments: NEA Data Bank packaged versions of MCNP4C2 for PC (CCC-0701/01) and of cross-section libraries (DLC-0200/03) were used. In the main study, the .61c (delayed neutron) set was used. The .49c (unresolved resonance data tables) set was used in the evaluation of reactivity influences of selected Pu and Cm nuclides. Both are based on ENDF/B-VI. The cross-sections for some of the fission products are based on ENDF/B-V. The cross-sections are in continuous energy form. For each problem, 915 000 neutrons (3 000*305, of which only 15 000 were "inactive") were run. The standard deviations are between 0.00062 and 0.00076. K_{eff} based on combined collision, absorption and track length estimates.

Appendix III

A STUDY OF COMPUTER CODE AND DATA BEHAVIOUR FOR MOX PIN CELL CALCULATIONS

M.D. DeHart
Oak Ridge National Laboratory*
USA

Introduction

The charter of the OECD Burn-up Credit Working Group is the study of phenomena related to burn-up credit through inter-code comparisons. Such comparisons serve to highlight potential limitations or deficiencies in various code systems, data or modelling methods. The Phase IV-A benchmark specification [1], distributed to the working group in March 1998, describes calculations to be performed for the analysis of mixed oxide (MOX) fuel pins in a two-dimensional, infinite lattice configuration. Benchmark calculations based on this specification were recently completed at the Oak Ridge National Laboratory (ORNL) in the US. These calculations were performed using three different computer codes: XSDRNPM [2] (1-D discrete ordinates), NEWT [3] (2-D discrete ordinates with flexible geometry capabilities), and KENO-V.a [4] (3-D Monte Carlo). In addition, calculations were performed using each code with both the 238-group [5] and 44-group [6] versions of ENDF/B-V data available within the SCALE code system [7].

It was pointed out by A. Santamarina at the 1998 meeting of the Burn-up Credit Working Group that the Wigner-Seitz approximation for a pin cell in MOX fuel can produce erroneous results. The Wigner-Seitz approximation uses a cylindrical outer boundary and white boundary conditions to replace the square moderator boundary associated with a pin in a square lattice [8]. The exact geometry is depicted in Figure 1(a); the Wigner-Seitz approximation is shown in Figure 1(b). In the Wigner-Seitz equivalent cell, a radius is used such that the volume of the moderator is precisely the same as in the exact cell. White boundary conditions are applied in the approximate model because of computational difficulties associated with reflective boundary conditions on a cylindrical outer boundary. Because the approximation reduces a two-dimensional cell to a simpler one-dimensional form, it becomes more computationally efficient. In the past, this approximation has been found to be acceptable for UO_2 fuel pin-cell modelling.

To confirm the response of the Wigner-Seitz cell approximation for MOX fuel, and to try to understand the physics of the matter, ORNL volunteered to use two codes within the SCALE system to study this effect.

Approach

ORNL has the unique capability to study the behaviour of the pin-cell model based on discrete ordinates theory, using 1-D XSDRNPM calculations and 2-D NEWT calculations, using identical

* Managed by UT-Battelle, LLC, under contract DE-AC05-00OR22725 with the US Department of Energy.

Figure 1. Exact and Wigner-Seitz representations of a pin cell

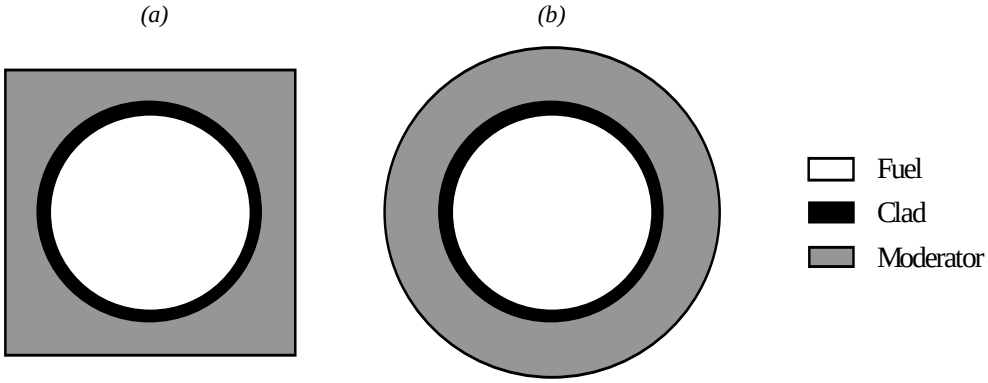

cross-section data and processing techniques. The 1-D nature of XSDRNPM requires the use of the Wigner-Seitz equivalent cell. In general, this approximation is also necessary in multi-dimensional discrete ordinates methods because of the constraints of orthogonal meshing schemes. However, the NEWT transport code allows a flexible, unstructured grid layout, such that the cylindrical fuel/clad region can be very closely approximated within an exact square pin cell boundary. Figure 2 illustrates a NEWT model for a fuel/clad/moderator pin cell. All computational cells within this model are polygons; irregular (non-rectangular) cells are used to closely approximate curved surfaces. In practice, symmetry would be used to reduce this problem to a 1/4 cell representation of a single quadrant. After NEWT and XSDRN calculations were completed, significant discrepancies were noted between results, especially for the SCALE 238-group library. Hence, KENO-V.a calculations were performed to assess which method was providing the largest error.

Figure 2. NEWT grid structure for a pin cell

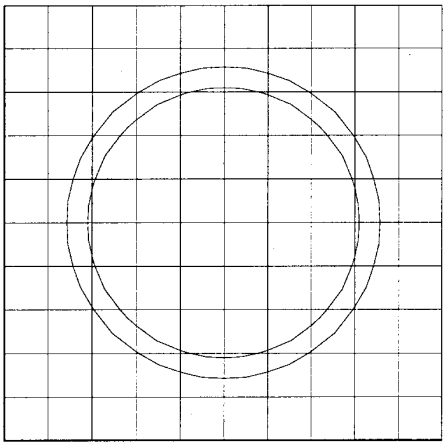

Results of benchmark calculations

Results of the six sets of calculations, as submitted to the Working Group, are listed in Table 1. The discrete ordinates solutions were performed using S_8 quadrature and P_3 scattering, with convergence criteria of 0.0001; KENO-V.a calculations also used P_3 scattering, and were based on 2×10^6 neutron

Table 1. ORNL Phase IV-A results submitted to the OECD Burn-up Credit Working Group

Case no.	XSDRNPM 44-group	NEWT 44-group	KENO-V.a 44-group	XSDRNPM 238-group	NEWT 238-group	KENO-V.a 238-group
1	1.2947	1.2980	1.2979(4)*	1.2916	1.2989	1.2978(5)
2	1.1779	1.1807	1.1802(4)	1.1741	1.1807	1.1795(4)
3	1.1081	1.1107	1.1108(4)	1.1041	1.1103	1.1093(4)
4	1.0523	1.0546	1.0543(4)	1.0480	1.0538	1.0527(4)
5	1.2385	1.2415	1.2413(4)	1.2342	1.2412	1.2406(4)
6	1.2013	1.2039	1.2041(4)	1.1961	1.2028	1.2017(4)
7	1.1728	1.1751	1.1755(4)	1.1669	1.1732	1.1724(4)
8	1.2386	1.2416	1.2416(4)	1.2340	1.2411	1.2407(4)
9	1.2033	1.2060	1.2053(4)	1.1975	1.2042	1.2027(4)
10	1.1795	1.1819	1.1812(4)	1.1724	1.1788	1.1778(4)
11	1.1317	1.1345	1.1345(4)	1.1278	1.1343	1.1333(4)
12	1.0519	1.0544	1.0542(4)	1.0480	1.0539	1.0539(4)
13	0.9882	0.9903	0.9908(3)	0.9843	0.9896	0.9891(4)
14	1.1955	1.1987	1.1985(4)	1.1908	1.1978	1.1957(4)
15	1.1514	1.1541	1.1537(4)	1.1461	1.1527	1.1516(4)
16	1.1196	1.1220	1.1217(4)	1.1138	1.1199	1.1196(4)
17	1.1957	1.1989	1.1983(4)	1.1908	1.1979	1.1968(4)
18	1.1538	1.1566	1.1563(4)	1.1480	1.1547	1.1539(4)
19	1.1274	1.1299	1.1301(4)	1.1206	1.1269	1.1259(4)
20	1.4162	1.4180	1.4182(4)	1.4102	1.4154	1.4146(4)
21	1.2221	1.2239	1.2242(4)	1.2189	1.2243	1.2239(4)
22	1.1106	1.1123	1.1122(3)	1.1078	1.1129	1.1129(4)
23	1.0322	1.0337	1.0341(4)	1.0290	1.0337	1.0322(4)
24	1.2918	1.2937	1.2934(4)	1.2884	1.2942	1.2934(5)
25	1.2160	1.2176	1.2180(4)	1.2129	1.2182	1.2172(4)
26	1.1667	1.1678	1.1676(4)	1.1623	1.1674	1.1675(4)
27	1.2918	1.2937	1.2937(4)	1.2884	1.2941	1.2933(4)
28	1.2164	1.2180	1.2170(4)	1.2131	1.2184	1.2176(4)
29	1.1694	1.1705	1.1700(4)	1.1645	1.1696	1.1688(4)
30	1.1958	1.1975	1.1971(4)	1.1924	1.1976	1.1972(4)
31	1.0623	1.0639	1.0641(3)	1.0595	1.0643	1.0639(4)
32	0.9706	0.9719	0.9722(3)	0.9676	0.9719	0.9715(4)
33	1.2699	1.2719	1.2725(4)	1.2662	1.2719	1.2720(4)
34	1.1766	1.1784	1.1780(4)	1.1733	1.1785	1.1777(4)
35	1.1192	1.1203	1.1195(3)	1.1147	1.1197	1.1188(4)
36	1.2699	1.2720	1.2718(4)	1.2662	1.2719	1.2703(4)
37	1.1771	1.1789	1.1785(4)	1.1736	1.1788	1.1781(4)
38	1.1222	1.1234	1.1235(4)	1.1173	1.1223	1.1217(4)
39	1.1887	1.1927	1.1911(4)	1.1866	1.1948	1.1931(4)
40	1.1063	1.1101	1.1091(4)	1.1013	1.1090	1.1070(4)
41	1.0633	1.0669	1.0665(4)	1.0574	1.0646	1.0628(4)
42	1.0271	1.0304	1.0299(4)	1.0208	1.0277	1.0261(4)
43	1.1067	1.1105	1.1096(4)	1.1013	1.1090	1.1080(4)
44	1.0683	1.0720	1.0713(4)	1.0613	1.0687	1.0675(5)
45	1.0407	1.0443	1.0440(4)	1.0329	1.0401	1.0383(4)
46	1.1590	1.1630	1.1627(4)	1.1531	1.1613	1.1591(5)
47	1.1448	1.1485	1.1477(4)	1.1372	1.1450	1.1437(4)
48	1.1335	1.1368	1.1364(4)	1.1249	1.1324	1.1306(4)
49	1.1594	1.1634	1.1625(4)	1.1530	1.1611	1.1593(4)
50	1.1496	1.1535	1.1526(4)	1.1407	1.1487	1.1471(4)
51	1.1470	1.1506	1.1497(4)	1.1364	1.1442	1.1423(4)
52	1.0530	1.0567	1.0569(4)	1.0482	1.0556	1.0539(4)
53	1.0035	1.0069	1.0067(4)	0.99802	1.0050	1.0039(4)
54	0.9622	0.9653	0.9656(3)	0.9565	0.9630	0.9617(4)

* 1.2979(4) should be read as 1.2979 ± 0.0004.

Table 1. ORNL Phase IV-A results submitted to the OECD Burn-up Credit Working Group (*cont.*)

Case no.	XSDRNPM 44-group	NEWT 44-group	KENO-V.a 44-group	XSDRNPM 238-group	NEWT 238-group	KENO-V.a 238-group
55	1.0536	1.0574	1.0575(4)	1.0485	1.0560	1.0546(4)
56	1.0093	1.0129	1.0118(4)	1.0029	1.0100	1.0085(4)
57	0.9772	0.9806	0.9799(3)	0.9702	0.9770	0.9759(4)
58	1.1080	1.1120	1.1114(4)	1.1021	1.1102	1.1087(4)
59	1.0896	1.0934	1.0930(4)	1.0822	1.0900	1.0890(4)
60	1.0766	1.0800	1.0794(4)	1.0683	1.0757	1.0739(4)
61	1.1086	1.1127	1.1125(4)	1.1023	1.1104	1.1090(4)
62	1.0953	1.0993	1.0991(4)	1.0868	1.0947	1.0935(4)
63	1.0918	1.0955	1.0950(4)	1.0818	1.0895	1.0875(4)

* 1.2979(4) should be read as 1.2979 ± 0.0004.

histories. Overall, results show good agreement between NEWT and KENO-V.a for each of the two cross-section libraries. Differences between these results for each code and cross-section library are illustrated in Figure 3, which shows the error of each solution relative to the KENO-V.a solution for each case. One-sigma error bars are shown for each of the KENO-V.a calculations; deterministic calculations have an error term on the order of ±0.0001.

Figure 3. Difference between k_{eff} calculated by KENO-V.a/238g and other solutions

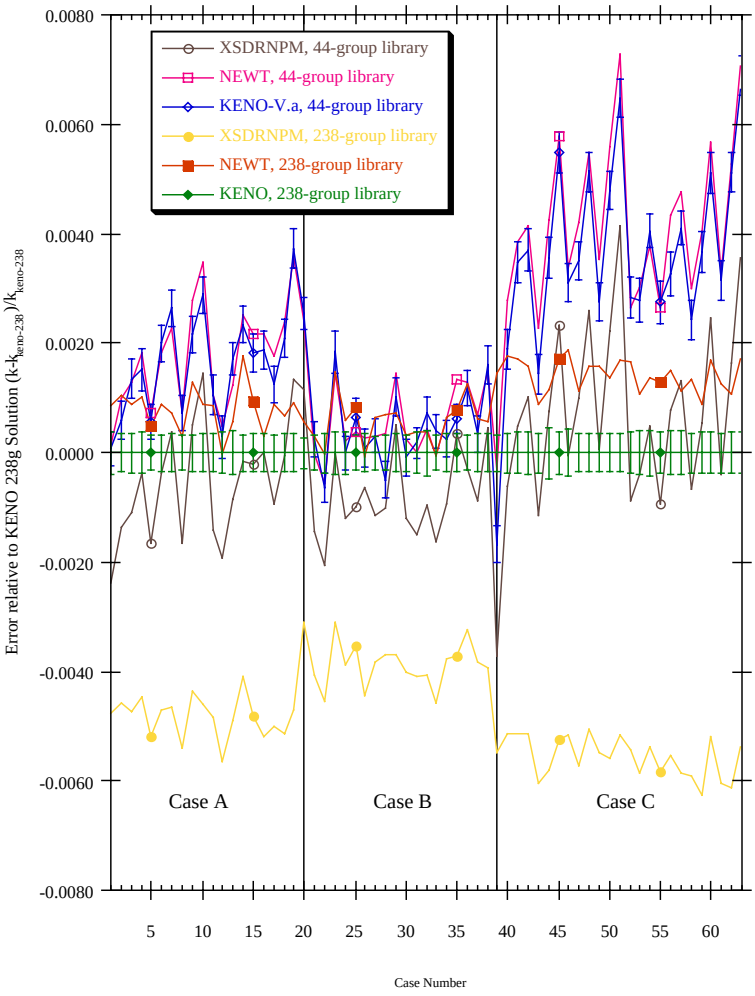

Discussion

Figure 3 illustrates significant differences between solutions for the various codes. Since there is no absolute solution, all calculations are compared to 238-group KENO-V.a results. This is not meant to imply that KENO provides the best solution; it is simply used as a reference solution for comparison of relative error terms.

Numerous features are observed in the data of Table 1 and the plots of Figure 3, as listed below:

- Both NEWT and KENO-V.a are in good agreement. On the average, NEWT is 0.098% higher than KENO with the 238-group library. The agreement is improved with the 44-group library, with NEWT being 0.026% higher on the average.

- All calculations show the best agreement for Case B (weapons Pu) fuel. Agreement is not as good for Case A (first generation recycle), and is worst for Case C (later generation recycle). The trend mirrors relative concentrations of ^{238}Pu, ^{240}Pu and ^{242}Pu in the fuels, which are lowest for Case B, higher in Case A and highest in Case C.

- The change in bias with fuel type relative to the KENO/238g solution is in a positive direction for all codes and data, with the exception of the 238g XSDRNPM solution, which is in a negative direction.

- There are definite group structure effects – 44-group calculations show more variation with burn-up than 238-group calculations, relative to KENO 238-group calculations. The relative error increases with increasing burn-up.

- The largest variation between 238-group and 44-group results is seen for cases with no fission products and *all* actinides. The error is significantly larger than for cases with no fission products and *major* actinides. This group structure effect must therefore be due to treatment of curium nuclides.

- The XSDRNPM 238-group calculations are on the average 0.47% lower than corresponding 44-group XSDRNPM calculations and 0.48% lower than KENO 238-group calculations. The 44-group XSDRNPM solutions average 0.22% less than average 44-group KENO solutions.

Differences between 44-group and 238-group libraries are most likely the result of differences between the group structures in the SCALE libraries. Although the broad group structure of the 44-group library retains much of the thermal range structure of its parent 238-group library, lower energy resonances in plutonium may not be properly captured. In addition, the 44-group library was collapsed from the 238-group library assuming a fresh-fuel UO_2 pin spectrum. This collapsing spectrum may be inadequate to capture the effects of high concentrations of plutonium in MOX fuels.

The behaviour of the XSDRNPM solutions relative to KENO and NEWT solutions is believed to be a result of the Wigner-Seitz approximation. This approximation has two components: (1) a cylindrical moderator region in place of the actual square region, and (2) a white boundary condition rather than a more realistic reflective boundary. If the discrepancy between Wigner-Seitz and an exact model is due solely to the first item, then the behaviour most likely results from different moderating mechanisms between the two different moderator regions. If the differences result from the application of a white boundary condition, then inter-cell streaming effects are important; inter-cell streaming would not occur with a white boundary condition. To investigate these phenomena further, additional NEWT calculations were performed to simulate these effects. To test the effect of a white boundary condition, the NEWT

calculations performed earlier were modified by replacing the reflective boundary conditions on the moderator boundaries with white boundary conditions. Results (relative to 238-group KENO-V.a calculations) are illustrated in Figure 4, and show that the white boundary condition has very little effect on the calculation of k_{eff} for the MOX benchmarks.

Figure 4. Effect of white boundary conditions in NEWT calculations

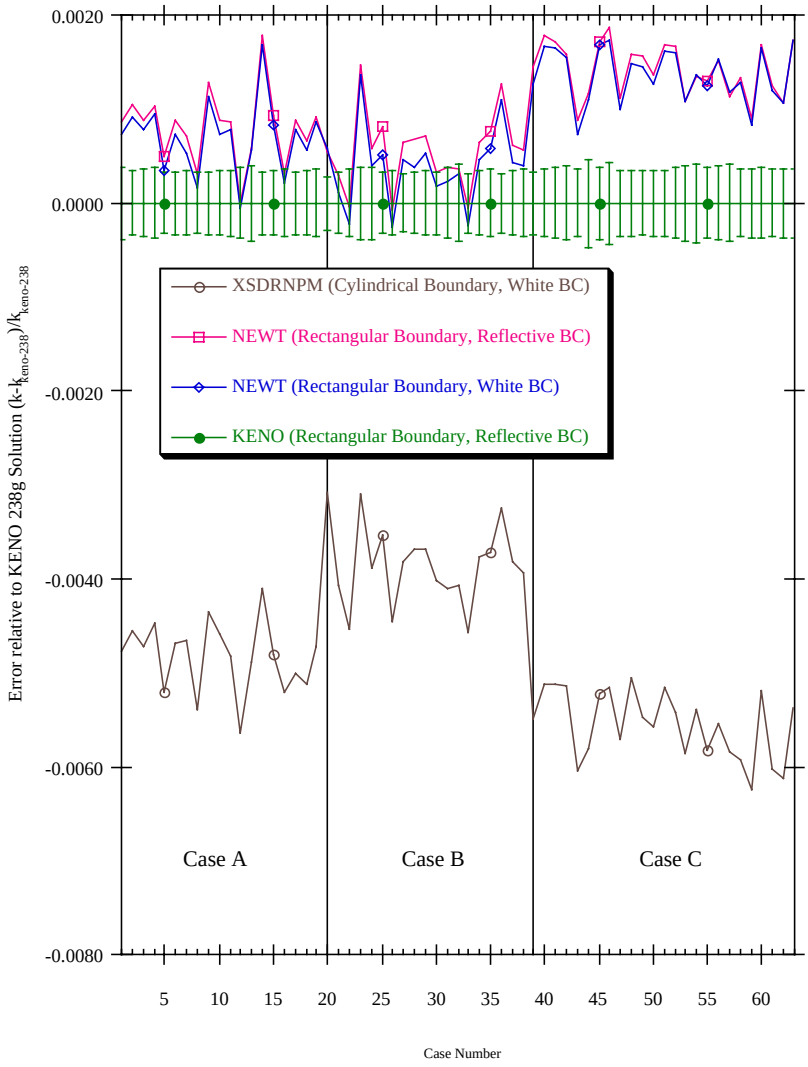

Next, calculations were performed to simulate the Wigner-Seitz approximation within NEWT. This approximation cannot be implemented directly within NEWT, since NEWT is a two-dimensional code based on a Cartesian co-ordinate system. However, the cylindrical cell was approximated using a cylindrical moderator region surrounded by a white media and white boundary conditions, as depicted in Figure 5. The white media is a fictitious material with a total and within-group scattering cross-section of 1 barn. In the NEWT solution, this has the effect of isotropically distributing neutrons within each energy group, which would look like a boundary condition beyond the moderator boundary. Figure 6 shows the results plotted in Figure 4, with the addition of the NEWT calculated using a simulated Wigner-Seitz cell. The NEWT calculations with the simulated Wigner-Seitz approximation are in close agreement with 1-D XSDRNPM calculations. These results seem to indicate that the underestimate of k_{eff} by XSDRNPM is the result of the cylindrical approximation of the moderator region.

Figure 5. Wigner-Seitz cell representation using NEWT

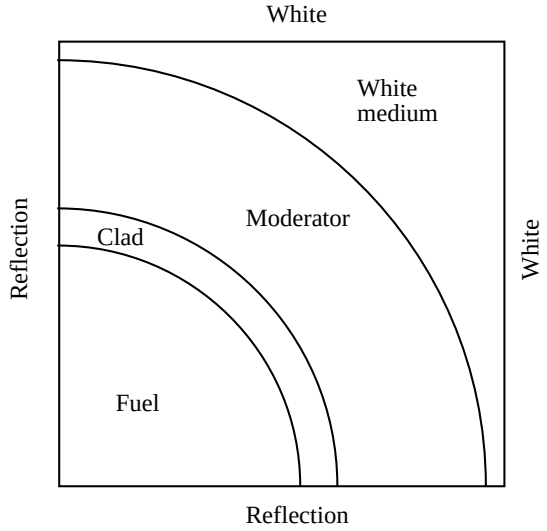

Incidentally, Figure 6 also shows closest agreement between XSDRNPM and NEWT for Case C fuel. This is inconsistent with other calculations, for which the closest agreement is always seen with Case B. It is suspected that the close agreement for Case C is coincidental; it is more likely that there is a general 0.1% bias between XSDRNPM and NEWT, which offsets the bias between the two results for Case C. Such a bias could result from the simulated Wigner-Seitz cell in NEWT. However, no effort was made to determine if such a bias was present; the goal was to demonstrate the similarity of error in the cylindrical approximation for two independent computer codes.

It can be shown that the average moderator thickness for a cylindrical cell (moderator radius/fuel radius) is always less than that of a square cell (average moderator radius/fuel radius). Thus, even though the Wigner-Seitz approximation provides equivalent moderator volumes, the effective moderator thickness seen by a neutron leaving the fuel region is larger. This may result in increased moderation in the square cell relative to the cylindrical approximation. Because uranium is relatively insensitive to small spectral changes, the effect of the cylindrical approximation would be small. However, in MOX fuel, because of the ~0.3eV resonances in ^{239}Pu and ^{241}Pu (primarily the former), and the 1.1 eV resonance in ^{240}Pu, plutonium fuels are more sensitive to spectral changes. It appears that because the broad-group structure of the SCALE 44-group library smears low-resonance-energy cross-sections of its parent 238-group library, the 44-group library is not as sensitive to the spectral effects of the cell approximation.

Summary

The purpose of the OECD suite of benchmarks is to obtain a better understanding of computer code and data behaviour with respect to well-defined burn-up credit problems. The Phase IV-A benchmark provides a new twist on burn-up credit analyses, with significant amounts of plutonium present. The low-energy resonances in plutonium nuclides create special computational problems that are not seen in uranium fuels. Specifically, group structure effects in multi-group methods may be more pronounced, especially for broad group libraries not tailored for MOX systems. Furthermore, because of the sensitivity of k_{eff} to the thermal spectrum in MOX fuel, the 1-D Wigner-Seitz cell approximation may be inadequate for MOX fuel pin cells. The error has been found to be as large as ~0.5% $\Delta k/k$ in this study, and is therefore an important consideration in the analysis of MOX fuel.

Figure 6. NEWT calculations with simulated Wigner-Seitz boundary

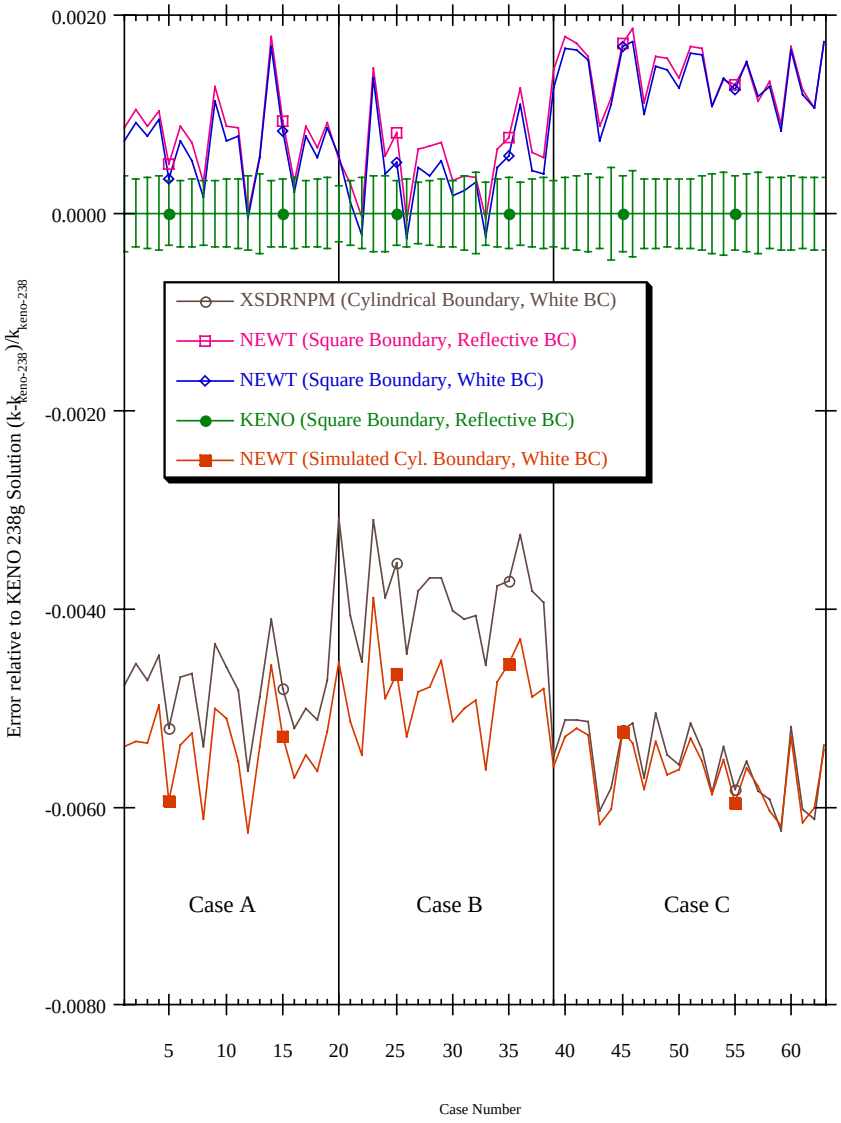

REFERENCES

[1] R.L. Bowden and P.R. Thorne, "Problem Specification for the OECD/NEA NSC Burn-up Credit Benchmark Phase IV-A: Mixed Oxide (MOX) Fuels", Version 1, March 1998.

[2] N.M. Greene and L.M. Petrie, "XSDRNPM: A One-dimensional Discrete-ordinates Code for Transport Analysis", Sect. F3 of *SCALE: A Modular Code System for Performing Standardized Computer Analyses for Licensing Evaluation*, NUREG/CR-0200, Rev. 4 (ORNL/NUREG/CSD-2/R4), Vols. I, II and III (April 1995). Available from Radiation Shielding Information Center as CCC-545.

[3] M. D. DeHart, "An Advanced Deterministic Method for Spent-fuel Criticality Safety Analysis", *Trans. Am. Nucl. Soc*., 78, 170 (1998).

[4] L.M. Petrie and N.F. Landers, "KENO V.a: An Improved Monte Carlo Criticality Program with Supergrouping", Sect. F11 of *SCALE: A Modular Code System for Performing Standardized Computer Analyses for Licensing Evaluation*, NUREG/CR-0200, Rev. 4 (ORNL/NUREG/CSD-2/R4), Vols. I, II and III (April 1995). Available from Radiation Shielding Information Center as CCC-545.

[5] N.M. Greene, *et al*., "The LAW Library – A Multi-group Cross-section Library for Use in Radioactive Waste Analysis Calculations", ORNL/TM-12370, Oak Ridge National Laboratory, Martin Marietta Energy Systems, Inc. (1994).

[6] M.D. DeHart and S.M. Bowman, "Validation of the SCALE Broad Structure 44-group ENDF/B-V Cross-section Library for Use in Criticality Safety Analyses", NUREG/CR-6102 (ORNL/TM-12460), Martin Marietta Energy Systems, Inc., Oak Ridge National Laboratory (1994).

[7] "SCALE: A Modular Code System for Performing Standardized Computer Analyses for Licensing Evaluation", NUREG/CR-0200, Rev. 4 (ORNL/NUREG/CSD-2/R4), Vols. I, II and III (April 1995). Available from Radiation Shielding Information Center as CCC-545.

[8] E.E. Lewis and W.F. Miller, Jr., "Computational Methods of Neutron Transport", John Wiley and Sons, New York (1984).

Appendix IV

EMS MOX FUEL ROD INFINITE ARRAY STUDY

Dennis Mennerdahl
E. Mennerdahl Systems (EMS)

Infinite array of MOX fuel rods with uniform burn-up

This phase contains a very simple geometry model; an infinitely long cylindrical PWR fuel rod with cladding in a square cell. The 63 cases contain many different types of fresh and irradiated fuel. The calculation cases are useful for comparison of cross-section data. SCALE and MCNP have been used with different cross-section sets. Some of them lack some of the curium isotopes, but most of the problems can still be calculated.

The Expert Group results

The results of the EG are not yet published, but an average of the first 37 contributions for each case is used here as a reference. It is just an average and not the best estimate of each case. A large deviation does not necessarily indicate a poor result. As described below, many of the SCALE results are based on 1-D calculations which are not very good for this study. There is a very clear negative bias in those results.

One-dimensional approximation of a square fuel cell

The first comparison of the OECD/NEA NSC Expert Group (EG) results showed that many of the SCALE CSAS1X values of k_{eff} were unexpectedly low. The differences in k_{eff} between the 44-group and the 238-group ENDF/B-V libraries were very large. The CSAS1X calculation sequence in SCALE uses 1-D approximations of the fuel cell. The square fuel cell boundary is converted to a cylindrical boundary with "white" reflection. This has been found to be an adequate procedure in the past for uranium dioxide fuel. The procedure is used to obtain values of k_{∞} with the XSDRNPM deterministic code in SCALE. It is also used to obtain homogenised cross-sections for fuel assemblies in transport casks and storage pools. Another application is depletion calculations.

During the OECD/NEA study, DeHart demonstrated that the 1-D approximation is not as good for MOX fuel. New results with CSAS1X and CSAS25 with identical cross-sections show this clearly. The bias is largest for the 238-group library. It is negative, consistent for all cases and between 0.2 and 0.6% of k_{eff}.

My first impression of the Phase IV-A calculation results (CSAS1X) was that the 238-group library for SCALE is not as reliable as I had previously thought. The large difference between CSAS1X and CSAS25 results did not change this impression. However, after the additional studies by DeHart

and now by myself, it is clear that the larger differences for the 238-group cross-section library than for the 44-group and 27-group burn-up libraries correspond to real physics behaviour. The larger differences actually demonstrate that the 238-group library is better than the others. The MCNP calculation results confirm this.

Table 1 includes SCALE4.3 CSAS1X and SCALE4.4 CSAS25 calculations using three different cross-section libraries. The 27-group burn-up library is based on ENDF/B-IV and does not include all the curium isotopes required to complete all calculation cases. The 44-group and 238-group libraries are based on ENDF/B-V and include all nuclides needed for the 63 calculation cases.

Table 1. Comparison of the SCALE sequences CSAS1X and CSAS25

Case	EG-Av k_{eff}	SCALE 4.3 – 10^2 * Δk_{eff} – Difference to EG average – 1-D approximations					
		27 group BU ENDF/B-IV		44 group ENDF/B-V		238 group ENDF/B-V	
		CSAS1X	CSAS25	CSAS1X	CSAS25	CSAS1X	CSAS25
1	1.3002	-0.02	0.35	-0.28	-0.29	-0.86	-0.36
2	1.1816	0.11	0.55	-0.37	-0.15	-0.75	-0.20
3	1.1108	0.02	0.35	-0.27	-0.01	-0.67	-0.20
4	1.0540	-0.09	0.32	-0.16	0.04	-0.60	-0.11
5	1.2429	-0.01	0.32	-0.43	-0.24	-0.87	-0.20
6	1.2051	-0.08	0.26	-0.38	-0.22	-0.90	-0.22
7	1.1755	-0.13	0.19	-0.26	-0.11	-0.85	-0.46
8	1.2425			-0.39	-0.14	-0.85	-0.26
9	1.2063			-0.30	-0.08	-0.88	-0.33
10	1.1811			-0.16	0.12	-0.87	-0.39
11	1.1345	-0.07	0.29	-0.28	-0.14	-0.66	-0.08
12	1.0539	-0.14	0.20	-0.20	0.08	-0.59	-0.13
13	0.9893	-0.18	0.10	-0.10	0.06	-0.50	0.08
14	1.1989	-0.23	0.17	-0.34	-0.14	-0.81	-0.25
15	1.1540	-0.28	0.05	-0.26	0.03	-0.79	-0.26
16	1.1215	-0.34	-0.01	-0.18	-0.03	-0.77	-0.33
17	1.1988			-0.31	0.01	-0.80	-0.19
18	1.1559			-0.20	0.13	-0.79	-0.42
19	1.1285			-0.11	0.18	-0.79	-0.26
20	1.4144	-0.75	-0.52	0.17	0.41	-0.41	-0.07
21	1.2238	-0.24	0.02	-0.17	0.06	-0.48	-0.02
22	1.1129	-0.16	0.17	-0.22	-0.06	-0.50	-0.06
23	1.0337	-0.22	0.10	-0.14	0.02	-0.47	-0.06
24	1.2943	-0.37	-0.05	-0.25	-0.01	-0.59	-0.16
25	1.2194	-0.22	0.03	-0.34	-0.14	-0.67	-0.19
26	1.1691	-0.22	0.05	-0.26	-0.09	-0.68	-0.11
27	1.2944			-0.26	-0.13	-0.60	-0.01
28	1.2198			-0.34	-0.12	-0.68	-0.19
29	1.1716			-0.25	-0.03	-0.71	-0.24
30	1.1971	-0.31	0.04	-0.13	0.01	-0.47	0.01
31	1.0638	-0.20	0.12	-0.14	0.02	-0.42	-0.02
32	0.9714	-0.22	0.09	-0.07	0.10	-0.38	-0.02

Table 1. Comparison of the SCALE sequences CSAS1X and CSAS25 (*cont.*)

Case	EG-Av k_{eff}	SCALE 4.3 – 10^2 * Δk_{eff} – Difference to EG average – 1-D approximations					
		27 group BU ENDF/B-IV		44 group ENDF/B-V		238 group ENDF/B-V	
		CSAS1X	CSAS25	CSAS1X	CSAS25	CSAS1X	CSAS25
33	1.2719	-0.47	-0.16	-0.20	0.02	-0.57	-0.11
34	1.1791	-0.35	-0.18	-0.25	-0.18	-0.60	-0.16
35	1.1209	-0.36	-0.11	-0.20	-0.03	-0.62	-0.31
36	1.2722			-0.23	-0.03	-0.60	-0.24
37	1.1800			-0.29	-0.11	-0.66	-0.25
38	1.1239			-0.20	-0.05	-0.66	-0.14
39	1.1958	0.28	0.57	-0.71	-0.39	-0.92	-0.19
40	1.1103	0.20	0.63	-0.40	-0.02	-0.90	-0.20
41	1.0654	0.05	0.43	-0.20	0.06	-0.80	-0.24
42	1.0281	-0.11	0.25	-0.09	0.15	-0.73	-0.14
43	1.1095			-0.27	0.05	-0.82	-0.21
44	1.0691			-0.07	0.12	-0.78	-0.20
45	1.0400			0.08	0.39	-0.71	-0.11
46	1.1631	0.14	0.60	-0.40	-0.04	-0.99	-0.33
47	1.1475	-0.05	0.34	-0.26	0.05	-1.03	-0.42
48	1.1349	-0.19	0.19	-0.13	0.22	-1.00	-0.29
49	1.1626			-0.32	-0.04	-0.96	-0.33
50	1.1509			-0.12	0.18	-1.02	-0.36
51	1.1461			0.10	0.38	-0.97	-0.34
52	1.0560	-0.01	0.48	-0.30	-0.03	-0.78	-0.22
53	1.0048	-0.14	0.29	-0.13	0.15	-0.68	-0.13
54	0.9624	-0.23	0.17	-0.02	0.24	-0.59	-0.07
55	1.0560			-0.23	0.11	-0.75	-0.19
56	1.0096			-0.03	0.25	-0.67	-0.08
57	0.9764			0.09	0.43	-0.62	-0.01
58	1.1112	-0.13	0.25	-0.32	0.10	-0.90	-0.31
59	1.0913	-0.30	0.09	-0.17	0.08	-0.91	-0.28
60	1.0771	-0.41	-0.04	-0.05	0.20	-0.87	-0.29
61	1.1114			-0.28	-0.02	-0.91	-0.22
62	1.0958			-0.05	0.16	-0.90	-0.20
63	1.0911			0.07	0.39	-0.93	-0.26
The standard deviations are about 0.0007 (900 000 neutrons)							
Diff	0.0000	-0.16	0.18	-0.21	0.03	-0.74	-0.20
Max+	0.0000	0.28	0.63	0.17	0.43	-0.38	0.08
Max-	0.0000	-0.75	-0.52	-0.71	-0.39	-1.03	-0.46

Figure 1 shows the large negative biases that can be expected if CSAS1X is used with the 238-group cross-section library for MOX fuel rod lattices. Simulations of the same approximations using MCNP are also shown. Individual pairs of results should not be compared due to insufficient statistics (900 000 neutrons). Case 39 is an exception, using 9 million neutrons.

Figure 1. Influence of 1-D approximations – SCALE and MCNP evaluation

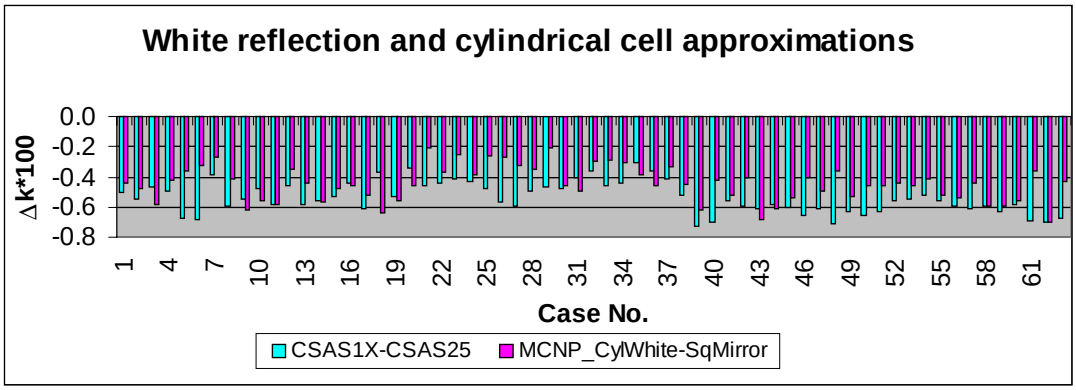

MCNP4C2 with various combinations of square and cylindrical fuel cells with either mirror or white reflection boundary conditions gave similar differences as those found using SCALE. For Case 39, the white reflection in MCNP4C2 with Ur .49c cross-sections gave a k_{eff} of 1.1934 with a σ of 0.0002. The corresponding result for mirror reflection was 1.1968. MCNP with a cylindrical fuel cell and white boundary conditions gave a k_{eff} of 1.1906. The total difference between results for a realistic fuel cell with mirror boundary conditions and a cylindrical fuel cell with white boundary conditions is 0.0062 using MCNP and 0.0073 using SCALE. The results are similar. These calculations were obtained with about 9 million neutron histories.

The remaining cases for Phase IV-A were also calculated, using only 900 000 neutron histories. The results for each case are given in Figure 1 and in Table 2 in the form of differences to the OECD/NEA average results. Except for Case 39, the statistics are not sufficient for comparisons of SCALE and MCNP for individual cases.

In Figure 2 the average deviation for all cases is given. It is clear that the total influence of the MCNP approximation with cylindrical cell and white reflection is similar in magnitude to the difference between SCALE CSAS1X and CSAS25. Further, and contrary to the results of DeHart, the major reason for the deviation appears to be the white reflection approximation as opposed to the cylindrical approximation. However, the effects are not independent. Both approximations contribute with moderation and self-shielding effects. The total effect is probably less than the sum of each individual effect on its own. In that case the first effect (white instead of mirror reflection) based on direct calculation is overestimated. The second effect (cylindrical instead of square cell) is underestimated when it is determined from the difference between the total and the first effect.

The 1-D cylindrical approximation with mirror reflection does not work at all. This is the reason it is not used in neutron physics calculations. An MCNP calculation of Case 39 using a cylindrical cell with mirror reflection was run. The result was 1.2483, which should be compared with 1.1968 for the square cell with mirror reflection. It is not a realistic physics simulation for neutrons. For this reason it is not easy to determine the exact influence of the cylindrical cell approximation separately. It can only be determined as a second approximation.

The white boundary condition results in slightly different moderation and self-shielding properties of the fuel cell than with mirror reflection. The cylindrical model of the square fuel cell also results in slightly different moderation and self-shielding. DeHart pointed out that the average moderator thickness is larger for the square cell than for the cylindrical cell. A comparison of the detailed neutron energy spectra in various parts of the fuel cell and in specific resonance energy regions may be of interest.

For under-moderated lattices, the cylindrical approximation is non-conservative. The opposite should be true for over-moderated lattices. If the cell material outside the fuel is not a moderator but a strong neutron absorber with resonances, the situation would be very different. An example is the storage of fuel rods in an iron matrix.

If the neutron energy spectrum using 1-D approximations is not adequate, the depletion results could be significantly incorrect. The build-up of actinides is strongly dependent on the neutron energy spectrum. Early results from Phase IV-B, which I have not yet participated in, indicate large differences.

Comparison of cross-section libraries for SCALE and MCNP4C2

Table 2 presents a comparison of the Expert Group (EG) average and a number of Monte Carlo calculations. Three cross-section libraries in SCALE4.4 and various cross-section sets obtained for use with MCNP4C2 were used. The SCALE cross-section libraries are the same as those used in the previous section (the 27-group ENDF/B-IV burn-up library together with the 44-group and 238-group ENDF/B-V libraries). The MCNP4C2 cross-sections were all in the continuous format. From the Los Alamos data library, four different sets of cross-sections for the actinides were selected. Three of them, DN (delayed neutrons using .61c identifiers), USM (tabular data for unresolved resonances using .49c and .48c identifiers and square cell with mirror reflection) and .60c standard cross-sections were based on ENDF/B-VI.2 or earlier. Most of the cross-sections for the fission products are based on ENDF/B-V. Two additional models of all cases were run using the unresolved resonance library. These are identified by USW (square cell, white reflection) and UCW (cylindrical cell, white reflection). The fourth set of LANL actinide cross-sections is based on ENDF/B-V.0 (.50c identifiers). Two other cross-section libraries were also used. One is the JEFF-2.2 library and the other is a Korean library based on ENDF/B-VI.5. All codes and data libraries were obtained from the NEA Data Bank.

Table 2. Comparison of SCALE and MCNP with Expert Group average results

Case	EG-Av k_{eff}	$10^2 * \Delta k_{eff}$ – Difference to Expert Group average – Monte Carlo only										
		SCALE 4.4-CSAS25			MCNP4C2							
		Δ27 E-4	Δ44 E-5	Δ238 E-5	Δ.60c E-6.0	ΔDN E-6.1	ΔUSM E-6.1	ΔUSW E-6.1	ΔUCW E-6.1	Δ.50c E-5	ΔE65 E-6.5	ΔJ22 JEF22
1	1.3002	0.35	-0.29	-0.36	-0.21	-0.21	0.03	-0.24	-0.41	-0.07	0.20	0.33
2	1.1816	0.55	-0.15	-0.20	-0.13	-0.07	0.01	-0.36	-0.47	-0.16	0.20	0.15
3	1.1108	0.35	-0.01	-0.20	-0.12	0.00	0.10	-0.28	-0.48	0.05	0.16	0.13
4	1.0540	0.32	0.04	-0.11	-0.14	-0.15	-0.09	-0.25	-0.51	-0.11	0.02	0.10
5	1.2429	0.32	-0.24	-0.20	-0.18	-0.33	-0.10	-0.30	-0.46	-0.04	0.17	0.24
6	1.2051	0.26	-0.22	-0.22	-0.22	-0.08	-0.22	-0.38	-0.54	-0.23	0.15	0.41
7	1.1755	0.19	-0.11	-0.46	-0.22	-0.11	-0.17	-0.39	-0.44	-0.11	0.12	0.29
8	1.2425		-0.14	-0.26	-0.15	-0.17	-0.09	-0.38	-0.50		0.28	0.30
9	1.2063		-0.08	-0.33	-0.04	-0.14	0.06	-0.33	-0.56		0.21	0.34
10	1.1811		0.12	-0.39	-0.13	-0.17	-0.01	-0.47	-0.57		0.06	0.18
11	1.1345	0.29	-0.14	-0.08	-0.02	-0.22	0.05	-0.17	-0.53	-0.01	0.15	0.04
12	1.0539	0.20	0.08	-0.13	-0.17	-0.16	-0.09	-0.32	-0.44	0.03	0.13	-0.06
13	0.9893	0.10	0.06	0.08	0.02	-0.02	-0.06	-0.25	-0.50	0.12	-0.05	0.17
14	1.1989	0.17	-0.14	-0.25	-0.19	-0.23	0.02	-0.32	-0.55	-0.04	0.14	0.14
15	1.1540	0.05	0.03	-0.26	-0.21	-0.18	-0.10	-0.34	-0.58	-0.21	0.11	0.29
16	1.1215	-0.01	-0.03	-0.33	-0.19	-0.22	-0.08	-0.45	-0.54	-0.09	0.07	0.07
17	1.1988		0.01	-0.19	-0.29	-0.25	0.06	-0.36	-0.46		0.32	0.26
18	1.1559		0.13	-0.42	0.02	-0.18	-0.01	-0.32	-0.65		0.24	0.21
19	1.1285		0.18	-0.26	-0.20	-0.16	0.02	-0.44	-0.54		0.17	0.17
20	1.4144	-0.52	0.41	-0.07	-0.45	-0.34	0.20	-0.11	-0.26	0.26	0.38	0.04

Table 2. Comparison of SCALE and MCNP with Expert Group average results (*cont.*)

Case	EG-Av k_{eff}	$10^2 * \Delta k_{eff}$ – Difference to Expert Group average – Monte Carlo only										
		SCALE 4.4-CSAS25			MCNP4C2							
		Δ27 E-4	Δ44 E-5	Δ238 E-5	Δ.60c E-6.0	ΔDN E-6.1	ΔUSM E-6.1	ΔUSW E-6.1	ΔUCW E-6.1	Δ.50c E-5	ΔE65 E-6.5	ΔJ22 JEF22
21	1.2238	0.02	0.06	-0.02	-0.13	-0.25	0.10	-0.26	-0.11	0.16	0.23	0.18
22	1.1129	0.17	-0.06	-0.06	-0.06	-0.07	0.01	-0.21	-0.36	0.02	0.03	0.18
23	1.0337	0.10	0.02	-0.06	-0.01	-0.09	-0.08	-0.24	-0.33	0.08	0.10	0.20
24	1.2943	-0.05	-0.01	-0.16	-0.29	-0.12	0.11	-0.12	-0.28	-0.01	0.30	0.12
25	1.2194	0.03	-0.14	-0.19	-0.16	-0.24	-0.22	-0.25	-0.48	0.11	0.21	0.31
26	1.1691	0.05	-0.09	-0.11	-0.19	-0.23	-0.22	-0.23	-0.49	-0.13	0.18	0.31
27	1.2944		-0.13	-0.01	-0.10	-0.15	0.11	-0.29	-0.21		0.34	0.30
28	1.2198		-0.12	-0.19	-0.27	-0.16	-0.07	-0.15	-0.42		0.22	0.30
29	1.1716		-0.03	-0.24	-0.20	-0.11	-0.17	-0.38	-0.38		0.18	0.38
30	1.1971	0.04	0.01	0.01	-0.34	-0.15	0.09	-0.19	-0.37	0.02	0.11	0.05
31	1.0638	0.12	0.02	-0.02	0.04	-0.17	0.21	-0.16	-0.28	0.13	0.20	0.08
32	0.9714	0.09	0.10	-0.02	-0.11	-0.15	-0.04	-0.23	-0.34	0.10	-0.05	0.07
33	1.2719	-0.16	0.02	-0.11	-0.30	-0.18	0.02	-0.22	-0.27	0.11	0.18	0.16
34	1.1791	-0.18	-0.18	-0.16	-0.14	-0.19	-0.04	-0.18	-0.35	0.04	0.25	0.12
35	1.1209	-0.11	-0.03	-0.31	-0.28	-0.34	-0.05	-0.36	-0.44	0.07	0.19	0.07
36	1.2722		-0.03	-0.24	-0.33	-0.25	0.07	-0.12	-0.39		0.30	0.24
37	1.1800		-0.11	-0.25	-0.23	-0.26	-0.13	-0.33	-0.46		0.16	-0.02
38	1.1239		-0.05	-0.14	-0.30	-0.21	-0.04	-0.41	-0.49		0.06	0.08
39	1.1958	0.57	-0.39	-0.19	-0.04	-0.13	0.10	-0.24	-0.52	-0.19	0.31	0.46
40	1.1103	0.63	-0.02	-0.20	-0.01	-0.18	-0.08	-0.38	-0.50	-0.16	0.10	0.19
41	1.0654	0.43	0.06	-0.24	-0.09	-0.20	-0.17	-0.33	-0.69	-0.15	-0.02	0.06
42	1.0281	0.25	0.15	-0.14	0.06	-0.07	-0.13	-0.40	-0.53	-0.09	-0.10	0.04
43	1.1095		0.05	-0.21	0.07	0.02	0.14	-0.21	-0.54		0.09	0.15
44	1.0691		0.12	-0.20	-0.06	0.01	-0.05	-0.43	-0.66		-0.05	0.06
45	1.0400		0.39	-0.11	-0.06	-0.05	-0.05	-0.60	-0.59		0.04	-0.08
46	1.1631	0.60	-0.04	-0.33	-0.12	-0.17	-0.15	-0.38	-0.55	-0.27	0.20	0.26
47	1.1475	0.34	0.05	-0.42	-0.26	-0.26	-0.15	-0.61	-0.64	-0.21	0.18	0.21
48	1.1349	0.19	0.22	-0.29	-0.15	-0.11	0.05	-0.53	-0.62	-0.04	0.12	0.17
49	1.1626		-0.04	-0.33	-0.01	-0.19	-0.09	-0.31	-0.62		0.24	0.29
50	1.1509		0.18	-0.36	-0.25	-0.15	-0.14	-0.69	-0.60		0.03	0.33
51	1.1461		0.38	-0.34	-0.02	-0.18	-0.08	-0.46	-0.54		0.26	0.40
52	1.0560	0.48	-0.03	-0.22	0.01	-0.03	-0.05	-0.44	-0.49	0.07	0.05	0.13
53	1.0048	0.29	0.15	-0.13	0.08	-0.08	-0.02	-0.34	-0.48	0.02	0.11	0.14
54	0.9624	0.17	0.24	-0.07	-0.09	-0.11	-0.05	-0.30	-0.46	0.07	0.09	0.10
55	1.0560		0.11	-0.19	-0.11	-0.05	0.06	-0.16	-0.46		0.01	0.07
56	1.0096		0.25	-0.08	-0.02	-0.10	-0.05	-0.38	-0.59		-0.09	0.07
57	0.9764		0.43	-0.01	-0.11	-0.12	-0.13	-0.42	-0.57		0.03	0.12
58	1.1112	0.25	0.10	-0.31	-0.15	-0.11	0.05	-0.44	-0.54	-0.04	0.12	0.17
59	1.0913	0.09	0.08	-0.28	-0.12	-0.17	-0.03	-0.30	-0.62	-0.16	0.16	0.16
60	1.0771	-0.04	0.20	-0.29	-0.24	-0.29	-0.20	-0.50	-0.76	0.01	0.23	0.08
61	1.1114		-0.02	-0.22	-0.15	-0.24	-0.20	-0.33	-0.56		0.21	0.19
62	1.0958		0.16	-0.20	-0.25	-0.20	-0.08	-0.45	-0.78		0.13	0.10
63	1.0911		0.39	-0.26	-0.31	-0.20	-0.23	-0.41	-0.66		0.07	0.02
The standard deviations are about 0.0007 (900 000 neutrons)												
Diff	0.0000	0.18	0.03	-0.20	-0.14	-0.16	-0.05	-0.33	-0.49	-0.03	0.14	0.17
Max+	0.0000	0.63	0.43	0.08	0.08	0.02	0.21	-0.11	-0.11	0.26	0.38	0.46
Max–	0.0000	-0.52	-0.39	-0.46	-0.45	-0.34	-0.26	-0.69	-0.78	-0.27	-0.10	-0.08

Figure 2 shows average, maximum and minimum deviations of various SCALE and MCNP cross-section sets, compared with the Expert Group average. The results for CSAS1X are included. The range of results does not appear to be a problem for criticality safety. There are consistent differences between different libraries. JEFF-2.2 and ENDF/B-VI.5 provide similar results which are higher than for older data. The SCALE 27-group and 44-group libraries appear to give larger spreads in the results than the SCALE 238-group library, which behaves more like the continuous cross-section sets. As mentioned before, the SCALE CSAS1X sequence with 1-D approximations is not so good for these cases. Some caution should be exercised when comparing results from individual calculations. Editorial mistakes cannot be excluded.

Figure 2. Comparison with Expert Group average results

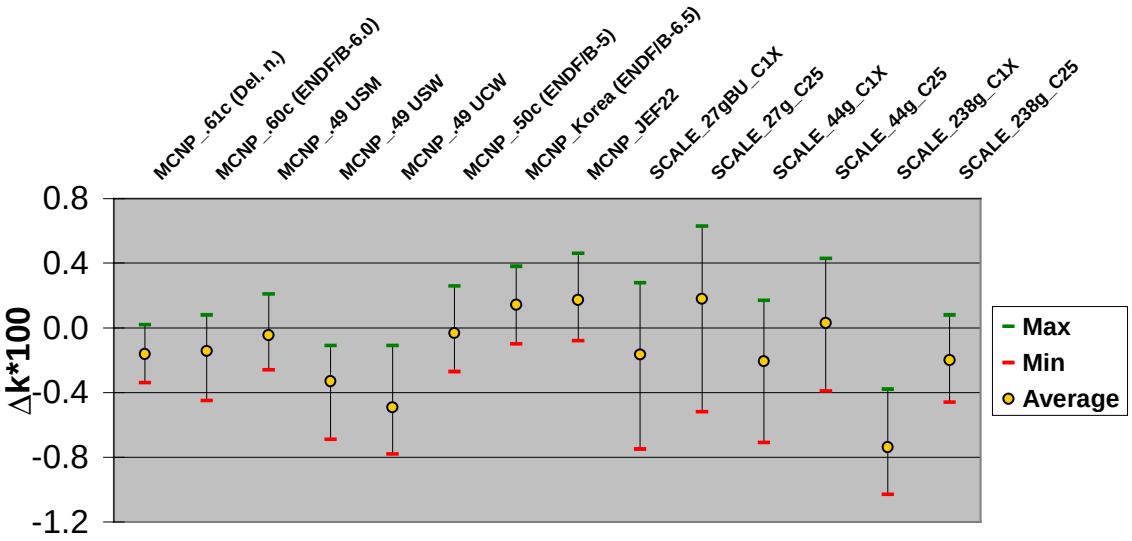

Evaluation of ^{238}Pu, ^{242}Pu, ^{244}Cm and ^{245}Cm nuclide importances

The Expert Group co-ordinator requested further information on the reactivity importance of the nuclides ^{238}Pu and ^{242}Pu for Case 39 as well as ^{244}Cm and ^{245}Cm for Case 63. These reactivities have been calculated using both SCALE4.4 and MCNP4C2 together with different cross-section libraries. Table 3 shows some of the results. For Case 63, some libraries did not include all the requested Cm isotopes. The reactivity values agree very well between the different methods.

Table 3. Reactivity influence of some Pu and Cm isotopes

Cases 39 and 63 – Δk/k * 100 of the nuclides ^{238}Pu, ^{242}Pu, ^{244}Cm and ^{245}Cm									
Case and removed nuclide(s)	**S-C25 238**	**S-C25 44**	**S-C25 27**	**M-Dn .61c**	**M-Ur .49c**	**M-E5 .50c**	**M-K6.5 .60c**	**M-JEF 2.2**	**Mean**
39 – ^{238}Pu	-1.4	-1.4	-1.5	-1.4	-1.4	-1.6	-1.5	-1.4	-1.4
39 – ^{242}Pu	-3.2	-3.1	-3.2	-3.2	-3.3	-3.2	-3.2	-3.2	-3.2
39 – $^{238+242}$Pu	-4.7	-4.7	-4.7	-4.8	-4.8	-4.8	-4.7	-4.7	-4.7
63 – ^{244}Cm	-0.5	-0.3		-0.5	-0.4		-0.5	-0.6	-0.5
63 – ^{245}Cm	1.7	1.7		1.7	1.5		1.6	1.6	1.7
63 – $^{244+245}$Cm	1.1	1.3		1.3	1.1		1.3	1.1	1.1

First, the calculations with SCALE were made with the CSAS1X sequence. Due to the previously reported problems with this sequence, the calculations were repeated with the CSAS25 sequence. The 238-group, 44-group and 27-group burn-up libraries were used with SCALE4.4.

The MCNP4C2 calculations were made with several different continuous energy cross-section libraries. As with SCALE, all results in Table B10-3 are based on differences between two separate calculations. The delayed neutron ENDF/B-VI.2 library set (Dn .61c), the unresolved resonance ENDF/B-VI.2 library set (Ur .49c) and the ENDF/B-V library sets (E5) were taken from the LANL cross-section library collection. The Korean ENDF/B-VI.5 (K6.5 .60c) and the European JEF-2.2 cross-section libraries were also used.

MCNP4C2 contains an option to calculate differences using first and second order perturbations. This has worked well with some perturbations but did not work out with ^{242}Pu. Smaller perturbations give reasonable results, but the trend cannot be extrapolated. It is not linear.

The first attempt was to calculate the total ^{242}Pu influence with the perturbation method of MCNP. The results depend strongly on the basic reference model. The fraction of the nominal ^{242}Pu density of Case 39 is used as a basic reference for each curve. Perturbations starting from a fraction result in a curve. The direct calculations of k_{eff} for different ^{242}Pu fractions of the nominal (Case 39) density were made with various cross-section sets. Only the "delayed neutron" set .61c is shown in Figure 3, since the other sets gave essentially identical results. Other curves show different basic reference models. The direct curve refers to the difference between k_{eff} results from separate calculations. The ratio of the second order perturbation to the total perturbation should be less than 20% according to the MCNP documentation. Some results shown in the charts had higher ratios than 20%. However, the limit had to be set to 15% or lower to get reasonable results.

Figure 3. Comparing MCNP direct difference and perturbation results for ^{242}Pu

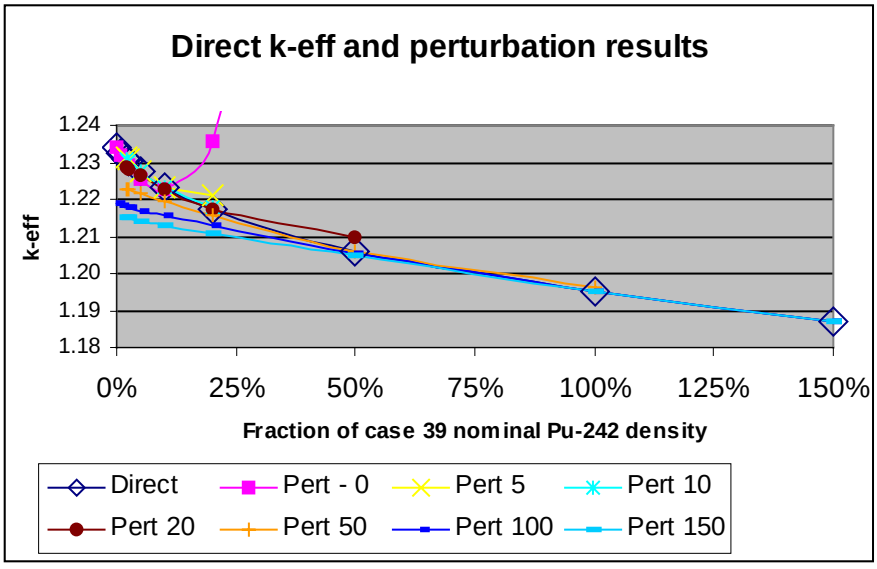

The advantage of the MCNP perturbation techniques is found when the results may be seriously influenced by the statistical nature of the calculations. For Case 39, the total ^{242}Pu reactivity influence is so large that the standard deviations from two separate calculations are not significant if a reasonable number of neutrons are run. In this case there is no advantage in using perturbation techniques. Figure 4 shows the deviation between the perturbed result and the differential k_{eff} value based on two

Figure 4. Deviations of perturbations and SCALE from MCNP direct k_{eff} results

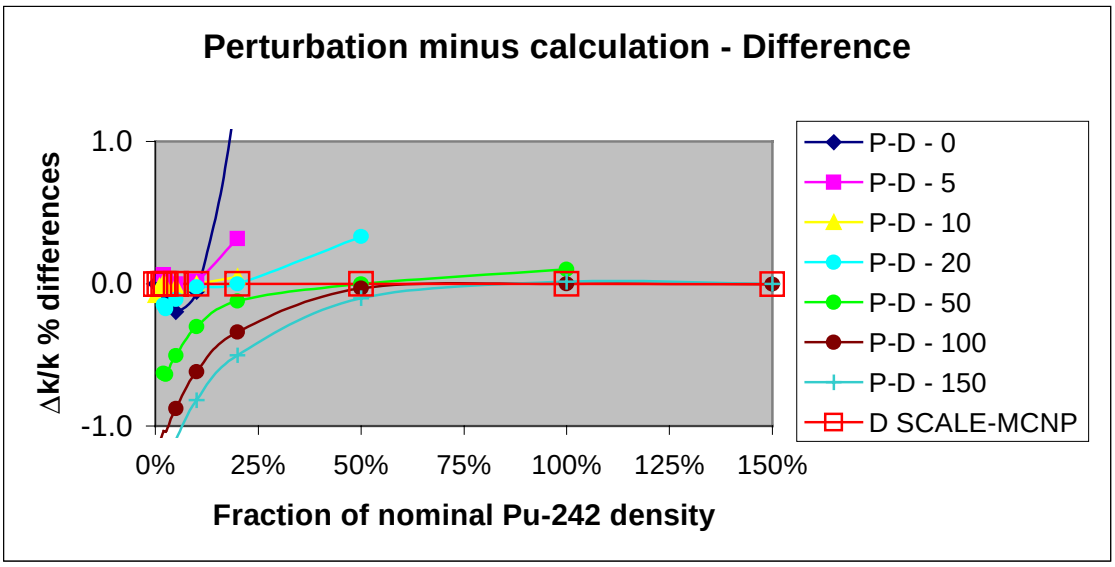

separate calculations. MCNP with the "delayed neutron" cross-section set and SCALE4.4 with the 238-group cross-section library gave essentially identical reactivity values for ^{242}Pu (the red line coincides with the 0.0 line). Figure 5 shows the same data for the lower range of ^{242}Pu fractions.

Figure 5. Deviations of perturbations and SCALE from MCNP direct k_{eff} results

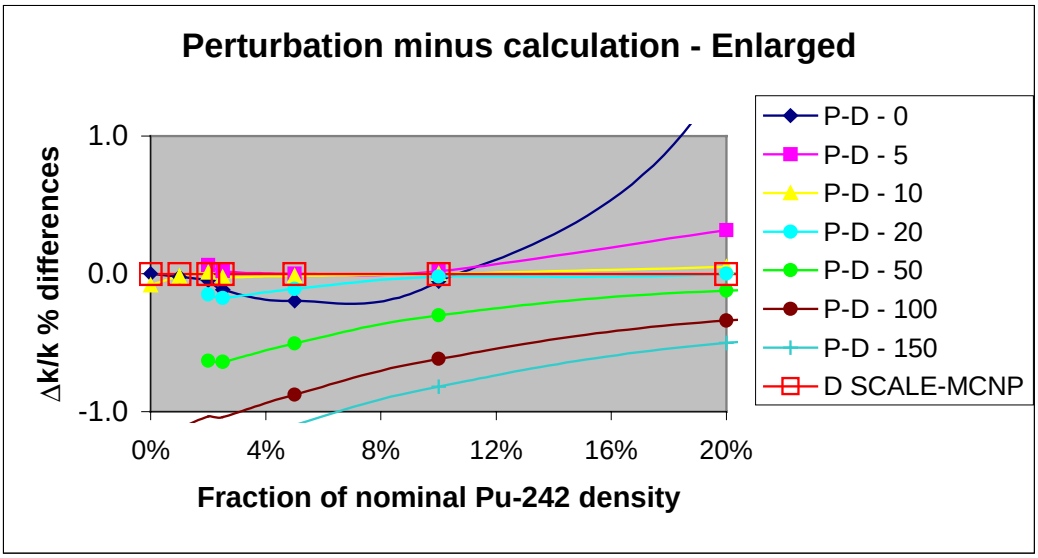

The total ^{242}Pu reactivity in Case 39 is about 3.2% and Δk is about 0.038. The first 10% of the ^{242}Pu nuclide addition is worth about 1% in reactivity, which is slightly more than the last 50% of the ^{242}Pu addition. The reactivity is reduced by a factor of five. Even though the geometry is very simple, the fuel composition seems to require many neutron histories for convergence with low ^{242}Pu presence. Nine million histories were run in each of those calculations, resulting in a σ of 0.0002.

The non-linear influence of ^{242}Pu is not surprising. All nuclides with large or many resonances should behave non-linearly. Also other nuclides, in particular those with large variations in the cross-sections in a particular energy range, are expected to give “saturation” effects. Here, ^{242}Pu removal was not compensated with other Pu isotopes, only with void. If the reactivity of replacing one nuclide with another is evaluated, more dramatic trend changes can be observed. A negative trend can become positive. Comparisons between ^{236}U and ^{238}U have shown such behaviour. Evaluation of steel thickness in water is another example. A thin plate may give a negative reactivity contribution, while a thicker plate gives a positive reactivity contribution.

Appendix V

INFINITE NEUTRON MULTIPLICATION FACTOR OF PWR ASSEMBLY WITH MOX FUELS

B. Roque, A. Santamarina
CEA/DRN Cadarache, F-13108 Saint Paul-lez-Durance, France

X. Boudin, E. Letang
IPSN BP6, F-92265 Fontenay-aux-Roses, France

Abstract

Phase IV of the Burn-up Credit Criticality Benchmark is devoted to mixed oxide (MOX) fuels.

French results of the Phase IV-A obtained with the APOLLO2 package, corresponding to infinite neutron multiplication factor calculations, are presented in this paper.

The reactivity loss, corresponding to burn-up credit, is analysed versus burn-up for cooling times T = 1 year and T = 5 years. The complementary reactivity worth linked to curium isotopes is also investigated.

1. Introduction

The aim of the OECD/NSC Burn-up Credit Group is to calculate relevant benchmarks in order to validate the safety-criticality codes and libraries for burn-up calculations.

To demonstrate the reliability of safety-criticality tools for calculation of LWR fuels, two kinds of benchmarks are required:

1) Benchmarks demonstrating that depletion calculation tools are well suited for fuel inventory determination.

2) Benchmarks demonstrating that the multiplication factor for spent fuel systems (transport cask, storage, ...) are well predicted.

Thus, the work of the OECD group is generally divided in phases related to different fuel types, and in each phase the two kinds of benchmarks presented above have to be calculated.

Three phases have been completed: Phase I related to simple PWR spent fuel cell, Phase II related to axial burn-up effects in spent fuel from PWRs and Phase III to burn-up credit in boiling water reactors.

Phase IV, currently being undertaken, is devoted to mixed oxide (MOX) fuels. Phase IV-A corresponds to calculations of infinite neutron multiplication factors of a MOX fuel pin [1].

This paper summarises the CEA results of Phase IV-A based on the powerful French code APOLLO2.

2. Calculation route

The calculations were performed with the French code APOLLO2 [2], which is extensively used in light water reactor studies [3] and in the CRISTAL safety-criticality package[4].

APOLLO2 is a modular code which solves both the Boltzmann integral equation and the integro-differential equation (S_n method).

APOLLO2 allows the use of several collision probability methods to solve the integral equation: exact 2-D P_{ij}, multi-cell P_{ij} based on the interface current method. The one used for the benchmark is the exact 2-D P_{ij} method; no hypothesis of pin cell cylindrisation has been made.

The neutron data library used is the “CEA93” library in a 172-group structure. These multi-group cross-sections and effective cross-sections were processed by NJOY from the JEF-2 European File.

The CEA93 library is currently benchmarked against specific French integral experiments [5].

The geometry described is the exact geometry of the lattice, that is, square cell with specular boundary (Figure 1).

In our calculations, the MOX fuel pin is divided in six concentric zones.

Figure 1. Geometry of MOX fuel pin cell for PWR

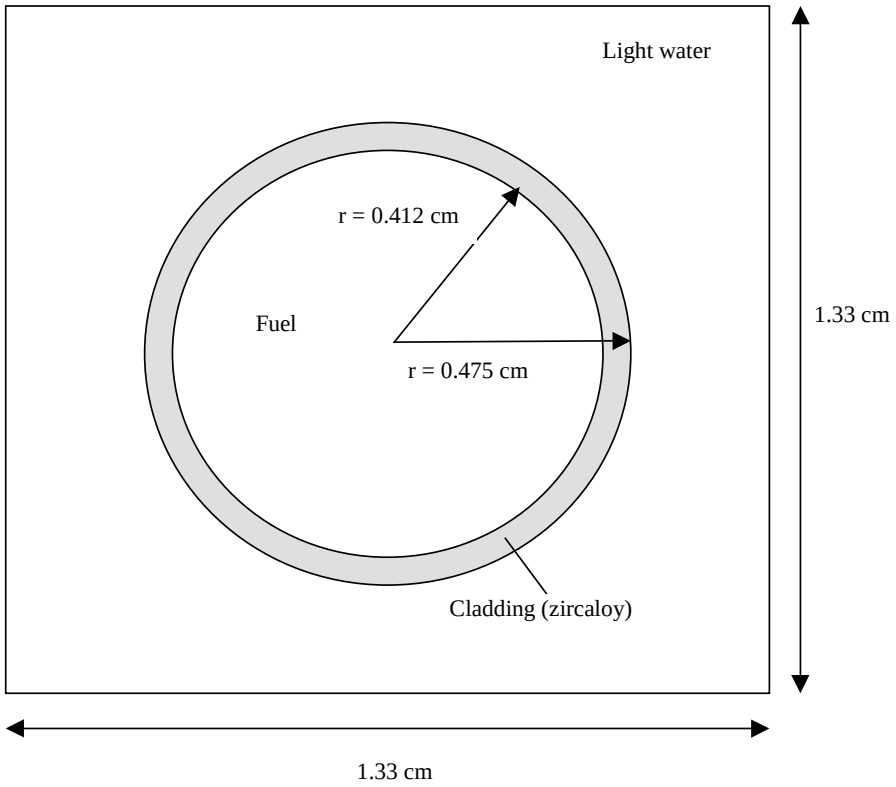

Self-shielded cross-sections are calculated for ^{238}U in each concentric zone. An accurate "background matrix" formalism [6] is used for resonant reaction rate calculation, allowing space-dependent resonance self-shielding and rim effect modelling.

For the other actinides, ^{240}Pu, ^{239}Pu, ^{241}Pu, ^{242}Pu, ^{238}Pu, ^{241}Am, ^{235}U and Zr, we used an "average self-shielding" formalism. The Dancoff effect and the self-shielded cross-sections are also obtained from 2-D P_{ij} collision probabilities.

The whole nuclide required for the benchmark is available in the CEA93 library.

Table 1. Nuclides required in the BUC benchmark (Phase IV-A)

Actinides	$^{234,235,236,238}U$ $^{238,239,240,241,242}Pu$ $^{241,243}Am$ ^{237}Np $^{242,243,244,245}Cm$
Fission products	^{95}Mo, ^{99}Tc, ^{101}Ru, ^{103}Rh, ^{109}Ag ^{133}Cs $^{143,145}Nd$ $^{147,149,150,151,152}Sm$ ^{153}Eu ^{155}Gd

3. Benchmark specification [1]

The selected parameters of benchmark Phase IV-A are the following. Three different MOX fuels are considered:

- Case A: "A reference MOX fuel case appropriate to a typical plutonium vector for material derived from the reprocessing of thermal reactor UO_2 fuels".
- Case B: "A MOX fuel case appropriate to the disposition of weapons plutonium in MOX".
- Case C: "Future MOX fuels that might be produced using the plutonium recovered from the reprocessing of irradiated MOX".

The plutonium isotopic compositions for these MOX are presented in Table 2.

Table 2. Plutonium isotopic composition in fresh MOX fuel

Nuclide	Isotopic composition, w/o in Pu_{total}		
	MOX Case A	MOX Case B	MOX Case C
^{238}Pu	1.8	0.05	4.0
^{239}Pu	59.0	93.6	36.0
^{240}Pu	23.0	6.0	28.0
^{241}Pu	12.2	0.3	12.0
^{242}Pu	4.0	0.05	20.0

Three burn-ups and two cooling times are studied: 20, 40 and 60 GWd/t with T = 1 and 5 years. Also, 63 cases have to be calculated.

4. Calculation results and analysis

4.1 Infinite multiplication factors

The infinite multiplication factor results corresponding to the benchmark requirements are given in Tables 3 to 5 for the three MOX cases.

Table 3. Infinite multiplication factor results for MOX Case A

MOX case	Cooling time	Fission products	Actinides	Burn-up			
				Fresh	20	40	60
A	1	Yes	Major	1.30454	1.18379	1.11189	1.05395
		No	Major		1.24680	1.20848	1.17884
			Major + Cm		1.24661	1.20967	1.18374
	5	Yes	Major		1.13566	1.05372	0.98807
		No	Major		1.20161	1.15636	1.12347
			Major + Cm		1.20156	1.15815	1.13009

Table 4. Infinite multiplication factor results for MOX Case B

MOX case	Cooling time	Fission products	Actinides	Burn-up			
				Fresh	20	40	60
B	1	Yes	Major	1.41628	1.22574	1.11411	1.03379
		No	Major		1.29813	1.22351	1.17295
			Major + Cm		1.29810	1.22370	1.17500
	5	Yes	Major		1.19806	1.06419	0.97063
		No	Major		1.27481	1.18225	1.12351
			Major + Cm		1.27479	1.18255	1.12608

Table 5. Infinite multiplication factor results for MOX Case C

MOX Case	Cooling time	Fission products	Actinides	Burn-up			
				Fresh	20	40	60
C	1	Yes	Major	1.20043	1.11156	1.06558	1.02697
			Major + Cm		1.11141	1.06919	1.03854
		No	Major		1.16616	1.14968	1.13667
			Major + Cm		1.16576	1.15241	1.14681
	5	Yes	Major		1.05637	1.00407	0.96053
			Major + Cm		1.05658	1.00880	0.97403
		No	Major		1.11306	1.09246	1.07790
			Major + Cm		1.11307	1.09653	1.09051

Design calculations using the cylindrical pin cell model were also performed. The infinite multiplication factor results of these cases differ by about -300 pcm from those given in Tables 3-5.

4.2 Reactivity loss and burn-up credit

The reactivity loss corresponding to burn-up credit is:

$$BUC = |\Delta\rho| = \rho(BU) - \rho(fresh)$$

The reactivity variation is defined as $\Delta\rho = \mathrm{Ln}\frac{K_{final}}{K_{initial}}$ and expressed in pcm (10^{-5}).

Tables 6-8 and Figures 2-4 summarise the BUC reactivity worth versus burn-up for cooling times of one and five years due to major actinides or fission products (FP). They show the high level of burn-up credit, which amounts to (PWR recycling, Case A, T = 1 year, BU = 40 GWd/t):

$$|\Delta\rho| = 15\,980 \text{ pcm (Actinide depletion + 15 FP)}$$

involving a $|\Delta\rho| = 7\,650$ pcm actinide component and $|\Delta\rho| = 8\,330$ FP component.

It should be noted that, due to ^{241}Pu decay, the actinide component becomes predominant as cooling time increases: $|\Delta\rho|_{Act} = 12\,057$ pcm at T = 5 years.

Table 6. Burn-up credit reactivity (pcm) versus burn-up for MOX Case A

	20	40	60
BUC TOTAL 1 year	-9 713	-15 979	-21 331
BUC ACT 1 year	-4 527	-7 649	-10 132
BUC PF 1 year	-5 186	-8 330	-11 199
BUC (AC + Cm) 1 year	-4 542	-7 550	-9 717
BUC TOTAL 5 years	-13 864	-21 352	-27 785
BUC ACT 5 years	-8 219	-12 057	-14 943
BUC PF 5 years	-5 645	-9 295	-12 842
BUC (AC + Cm) 5 years	-8 223	-11 903	-14 355

Table 7. Burn-up credit reactivity (pcm) versus burn-up for MOX Case B

	20	40	60
BUC TOTAL 1 year	-14 449	-23 998	-31 480
BUC ACT 1 year	-8 711	-14 631	-18 851
BUC PF 1 year	-5 738	-9 367	-12 629
BUC (AC + Cm) 1 year	-8 713	-14 615	-18 677
BUC TOTAL 5 years	-16 733	-28 582	-37 784
BUC ACT 5 years	-10 524	-18 061	-23 158
BUC PF 5 years	-6 209	-10 521	-14 627
BUC (AC + Cm) 5 years	-10 525	-18 036	-22 929

Table 8. Burn-up credit reactivity (pcm) versus burn-up for MOX Case C

	20	40	60
BUC TOTAL 1 year	-7 692	-11 916	-15 607
BUC ACT 1 year	-2 896	-4 320	-5 458
BUC PF 1 year	-4 795	-7 596	-10 149
BUC (AC + Cm) 1 year	-2 931	-4 082	-4 570
BUC (AC+Cm+PF) 1 year	-7 705	-11 578	-14 486
BUC TOTAL 5 years	-12 784	-17 862	-22 295
BUC ACT 5 years	-7 557	-9 425	-10 767
BUC PF 5 years	-5 227	-8 437	-11 528
BUC (AC+Cm) 5 years	-7 556	-9 053	-9 603
BUC (AC+Cm+PF) 5 years	-12 764	-17 392	-20 899

Figure 2. Burn-up credit for MOX Case A, T = 1 and 5 years

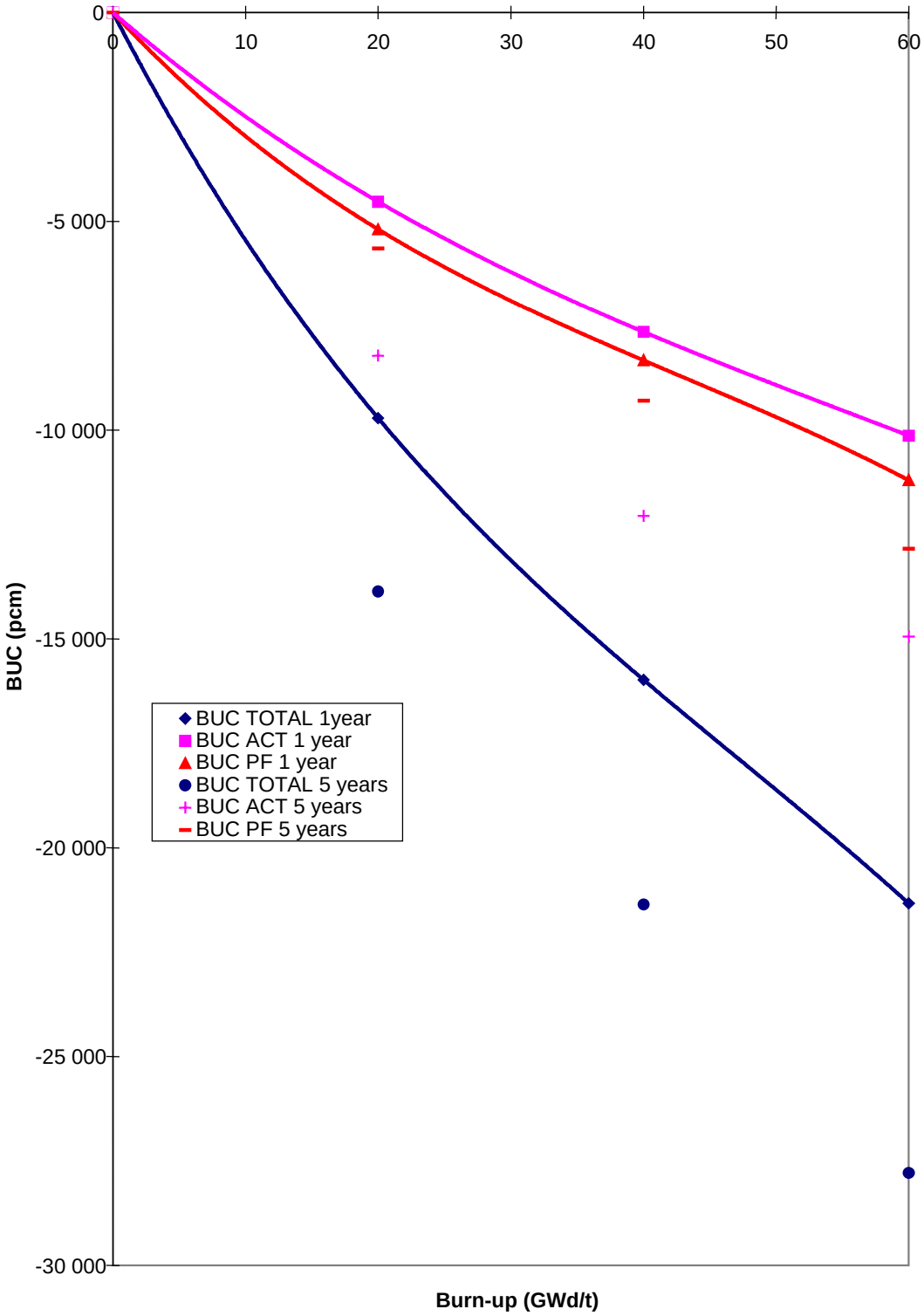

Figure 3. Burn-up credit for MOX Case B, T = 1 and 5 years

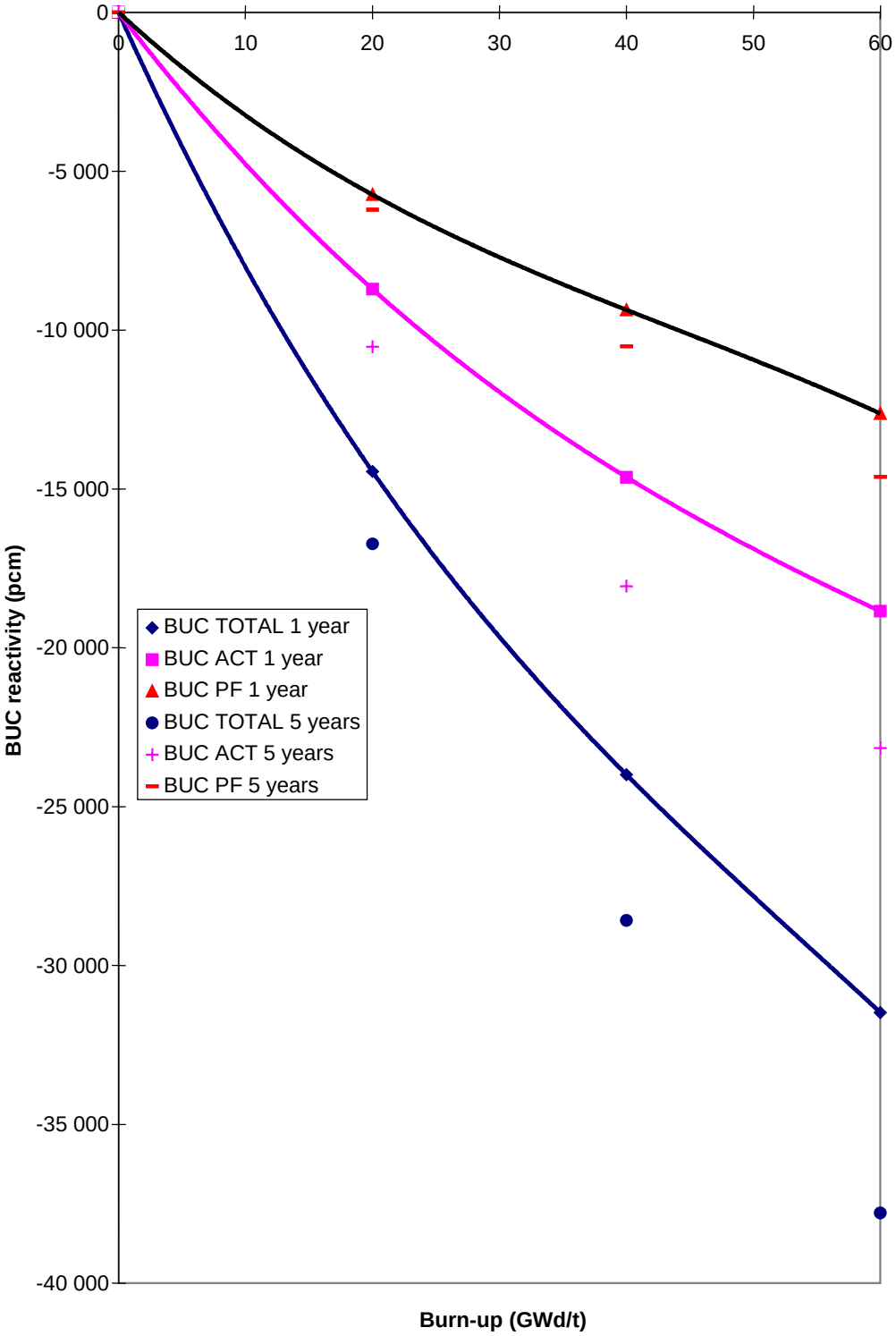

Figure 4. Burn-up credit for MOX Case C, T = 1 and 5 years

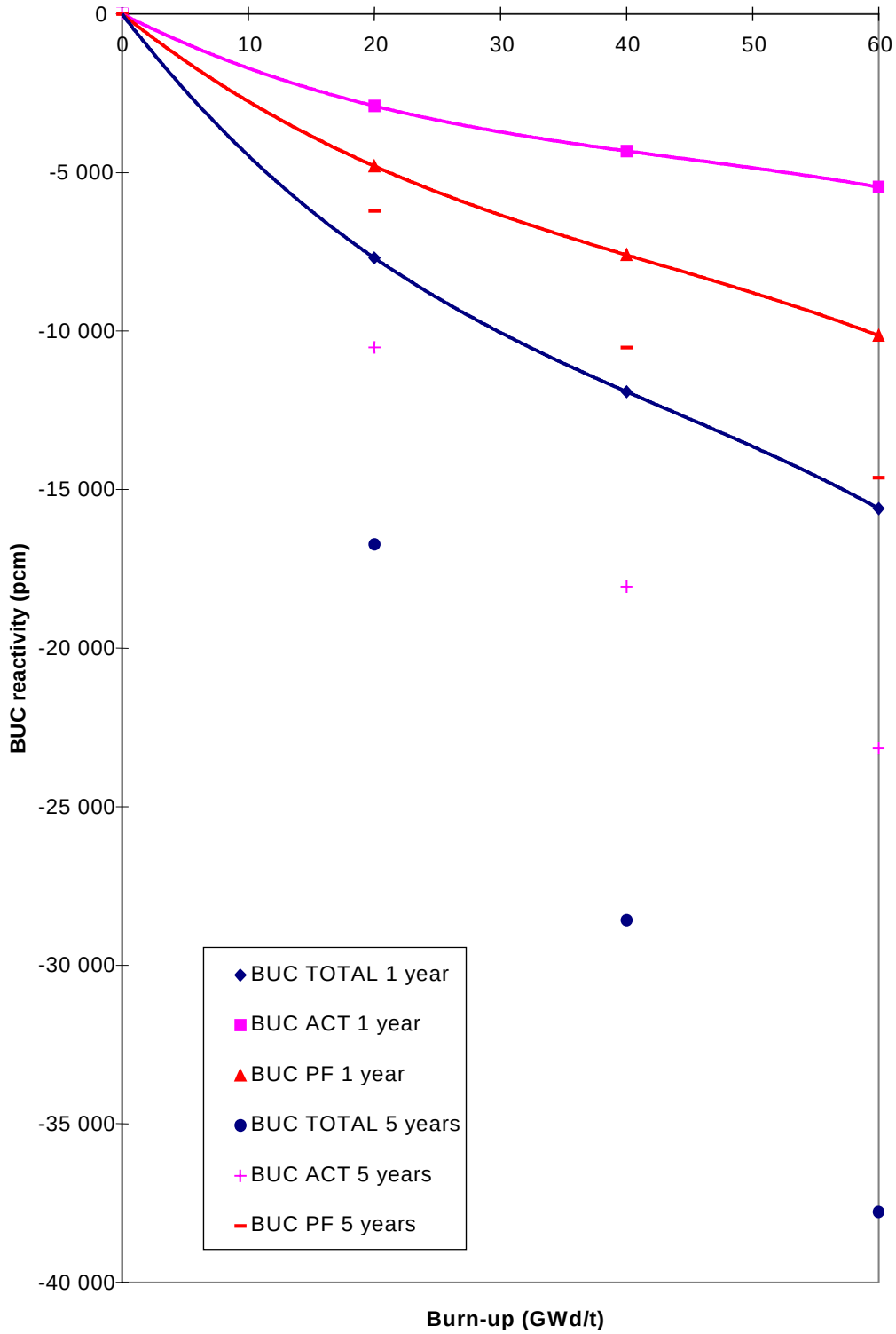

The results presented in Tables 6, 7, 8 demonstrate that burn-up credit is emphasised in weapons Pu MOX fuels; in these MOX fuels the plutonium is dominated by the ^{239}Pu isotope and the "actinide" reactivity loss with burn-up is raised to a maximum. On the other hand, the actinide BUC component is decreased in Cases A and C due to the high initial ^{240}Pu content and consequently to a better conversion factor.

These MOX benchmark results point out that burn-up credit is reduced in MOX lattices compared to the previous BUC results in UO_2 lattices [7]. This effect is mainly linked to the strong reduction of the actinide component: $|\Delta\rho|$ = 7 650 pcm at 40 GWd/t and T = 1 year, instead of $|\Delta\rho|$ = 19 000 pcm in the UO_2 lattice.

4.3 Curium reactivity worth

Figures 5-7 show the effect of the curium isotopes.

The plotted worth values represent the difference of reactivity between the calculation with and without the curium isotopes.

These results indicate that neglecting curium isotopes leads to an overestimation of the burn-up credit above BU > 30 GWd/t. At these high burn-ups, although the ^{244}Cm increases, its capture effect is less important than the positive reactivity worth effect due to the ^{245}Cm fissile isotope.

Figure 5. Effect of curium isotopes on BUC reactivity: MOX Case A

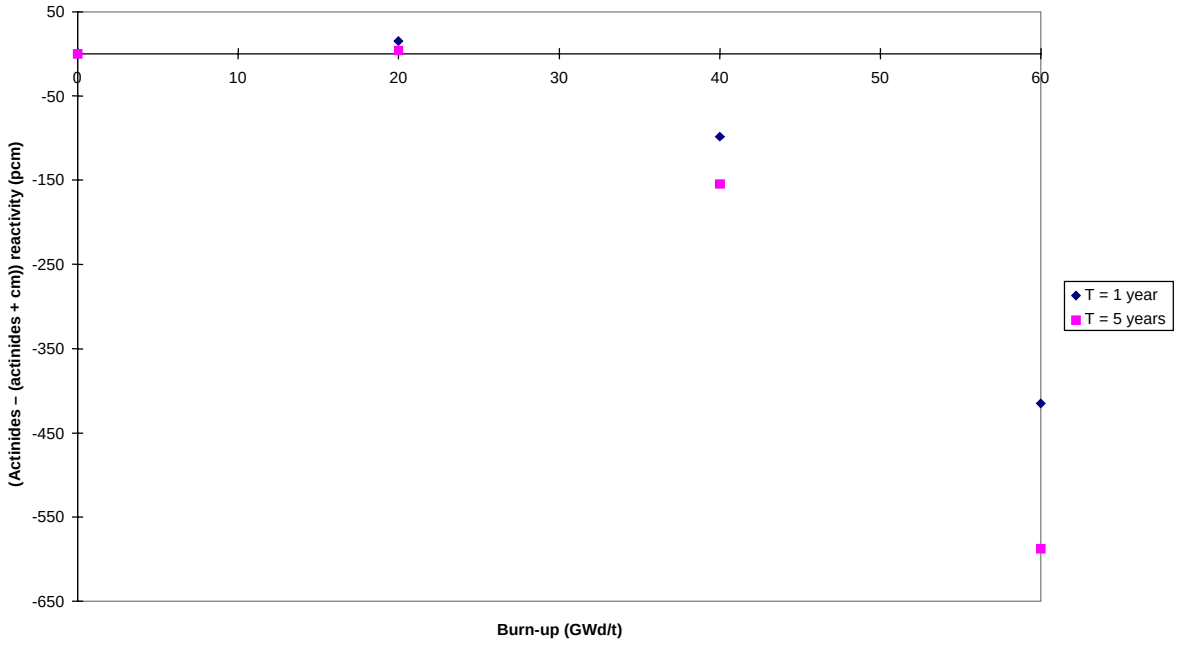

Figure 6. Effect of curium isotopes on BUC reactivity: MOX Case B

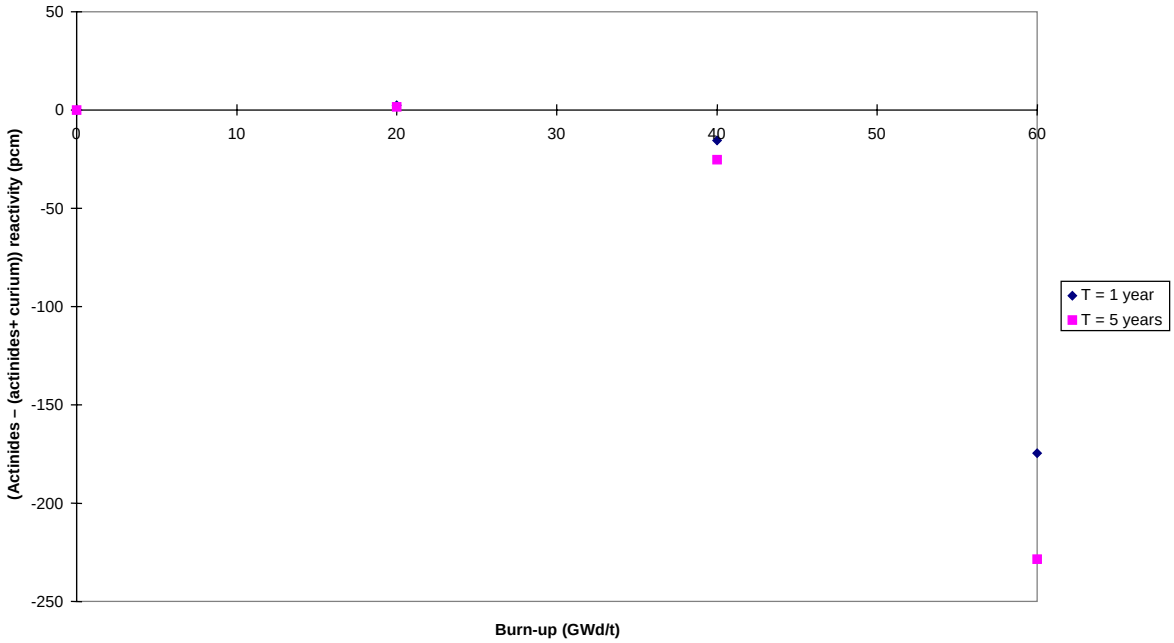

Figure 7. Effect of curium isotopes on BUC reactivity: MOX Case C

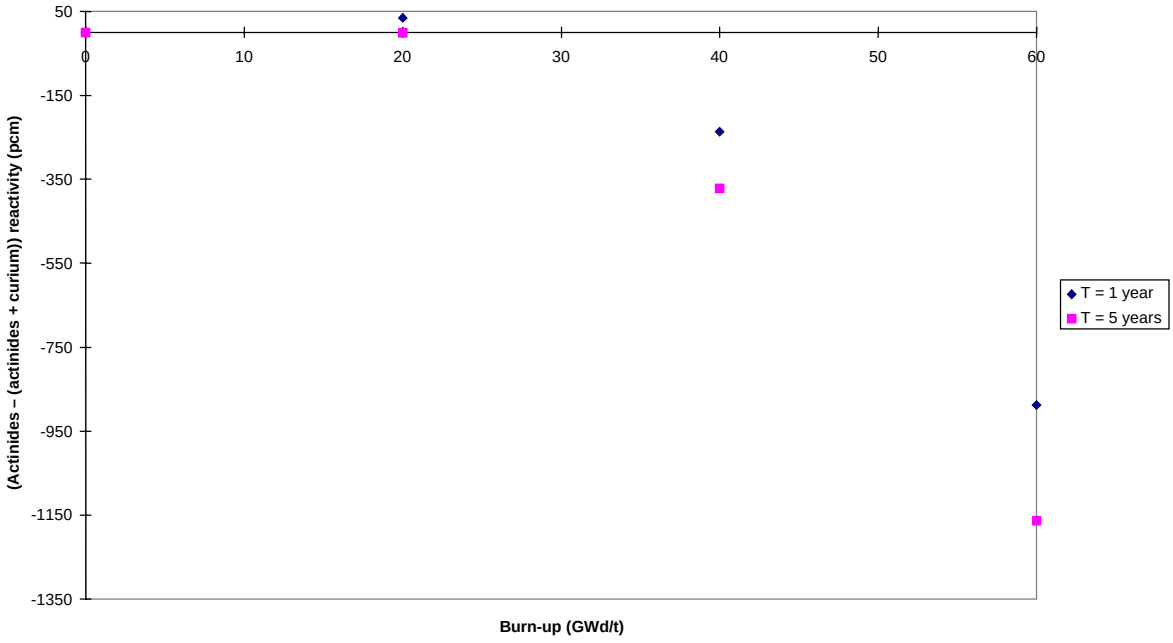

5. Conclusion

The Burn-up Credit Criticality Benchmark in MOX fuels was computed using the powerful 2-D lattice model implemented in the APOLLO2 code.

The BUC reactivity worth after one year cooling time amounts to 16 000 pcm in standard MOX fuel (Pu recycling in LWRs). The burn-up credit worth is linked to equivalent "actinide" and "fission product" components respectively 7 600 pcm and 8 400 pcm.

Due to the fertile ^{240}Pu isotope, the actinide BUC component is smaller in MOX fuel than in UOX assemblies. Therefore, for an equivalent T = 1 year cooling time, the burn-up credit in a MOX lattice is reduced by 45% compared to a UO_2 lattice.

This Phase IV of the BUC benchmark programme has stressed another specificity of the burn-up credit in MOX fuels: at high burn-ups, beyond 30 GWd/t, the Cm build-up must be accounted for, due to the large positive reactivity worth of the ^{245}Cm isotope.

REFERENCES

[1] R.L. Bowden, P.R. Thorne, "Problem Specification for the OECD/NEA NSC Burn-up Credit Benchmark Phase IV-A: Mixed Oxide (MOX) Fuels", this report.

[2] R. Sanchez, *et al.*, "APOLLO2: a User-oriented , Portable, Modular Code for Multi-group Transport Assembly Calculations", *Nucl. Sci. and Eng*., 100, 352 (1988).

[3] C. Chabert, A. Santamarina, J-C. Lefebvre, C. Poinot, V. Allais, "Experimental Validation of UOX and MOX Spent Fuel Isotopics Predictions", Proc. Int. Conf. on the Physics of Reactors (PHYSOR96), Mito, Japan, Sept. 1996.

[4] B. Roque, A. Santamarina, C. Mattera, "Validation of the New French Criticality-safety Package CRISTAL", Top. Meeting on Criticality-safety Challenges in the Next Decade, Chelan, USA, 7-11 September 1997.

[5] S. Cathalau, A. Benslimane, A. Magnhouj, P. Fougeras, V. Ukraintsev, "Qualification of the JEF-2.2 Cross-sections in the Epithermal and Thermal Energy Ranges Using a Statistical Approach", *Nucl. Sci. Eng*., 121, 326-333 (1995).

[6] P. Reuss, *Nucl. Sci. Eng*., 92, 261 (1986).

[7] M. Takano, "OECD/NEA Burn-up Credit Criticality Benchmark – Result of Phase I-A", OECD/NEA document NEA/NSC/DOC(93)22.

ALSO AVAILABLE

NEA Publications of General Interest

2001 Annual Report (2002) *Free: paper or Web.*

NEA News
ISSN 1605-9581 Yearly subscription: € 40 US$ 45 GBP 26 ¥ 4 800

Nuclear Science

Physics of Plutonium Recycling
Volume VII – BWR MOX Benchmark – Specification and Results (2003)
ISBN 92-64-19905-5 Price: € 45 US$ 45 GBP 29 ¥ 5 500
Volume VI – Multiple Pu Recycling in Advanced PWRs (2002)
ISBN 92-64-19957-8 Price: € 45 US$ 45 GBP 28 ¥ 5 250

Advanced Reactors with Innovative Fuels (2002)
ISBN 92-64-19847-4 Price: € 130 US$ 113 GBP 79 ¥ 15 000

Basic Studies in the Field of High-temperature Engineering (2002)
ISBN 92-64-19796-6 Price: € 75 US$ 66 GBP 46 ¥ 8 600

Fission Gas Behaviour in Water Reactor Fuels (2002)
ISBN 92-64-19715-X Price: € 120 US$ 107 GBP 74 ¥ 12 100

Shielding Aspects of Accelerators, Targets and Irradiation Facilities – SATIF 5 (2001)
ISBN 92-64-18691-3 Price: € 84 US$ 75 GBP 52 ¥ 8 450

Nuclear Production of Hydrogen (2001)
ISBN 92-64-18696-4 Price: € 55 US$ 49 GBP 34 ¥ 5 550

Utilisation and Reliability of High Power Proton Accelerators (2001)
ISBN 92-64-18749-9 Price: € 130 US$ 116 GBP 80 ¥ 13 100

Burn-up Credit Criticality Benchmark (2003) *Free: paper or web.*
Phase IV-A: Reactivity Prediction Calculations for Infinite Arrays of PWR MOX Fuel Pin Cells
ISBN 92-64-02123-X
Phase IV-B: Results and Analysis of MOX Fuel Depletion Calculations
ISBN 92-64-02124-8

CD-ROM Complete Collection of Published Reports (as of May 2003) *Free on request.*

Accelerator-driven Systems (ADS) and Fast Reactors (FR) in Advanced Nuclear Fuel Cycles (2002)
ISBN 92-64-18482-1 *Free: paper or web.*

Comparison Calculations for an Accelerator-driven Minor Actinide Burner (2002)
ISBN 92-64-18478-3 *Free: paper or web.*

Speciation, Techniques and Facilities for Radioactive Materials at Synchrotron Light Sources (2002)
Workshop Proceedings, Grenoble, France, 10-12 September 2000
ISBN 92-64-18485-5 *Free: paper or web.*

Pressurised Water Reactor Main Steam Line Break (MSLB) Benchmark (Volume III) (2002)
ISBN 92-64-18495-3 *Free: paper or web.*

A VVER-1000 LEU and MOX Assembly Computational Benchmark (2002)
Specification and Results
ISBN 92-64-18491-0 *Free: paper or web.*

Order form on reverse side.

ORDER FORM

OECD Nuclear Energy Agency, 12 boulevard des Iles, F-92130 Issy-les-Moulineaux, France
Tel. 33 (0)1 45 24 10 15, Fax 33 (0)1 45 24 11 10, E-mail: neapub@nea.fr**, Internet: www.nea.fr**

Qty	Title	ISBN	Price	Amount
			Total*	

* Prices include postage fees.

❑ Payment enclosed (cheque payable to OECD Publications).

Charge my credit card ❑ VISA ❑ Mastercard ❑ American Express

Card No.	Expiration date	Signature
Name		
Address	Country	
Telephone	Fax	
E-mail		

OECD PUBLICATIONS, 2 rue André-Pascal, 75775 PARIS CEDEX 16
Printed in France.